Experience-dependent connections in the brain

A thesis by:

Samuel E. Rasche

Submitted for the degree of

Doctor of Philosophy

Laboratory of Neurobiology, Department of Cell and Developmental Biology, Division of Biosciences

University College London

2023

DECLARATION

I, Samuel E. Rasche, confirm that the work presented in my thesis is my own. Where information has been derived from other sources, I confirm that this has been indicated in the thesis.

ABSTRACT

This thesis is an exploration of connections between cortical areas that become demonstrable through specific experiences, which I refer to as experience-dependent connections. By employing both univariate and multivariate analyses, the investigation delves into the neural mechanisms orchestrating various experiences, ranging from the conscious perception of single visual attributes to aesthetic experiences.

I begin by addressing the neural mechanisms involved in conscious perception in the Riddoch syndrome. These patients are blinded by damage to V1 yet can consciously perceive motion presented in their blind field. Previous evidence, as well as ours, suggests that this residual ability may be retained after damage if the visual area important for motion perception, V5, is intact and receives direct input from the subcortex. These connections with the subcortex are critical, as we demonstrate in one of our patients that even partial damage to these pathways can lead to loss of sight and to conditions that mimic the Riddoch syndrome. Moreover, we show that the patients' performance on visual discrimination tasks and their certainty of having seen motion strongly correlate, and specific neural activity patterns emerge in V5 only when a patient is conscious of motion. Thus, V1 is not necessary for conscious awareness of visual motion. Finally, we observed additional experiential states in these patients; they may, for example, experience hallucinations of motion. These experiences engaged additional areas, thereby revealing distinct brain connections depending on the experience.

Having thus established that awareness of a single visual attribute evokes specific neural activity patterns in visual sensory areas outside V1, we enquired whether such patterns also emerge with more complex experiences. To this end, we investigated the neural determinants of aesthetic experiences. Only when stimuli were experienced as beautiful or ugly did patterns emerge in face-perceptive areas and was there co-activity with the medial orbitofrontal cortex. Overall, these findings show that the existence and high specificity of functional connections become demonstrable during certain experiences.

IMPACT STATEMENT

A fundamental function of the brain is to acquire knowledge about the world by stabilising the everchanging signals it receives from it. One way of stabilising is through the sense of vision. For example, humans discard changes in spectral composition and visually experience constant colour categories. Our perceptions are thus not necessarily an exact representation of the external environment; instead, we can only perceive and become aware of that what our brain allows us to. It is therefore of critical importance to investigate the organisation of the brain, as only this can bring us closer to understanding how we experience the world we inhabit.

There are many ways of studying the organisation of the brain, one of them being examining patients. Because different parts of the brain perform different functions, different disabilities arise as a consequence of brain damage, depending on the affected region. Therefore, investigating changes in behaviour and phenomenological experience as a result of brain damage can deepen our understanding of the underlying mechanisms of the brain. The work presented here looked specifically at patients who lost sight by lesions in the primary visual cortex. Surprisingly, despite their injury, we, and others, have observed that they may retain some visual capacities. The work presented here scrutinises this residual capacity and reveals not only the underlying neural mechanisms of visual perception, but also offers patients more insight into their pathology and may improve their circumstances. For example, training programmes may be designed to enhance their capabilities, potentially improving their ability to navigate their environment despite their blindness. In short, these studies not only inform us about neurobiology; they may significantly improve clinical outcomes and enhance the quality of life of many patients rendered blind by lesions in the primary visual cortex.

Another way to study the organisation of the brain is by examining healthy individuals via non-invasive methods, such as through magnetic resonance imaging (MRI). Such studies are also included in this thesis; I specifically address the question of aesthetic experiences with functional MRI. These experiences, too, play a critical role in knowledge acquisition and guide our behaviour. This is well-illustrated by the fact that the world of beauty and art are extremely lucrative; many spend fortunes pursuing it. This global interest indicates that there may be a biological basis driving this behaviour. In fact, the

studies described here show that aesthetic experiences may not be simply 'in the eye of the beholder' and are more universal than intuitively thought. Beauty can thus not only teach us about cultural influences, but also directly about our biological origins. Moreover, even though the studies undertaken here on aesthetics do not involve patients directly, understanding the mechanisms involved in aesthetic experiences may nevertheless advance our understanding of neurological disorders as well, for example that of anhedonia, where patients are unable to experience beauty, joy or pleasure, and this insight may lead to the development of therapeutic treatments. Finally, comprehending the neural basis involved in the appreciation of aesthetic qualities in our environment may lead to new ways of increasing exposure to such pleasant stimuli, thereby improving the quality of life for the population at large.

UCL Research Paper Declaration Form

referencing the doctoral candidate's own published work(s)

For a research manuscript that has already been published:

a) **What is the title of the manuscript?**

The neural determinants of abstract beauty

b) **Please include a link to or doi for the work**

https://doi.org/10.1111/ejn.15912

c) **Where was the work published?**

European Journal of Neuroscience

d) **Who published the work?** (e.g. OUP)

Wiley

e) **When was the work published?**

January 12, 2023

f) **List the manuscript's authors in the order they appear on the publication**

Samuel E. Rasche*, Ahmad Beyh*, Marco Paolini, Semir Zeki

* Authors contributed equally.

g) **Was the work peer reviewed?**

Yes

h) **Have you retained the copyright?**

Yes, as an author of a published Wiley article, I have the right to reuse this article as part of my thesis.

i) **Was an earlier form of the manuscript uploaded to a preprint server?** (e.g. medRxiv). If 'Yes', please give a link or doi)

Yes - https://doi.org/10.1101/2022.07.13.499869

If 'No', please seek permission from the relevant publisher and check the box next to the below statement:

☒

*I acknowledge permission of the publisher named under **d** to include in this thesis portions of the publication named as included in **c**.*

For multi-authored work, please give a statement of contribution covering all authors

Ahmad Beyh, Samuel E. Rasche and Semir Zeki conceived of the experiment; Ahmad Beyh and Samuel E. Rasche conducted the experiments, analysed the data and, together with Semir Zeki, wrote the manuscript; Marco Paolini made the brain scanning

facilities available and made critical comments on the manuscript. Funding for this project was acquired by Semir Zeki.

In which chapter(s) of your thesis can this material be found?

Chapter 6 and in the summary of findings.

e-Signatures confirming that the information above is accurate (this form should be co-signed by the supervisor/ senior author unless this is not appropriate, e.g. if the paper was a single-author work)

Candidate

Samuel E. Rasche

Date:

12/10/2023

Supervisor/ Senior Author (where appropriate)

Semir Zeki

Date

12/10/2023

UCL Research Paper Declaration Form

referencing the doctoral candidate's own published work(s)

For a research manuscript that has already been published:

a) **What is the title of the manuscript?**

Neural patterns of conscious visual awareness in the Riddoch syndrome

b) **Please include a link to or doi for the work**

https://doi.org/10.1007/s00415-023-11861-5

c) **Where was the work published?**

Journal of Neurology

d) **Who published the work?** (e.g. OUP)

Springer

e) **When was the work published?**

July 10, 2023

f) **List the manuscript's authors in the order they appear on the publication**

Ahmad Beyh*, Samuel E. Rasche*, Alexander Leff, Dominic ffytche, Semir Zeki

* Authors contributed equally.

g) **Was the work peer reviewed?**

Yes

h) **Have you retained the copyright?**

Yes, as an author of a published Springer article, I have the right to reuse this article as part of my thesis.

i) **Was an earlier form of the manuscript uploaded to a preprint server?** (e.g. medRxiv). If 'Yes', please give a link or doi)

Yes - https://doi.org/10.1101/2023.04.20.537641

If 'No', please seek permission from the relevant publisher and check the box next to the below statement:

☒

*I acknowledge permission of the publisher named under **d** to include in this thesis portions of the publication named as included in **c**.*

For multi-authored work, please give a statement of contribution covering all authors

The study was conceptualised by all authors. Alexander Leff found suitable patients for the study. Ahmad Beyh and Samuel E. Rasche created the experimental tasks, collected the data, and analysed it. Ahmad Beyh analysed the diffusion weighted imaging data.

First draft was written by Ahmad Beyh, Samuel E. Rasche and Semir Zeki, which was reviewed and edited by all authors. Funding was acquired by Alexander Leff and Semir Zeki.

In which chapter(s) of your thesis can this material be found?

Chapter 2

e-Signatures confirming that the information above is accurate (this form should be co-signed by the supervisor/ senior author unless this is not appropriate, e.g. if the paper was a single-author work)

Candidate

Samuel E. Rasche

Date:

12/10/2023

Supervisor/ Senior Author (where appropriate)

Semir Zeki

Date

12/10/2023

UCL Research Paper Declaration Form

referencing the doctoral candidate's own published work(s)

For a research manuscript prepared for publication but that has not yet been published:

a) **What is the current title of the manuscript?**

A clinico-anatomical dissection of the magnocellular and parvocellular pathways in a patient with the Riddoch syndrome

b) **Has the manuscript been uploaded to a preprint server?** (e.g. medRxiv; if 'Yes', please give a link or doi)

No

c) **Where is the work intended to be published?** (e.g. journal names)

Journal of Neurology

d) **List the manuscript's authors in the intended authorship order**

Ahmad Beyh*, Samuel E. Rasche*, Alexander Leff, Dominic ffytche, Semir Zeki

* Authors contributed equally.

e) **Stage of publication** (e.g. in submission)

Ready for submission

For multi-authored work, please give a statement of contribution covering all authors

The study was conceptualised by Ahmad Beyh, Samuel E. Rasche and Semir Zeki. Alexander Leff found suitable patients for the study. Ahmad Beyh and Samuel E. Rasche created the experimental tasks, collected the data, and analysed it. Ahmad Beyh analysed the diffusion weighted imaging data. First draft was written by Ahmad Beyh, Samuel E. Rasche and Semir Zeki, which was reviewed and edited by all authors. Funding was acquired by Alexander Leff and Semir Zeki.

In which chapter(s) of your thesis can this material be found?

Chapter 4

e-Signatures confirming that the information above is accurate (this form should be co-signed by the supervisor/ senior author unless this is not appropriate, e.g. if the paper was a single-author work)

Candidate

Samuel E. Rasche

Date:

12/10/2023

Supervisor/ Senior Author (where appropriate)

Semir Zeki

Date

12/10/2023

UCL Research Paper Declaration Form

referencing the doctoral candidate's own published work(s)

For a research manuscript prepared for publication but that has not yet been published:

a) **What is the current title of the manuscript?**

Neural correlates of the experience of ugliness

b) **Has the manuscript been uploaded to a preprint server?** (e.g. medRxiv; if 'Yes', please give a link or doi)

No

c) **Where is the work intended to be published?** (e.g. journal names)

European Journal of Neuroscience

d) **List the manuscript's authors in the intended authorship order**

Samuel E. Rasche*, Ahmad Beyh*, Marco Paolini, Semir Zeki

* Authors contributed equally.

e) **Stage of publication** (e.g. in submission)

Ready for submission

For multi-authored work, please give a statement of contribution covering all authors

Ahmad Beyh, Samuel E. Rasche and Semir Zeki conceived of the experiment; Ahmad Beyh and Samuel E. Rasche conducted the experiments, analysed the data and, together with Semir Zeki, wrote the manuscript; Marco Paolini made the brain scanning facilities available and made critical comments on the manuscript. Funding for this project was acquired by Semir Zeki.

In which chapter(s) of your thesis can this material be found?

Chapter 7

e-Signatures confirming that the information above is accurate (this form should be co-signed by the supervisor/ senior author unless this is not appropriate, e.g. if the paper was a single-author work)

Candidate

Samuel E. Rasche

Date:

22/12/2023

Supervisor/ Senior Author (where appropriate)

Semir Zeki

Date

22/12/2023

ACKNOWLEDGEMENTS

First and foremost, I would like to thank my principal supervisor, Professor Semir Zeki, who has provided me with continuous support and guidance; I could not have wished for better mentorship. I would also like to express my sincere gratitude to my colleague and friend Dr. Ahmad Beyh, from whom I have learned so much in the past years. Without them, this work would not have been possible.

I extend my appreciation to those with whom I have collaborated on these projects and to those whose thoughtful input and valuable criticism have been crucial for the realisation of this thesis, including my subsidiary supervisor, Dr. Tobias Hauser, and my graduate departmental tutor, Professor Stephen Hunt.

I would also like to give special thanks to the members of the Platonic Academy London. Our discussions have proven to be extremely fruitful and truly inspirational, and have contributed, either directly or indirectly, to the conceptualisation of the work described in this thesis.

Finally, I am indebted to my partner and best friend, Jackie, my parents, brother, and the rest of my family and friends, who all have supported and encouraged me throughout this journey.

CONTENTS

ABBREVIATIONS

aCC – anterior cingulate cortex

BOLD – blood-oxygen-level-dependent

DMN – default mode network

DWI – diffusion weighted imaging

EPI – echo planar imaging

EVC – early visual cortex

FFA – fusiform face area

fMRI – functional magnetic resonance imaging

fODF – fibre orientation distribution function

FP – frontal pole

FWHM – full width at half maximum

GLM – general linear model

HC – hippocampus

HMOA – hindrance modulated orientational anisotropy

HRP – horseradish peroxidase

IFG – inferior frontal gyrus

IOG – inferior occipital gyrus

IPL – inferior parietal lobule

K – koniocellular

LGN – lateral geniculate nucleus

LOC – lateral occipital cortex

lOFC – lateral orbitofrontal cortex

M – magnocellular

mbCC – mid-body cingulate cortex

MNI – Montreal Neurological Institute

mOFC – medial orbitofrontal cortex

MOG – middle occipital gyrus

mPFC – medial prefrontal cortex

MPRAGE – magnetisation-prepared accelerated gradient echo

MRI – magnetic resonance imaging

MVPA – multivariate pattern analysis

OFA – occipital face area

P – parvocellular

pCC – posterior cingulate cortex

PPI – psychophysiological interaction

RDM – representational dissimilarity matrix

ROI – region of interest

RSA – representational similarity analysis

S – short-wavelength

SFG – superior frontal gyrus

TE – echo time

TR – repetition time

Type 2 ROC - type 2 receiver operating characteristic

vmPFC – ventromedial prefrontal cortex

2AFC – two-alternative forced choice

PROLOGUE

It is trite to say that the cerebral cortex is massively connected, with each area feeding many other areas and receiving a reciprocal input from them. Many of these connections have been demonstrated through straightforward anatomical tracing (for example with silver degeneration stains, horseradish peroxidase (HRP) uptake or viral tracing). Yet it is hard to believe that such 'static' pathways – in the sense that their trajectories can always be determined with the right anatomical method – are the only ones that populate the cortex. It is entirely likely, as I argue and demonstrate here, that other cerebral pathways, perhaps even a significant number of them, cannot be demonstrated by what I refer to as static anatomical methods. Instead, they must depend upon some kind of activity – elicited by an experience – to become active and therefore visibly demonstrable.

In fact, the advent of functional magnetic resonance imaging (fMRI) has demonstrated many such connections. This technique measures changes in blood flow and oxygenation in response to neural activity; it allows us to deduce which areas are involved during a particular experience, as active areas require delivery of oxygenated blood. Using this technique, studies have shown that different experiences activate different parts of the brain. For example, the visual cortex consists of visual areas that process distinct attributes of a visual stimulus, such as colour, form and motion [1]. Faces also have their dedicated brain area; when a face is perceived there is increased activity in sensory regions important for face-processing, such as the fusiform face area and the occipital face area, among others [2–5]. But, importantly, it is only when this face is experienced as beautiful that the medial orbitofrontal cortex (mOFC) – which plays a critical role in the experience of beauty, regardless of its source [6,7] – is also active [8]. Therefore, the experience of facial beauty reveals correlative connections between the fusiform gyrus and the mOFC which otherwise remain occult.

Thus, using fMRI, the involvement of each brain area in a particular experience can be estimated; this is usually done with the so-called univariate approach, in which the average activity in brain areas is compared across conditions through the general linear model (GLM) framework. The GLM estimates the amplitude of the blood-oxygen-level-dependent (BOLD) signal (or time-series) that is derived from fMRI. It does so in every voxel; these are cubes, often of a size of 3 mm^3, that represent a piece of brain tissue in

the fMRI image. The estimation is done for every single voxel in the brain independently (hence the name 'univariate'), thereby identifying which voxels are involved in a particular task. An especially powerful way of assessing the fMRI data via the univariate approach is through parametric modulation; here, one estimates whether the BOLD signal increases as the declared intensity of the experience increases. Overall, the univariate method has proven to be very fruitful, as it has been able to identify neural correlates of many cognitive functions.

However, despite its success, there are situations in which the univariate approach may fail to detect involvement of certain brain areas. For instance, it may not be able to dissociate between conditions that activate the same areas to a similar extent but with different spatial activation patterns. Another approach, the so-called multivariate approach circumvents this issue by considering the distribution of activity (i.e. pattern) in multiple voxels (hence the name 'multivariate'). Two prominent types of multivariate analyses include multi-voxel pattern analysis (MVPA) [9,10] and representational similarity analysis (RSA) [11]; the former uses classification algorithms to assess the pattern (dis)similarity of specific conditions, whereas the latter uses distance metrics to calculate the pattern (dis)similarity between trials. Of course, assessing a specific pattern of activity remains imprecise due to the presence of approximately one million neurons within a voxel [12]. Nevertheless, the multivariate approach has proven to be a powerful tool in the analysis of fMRI data, demonstrating that different mental states can correlate with different spatial patterns in one or more brain areas [13].

THESIS OVERVIEW

My aim is to reveal dormant brain connections by addressing various conditions in which activity patterns emerge and areas become co-active. I have investigated the neural mechanisms of experiences that are of special interest to me, namely those of visual awareness and aesthetic experiences. By supplementing the univariate analysis with the multivariate analysis, neural networks can be detected that underly particular experiences; we therefore performed categorical and parametric univariate analyses to detect changes in amplitude of activity and RSA to detect neural activity patterns. RSA was the preferred method over MVPA for our purposes, as this method is not sensitive to overall amplitude [11].

Part I: neural patterns of visual awareness in the Riddoch syndrome

First, I will discuss studies that I, together with my colleagues, have performed on patients with the Riddoch syndrome. These patients are blind due to lesions in the primary visual cortex (V1) but can nevertheless experience visual motion consciously [14]. This is a very curious phenomenon, as V1 is known to be a pivotal area in visual processing and a lesion in it leads to loss of sight [15,16].

If visual motion perception, however crude, can occur without V1, it means that V1 is not a necessary component of visual motion perception. What then are the minimal neural requirements to become aware of a single visual attribute, such as motion, without the involvement of V1? Visual motion is known to activate V5 [1], even in the absence of V1 [14,17–19]. However, previous research has shown that both perceived and unperceived motion can activate this area [14,20,21]. Increased activity in V5 is thus not an adequate indicator of awareness of motion. We therefore conjectured that it is not increases in activity per se, but rather a certain pattern of activity within V5 that enables a conscious experience of visual motion. One way of demonstrating such a pattern is through the multivariate approach.

To test this hypothesis, we presented patients suffering from the Riddoch syndrome with moving visual stimuli while simultaneously measuring the neural activity in the brain. The neuroimaging data included structural, diffusion and functional imaging, which was scrutinised with advanced statistical methods, including univariate and multivariate analyses. We found that when a Riddoch patient consciously perceives a visual motion, specific spatial arrangements (patterns) of neural activity emerged in the visual area specialised for the processing of visual motion, i.e., V5. Additional brain areas appeared to be involved as well, but their involvement depended upon the stimulus properties, which induced different perceptual states (i.e. experiences) in the patient (explained in detail in chapter 2).

Specifically, we investigated whether the ability to discriminate between coloured stimuli and black-white stimuli in the blind field persisted. Our patient was indeed able to discriminate these stimuli, and this ability, too, correlated with the emergence of neural patterns in the visual areas specialised for the processing of that visual attribute, in this case the V4 complex.

Finally, we examined a peculiar case of a patient who exhibited symptoms of the Riddoch syndrome yet had an intact V1, which was instead partially deafferented. Our investigation suggests that a selective loss of parvocellular input into V1 lies at the basis of this curious phenomenon.

To sum up, by studying the reduced neural system of the Riddoch syndrome, we were able to investigate the neural determinants of the conscious experience of a specific visual attribute, thus coming closer to specifying what the minimal neural conditions for conscious experience may be.

Part II: neural patterns in aesthetic experiences

The conscious experience of a single visual attribute correlated with the emergence of neural activity patterns, not only in the sensory area relevant for its processing, but also in additional areas, depending upon the experience that the various stimuli induced. I refer to these co-activations as experience-dependent connections. These remarkable findings motivated us to further explore conditions in which these neural patterns emerge. We therefore asked a second research question, which is addressed in the second part of this thesis: do neural activity patterns only correlate with perception of "low-level" visual attributes? Or do more abstract cognitive processes, such as the experience of beauty and ugliness, also correlate with specific detectable patterns and, if so, where in the brain do these patterns emerge? We found that such patterns did indeed emerge with aesthetic experiences, and again in the visual sensory area relevant for the processing of that specific stimulus, indicating that the aesthetic impression induced by such a stimulus is registered in these areas. Moreover, only when such a stimulus was of a particular aesthetic status was there co-activity in the medial orbitofrontal cortex, demonstrating again an experience-dependent connection in the brain.

Overall, the investigations described in this thesis are an attempt to advance our understanding of the neurobiology underlying various experiences. Using both univariate and multivariate analysis tools, we have investigated whether neural activity patterns emerge when experiencing single perceptual attributes (often referred to as "low-level" features, involving sensory areas of the brain) as well as complex stimuli (often referred to as 'higher' cognitive functions, typically involving additional areas such as the frontal lobe [22]) and found involvement of specific networks of brain regions which only become apparent through these specific experiences. This thesis therefore concentrates on making occult connections demonstrable through experience-dependent correlated activity.

REFERENCES

1. Zeki, S., Watson, J., Lueck, C., Friston, K., Kennard, C., and Frackowiak, R. (1991). A direct demonstration of functional specialization in human visual cortex. The Journal of Neuroscience *11*, 641–649. 10.1523/JNEUROSCI.11-03-00641.1991.
2. Allison, T., Puce, A., Spencer, D.D., and McCarthy, G. (1999). Electrophysiological studies of human face perception. I: potentials generated in occipitotemporal cortex by face and non-face stimuli. Cerebral Cortex *9*, 415–430. 10.1093/cercor/9.5.415.
3. Sergent, J., Ohta, S., and Macdonald, B. (1992). Functional neuroanatomy of face and object processing: a positron emission tomography study. Brain *115*, 15–36. 10.1093/brain/115.1.15.
4. Haxby, J. V., Hoffman, E.A., and Gobbini, M.I. (2000). The distributed human neural system for face perception. Trends Cogn Sci *4*, 223–233. 10.1016/S1364-6613(00)01482-0.
5. Kanwisher, N., McDermott, J., and Chun, M.M. (1997). The fusiform face area: a module in human extrastriate cortex specialized for face perception. The Journal of Neuroscience *17*, 4302–4311. 10.1523/JNEUROSCI.17-11-04302.1997.
6. Ishizu, T., and Zeki, S. (2011). Toward a brain-based theory of beauty. PLoS One *6*, e21852. 10.1371/journal.pone.0021852.
7. Zeki, S., Romaya, J.P., Benincasa, D.M.T., and Atiyah, M.F. (2014). The experience of mathematical beauty and its neural correlates. Front Hum Neurosci *8*. 10.3389/fnhum.2014.00068.
8. Yang, T., Formuli, A., Paolini, M., and Zeki, S. (2022). The neural determinants of beauty. European Journal of Neuroscience *55*, 91–106. 10.1111/ejn.15543.
9. Haxby, J. V., Gobbini, M.I., Furey, M.L., Ishai, A., Schouten, J.L., and Pietrini, P. (2001). Distributed and overlapping representations of faces and objects in ventral temporal cortex. Science (1979) *293*, 2425–2430. 10.1126/science.1063736.
10. Cox, D.D., and Savoy, R.L. (2003). Functional magnetic resonance imaging (fMRI) "brain reading": detecting and classifying distributed patterns of fMRI activity in human visual cortex. Neuroimage *19*, 261–270. 10.1016/S1053-8119(03)00049-1.
11. Kriegeskorte, N. (2008). Representational similarity analysis – connecting the branches of systems neuroscience. Front Syst Neurosci *4*. 10.3389/neuro.06.004.2008.
12. Arthurs, O.J., and Boniface, S. (2002). How well do we understand the neural origins of the fMRI BOLD signal? Trends Neurosci *25*, 27–31. 10.1016/S0166-2236(00)01995-0.
13. Haynes, J.-D., and Rees, G. (2006). Decoding mental states from brain activity in humans. Nat Rev Neurosci *7*, 523–534. 10.1038/nrn1931.
14. Zeki, S., and ffytche, D. (1998). The Riddoch syndrome: insights into the neurobiology of conscious vision. Brain *121*, 25–45. 10.1093/brain/121.1.25.
15. Henschen, S.E. (1890). Klinische und anatomische beiträge zur pathologie des gehirns (Almquist & Wiksells).
16. Holmes, G. (1918). Disturbances of vision by cerebral lesions. British Journal of Ophthalmology *2*, 353–384. 10.1136/bjo.2.7.353.
17. Barbur, J.L., Watson, J.D.G., Frackowiak, R.S.J., and Zeki, S. (1993). Conscious visual perception without VI. Brain *116*, 1293–1302. 10.1093/brain/116.6.1293.

18. Ajina, S., Kennard, C., Rees, G., and Bridge, H. (2015). Motion area V5/MT+ response to global motion in the absence of V1 resembles early visual cortex. Brain *138*, 164–178. 10.1093/brain/awu328.

19. Arcaro, M.J., Thaler, L., Quinlan, D.J., Monaco, S., Khan, S., Valyear, K.F., Goebel, R., Dutton, G.N., Goodale, M.A., Kastner, S., et al. (2019). Psychophysical and neuroimaging responses to moving stimuli in a patient with the Riddoch phenomenon due to bilateral visual cortex lesions. Neuropsychologia *128*, 150–165. 10.1016/j.neuropsychologia.2018.05.008.

20. Moutoussis, K., and Zeki, S. (2006). Seeing invisible motion: a human fMRI study. Current Biology *16*, 574–579. 10.1016/j.cub.2006.01.062.

21. Itoh, K., Fujii, Y., Kwee, I.L., and Nakada, T. (2005). MT+/V5 activation without conscious motion perception: a high-field fMRI study. Magnetic Resonance in Medical Sciences *4*, 69–74. 10.2463/mrms.4.69.

22. Frith, C., and Dolan, R. (1996). The role of the prefrontal cortex in higher cognitive functions. Cognitive Brain Research *5*, 175–181. 10.1016/S0926-6410(96)00054-7.

Part I

1.

Primary Visual Cortex

After damage to the visual cortex, people suffer from a variety of visual disturbances, depending on the functional specialisation of the affected visual area. The consequence of damage to the primary visual cortex (V1) is blindness. Given its retinotopic organization, the extent and position of the blindness depends on the extent and position of the lesion in V1. Importantly, the patient may experience residual visual awareness of certain features of a stimulus within the blind field. This, however, does not fit with (classical) theories about the function of V1, which has led to discussions and confusions in the field, some of which remain unresolved.

1.1 V1 AS THE BEDROCK OF VISUAL CORTEX

The brain's visual system is often described as being hierarchically organised [1]. Cells in successive areas would combine the incoming information, relay this information onto the next visual area along the hierarchical stream which then further integrates information, until eventually regions are reached that respond to entire objects. This hierarchical doctrine was proposed by Hubel & Wiesel [2,3] after their discoveries of orientation selective cells in the primary visual cortex (also referred to as V1, striate cortex, calcarine cortex or Brodmann area 17), but the idea itself is much older. Lissauer [4] and Flechsig [5] made the distinction of seeing and understanding, an idea which can be traced back to Immanuel Kant [6]. Visual processing would consist of two stages – apperception and association – whereby first, incoming visual input is received, and second, the input is associated with concepts existing in the mind. This idea sat well with two observations; first, Flechsig [5] found that the primary visual cortex was myelinated at birth, whereas other areas became myelinated later, presumably as a consequence of experience and interaction with the external world. Second, V1 has a distinct cytoarchitectural appearance; it has a visible striation (hence striate cortex). This supported the idea that V1 has a different function, as it was generally believed that distinct cytoarchitectures meant distinct functions [7]. The prestriate cortex (visual areas adjacent to V1) also has a uniform cytoarchitecture; hence it was assumed that this entire region performed the function of associating received impressions with existing ideas (however, we now know that cytoarchitectural uniformity is not an adequate indicator of functional uniformity; the prestriate cortex consists of various specialised visual areas) [7]. Thus, this two-staged model put V1, because of its organisation, at the beginning of the hierarchy and conscious visual perception was attributed to it. V1 was surrounded by the 'association' cortex (prestriate cortex) which brought together past and present visual inputs, and combined visual inputs with inputs from other sources [8].

Before discussing the Riddoch syndrome, it is worth addressing the historical background of V1, as this will clarify where certain ideas about its function originate from. By 1890, Henschen had gathered enough clinical evidence to discover that damage to the striate cortex leads to blindness [9]. Although these observations were based on large lesions, Henschen nevertheless managed to locate the extent of the visual cortex that corresponded to the striate cortex [10]. He also studied the way the retina is represented in

it; with one relatively minor exception – namely that central vision is represented anteriorly and peripheral vision posteriorly – his findings have stood the test of time. One possible explanation for his mistake could be that he may have included an area anterior to V1 in his analysis, namely V4, which responds to central vision (the visual field also has a retinotopic representation in other visual areas outside of V1) [7,11].

The advent of war resulted in more specific cases of cortical blindness. In 1904-1905 the Russo-Japan war was fought during which the Russians used high velocity rifles with tiny bullets after an agreement on the prohibition of certain ammunition at the Hague Convention in 1899. These bullets were not as damaging and were less deadly than previously used bullets; they pierced through the body with clear entrance and exit wounds. This resulted in an increase in soldiers surviving a headshot wound, and consequently, led to an increase in brain damaged cases. The Japanese physician Tetsuo Inouye examined some of these cases and invented a device to locate the damaged tissue based on these wounds [10]. This allowed him to deduce how the visual field is represented in the brain and discovered its retinotopic organisation; lesions in the most posterior part of V1 (the occipital pole) lead to blindness in the centre of the visual field, whereas lesions in more anterior portions lead orderly to peripheral blindness [10,12].

Support for Inouye's findings was found by Holmes & Lister [13]. Again, war (in this case the first world war) brought about various cases of brain injury that made it possible to investigate the representation of the visual field further. Holmes clearly mapped out the retinotopic organisation of V1 and, following Henschen's [9] and Flechsig's [5] footsteps, claimed that V1 is the sole visual perceptive centre of the brain [14]. By doing so, he ignored observations made by George Riddoch a year earlier, in which Riddoch demonstrated that patients with V1 damage are still able to *consciously* perceive motion in their blind field [15]. The five patients whom Riddoch had investigated were able to detect moving objects that were otherwise imperceivable when presented stationary. The patients described their sensation as something 'vague' and 'shadowy', and were unable to describe any other visual features of the stimulus. Holmes acknowledged but brushed aside Riddoch's observations, despite himself a patient (case 11) who was capable of perceiving motion in his blind field after damage to V1, who described it as a 'dirty grey colour' [14]. This evidence did not convince him to change his views on V1 as the sole visual perceptive centre; he insisted that the ability of these patients to see motion was greatly

reduced, that they only perceive motion when it was abrupt, and that they were uncertain. Moreover, colour and shape were not recognised; he therefore concluded that there is no dissociation of visual features, including motion, and that the perception of all these attributes depends on V1 [14,16].

However, discoveries in the second half of the 20th century changed the status of V1 in the visual brain. Different visual areas outside of V1 were found to be specialised in the processing of different features [17,18]; V1 could therefore not be the only visual centre in the brain. Nevertheless, with the discoveries made by Hubel & Wiesel [2,3], V1 maintained its position as the entry point of all visual processing. They found that the cells in V1 were orientation selective and had very small receptive fields. That is, to get an optimal response from a cell, the line had to cover the receptive field and have a specific orientation. This set the stage for the hierarchical doctrine of the visual cortex. Instead of perceiving the entire visual field at once, it is reconstructed step-by-step. Cells in V1 would be 'simple cells' that respond to lines in small receptive fields; combined they would feed into cells higher up the cortical hierarchy, turning these cells into 'complex cells' which respond to larger receptive fields, until eventually 'pontifical' or 'grandmother' cells are reached that respond to entire concepts [19]. Given the assumed position of V1 as being the initial stage of the cortical hierarchy and assuming that the rest of the hierarchy depends on the processing of V1, it fitted well with the observation that damage to V1 leads to loss of sight. However, during late 1960s through the 1980s, anatomical evidence appeared demonstrating that there was direct subcortical input – from the lateral geniculate nucleus and pulvinar – into other regions outside of V1 [20–23]. These connections could hardly be superfluous, suggesting that not all visual processing started with V1. In fact, clinical evidence showed that patients blinded by lesions in V1 retained certain visual capacities [24,25], including direction discrimination of motion [26], confirming Riddoch's early observations. Yet despite these findings, the idea that V1 is necessary for *conscious* visual perception persisted, as is evident from "blindsight"; proponents of this phenomenon claim that patient blinded by lesions in V1 can perform well on visual discrimination tasks despite having no awareness of the stimulus [25,27]. However, the consequences of damage to this area are much more nuanced than previously thought.

1.2 BLINDSIGHT

Thus, up until the second half of the 20th century, V1 was considered to be the sole recipient area of visual signals and the centre for conscious visual perception. It was not until the 1970s that interest in the consequences of V1 damage revived again. Pöppel et al. [24] were the first of this decade to describe residual visual capacities in patients blinded by V1 damage; the patients were able to shift their gaze towards a stimulus that they claimed not to see. This had important implications, because it meant that information presented in the blind field could still be processed and the corresponding activity was strong enough to elicit a saccadic (motor) response. Weiskrantz et al. [25] went even further; they described a patient who denied seeing any of the presented stimuli, but he was nevertheless able to correctly 'guess' the location, form and colour of various stimuli on more occasions than would be expected by chance, sometimes even with a perfect score. The authors concluded that blinded patients can discriminate various visual stimuli without any awareness and called this phenomenon "blindsight" [27] (Figure 1.1). This made of V1 an essential processing stage for conscious vision; without it visual awareness is not possible.

Importantly, the awareness measures that were used by Weiskrantz et al. [25] are not clearly stated by them. As far as one can gather, the patient was assumed to be unaware on every trial, although this sits oddly with reports that the patient had a 'feeling' on some occasions. For example, it is stated that the patient reported a "stronger feeling of something being there" when presented with a green stimulus compared to a red one. In addition, when, for control purposes, blank trials were introduced in which no stimulus was presented, the patient reported having a feeling that on some occasions there was no stimulus at all. This evidently implies some form of awareness. Nevertheless, additional studies reported patients who were able to detect, localize and discriminate visual stimuli without any awareness [28,29]. By emphasizing the lack of consciousness, the phenomenon acquired widespread interest, not only in the field of neuroscience, but also among philosophers, and inspired theories of consciousness; for example, a popular proposed theory was that visual consciousness arises when neural signalling is fed back into V1, which makes V1 a necessary brain structure for visual consciousness [30,31].

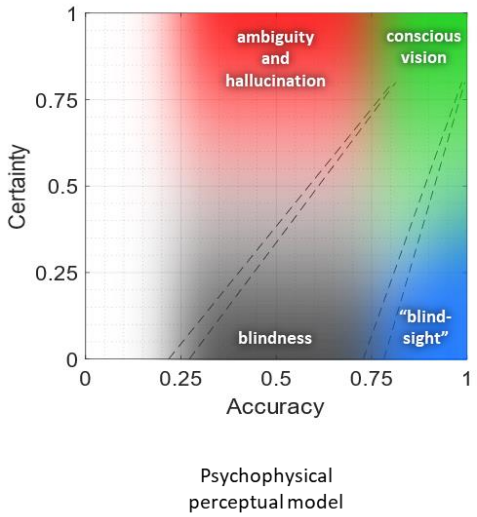

Figure 1.1. Psychophysical model of various perceptual states.
Accuracy, plotted on the x-axis, represents performance on a visual discrimination task; a score of '1' indicates perfect performance, whereas a score of '0.5' indicates chance performance. Certainty, plotted on the y-axis, represents confidence in perceiving a stimulus. Healthy subjects are highly certain and highly accurate on these type of discrimination tasks. A blind subject would not be certain and also perform at chance level. In blindsight, subjects perform well despite showing no certainty. Finally, there is high certainty but chance performance. This occurs when a subject perceives something that is not there (hallucination) or is be deceived by an ambiguous stimulus. The dashed lines represent the boundaries of the model under the binomial distribution at $p < .05$ and $p < .01$, calculated for 20 trials per condition.

However, the initial stance of blindsight, that is, the ability to discriminate visual stimuli without any conscious awareness, had to be revised in light of experiments showing that patients with damage to V1 were in fact, as observed by Riddoch in 1917 [15], able to consciously perceive visual motion [26,32]. Thus, the conscious dimension had to be included; to do so, Zeki and ffytche [32] coined the term 'Riddoch syndrome' (in honour of George Riddoch) to refer to conscious perception of visual motion after V1 damage. Proponents of blindsight, however, did not accept this definition; instead, they proposed that although there is some awareness, this awareness is not visual in nature, but rather a 'feeling' [33]. They integrated the conscious dimension by dividing blindsight into two types; 'type-1', referring to visual capacities with no visual awareness, and 'type-2', referring to visual capacities that are accompanied by a non-visual 'feeling' [33,34]. By omitting the visual aspect of the conscious experience, V1 continued to be a neural correlate of *visual* awareness.

Several weaknesses become apparent with this division. First of all, it implies two different neural mechanisms for each state; Sahraie et al. [35] propose that the unaware mode is driven by subcortical activity, whereas the aware mode relies on cortical activations. This was however contradicted by Zeki and ffytche [32], who found increased activity in the reticular formation when a "blindsight" patient was aware. Nevertheless, the dichotomy implied by the two types further reinforces the notion that behavioural performance and awareness are categorically distinct and can be dissociated, instead of being strongly linked to each other.

Second, patients typically exhibit both blindsight type-1 and type-2, depending upon stimulus properties (such as speed, contrast and spatial frequency) [32]. In fact, it is unclear whether a strictly type-1 blindsight patient exists, that is, one who has good performance and does not exhibit type-2 blindsight. There may be trials on which the patient reports no awareness, yet is correct, however, it would be premature to assume that the patient was truly unconscious on these trials, because stimuli that produce a weak impression may be reported as 'not seen' especially in binary judgements [36–39]. Binary reports (visible or not visible) may therefore not adequately cover the awareness spectrum; in fact, Overgaard et al. [40] demonstrated that a V1-damaged patient displayed type-1 blindsight when tested with a binary report, but, when using a more sensitive 'Perceptual Awareness Scale' to assess the level of awareness, the same patient reported some level of awareness and thus did no longer display type-1 blindsight. Similar findings were found by Mazzi et al. [41]. Thus, one must be selective in the awareness measures used. The possibility exists that type-1 blindsight may not occur at all; very minor residual capacities, such a shift in gaze or performance just above chance, may possibly occur without awareness, but a near perfect performance on discrimination tasks without any awareness is highly unlikely and, indeed, careful reading of traditional "blindsight" papers suggests that the patients showed some degree of awareness [32].

Finally, it is claimed that the 'feeling' in type-2 blindsight is not visual in nature, but instead a 'contentless kind of awareness' [34,42]. This proposal circumvents the natural assumption that perception of a visual stimulus, processed by the visual system, should lead to a visual experience, and makes V1 necessary for *visual* awareness. This roused many phenomenological debates about what it is like to have this 'feeling' and whether it is visual or not [43–50]. It is important to consider the difficulty the patients experience in

describing their sensation. Given that visual features such as motion are, under normal circumstances, not perceived in isolation, it is only natural not to be able to find the right words to describe such a degraded form of vision. Patients often resort to words such as 'shadow', 'feeling', 'flash' or 'foggy' [15,32,35,43]. For example, a much-studied patient called G.Y. described his experience of motion as a 'shadow' [32] (which bears resemblance to Riddoch's [15] and Holmes [14] early studies in which patients described their experience as 'vague' and 'shadowy', or as 'through a mist' and as a 'dirty grey colour'), but in other studies as a 'feeling' [35,51].

In summary, blindsight, and its division into two types, has created a number of confusions in the field. Are type-1 and type-2 two distinct categories with different underlying neural mechanisms, or is it same phenomenon? Does type-1 blindsight truly occur, or is it a result of inadequate awareness measures? Is the conscious experience of visual stimuli without V1 simply a feeling or contentless thought, or does it have visual 'qualia'? Finally, if it is true that V1 is not necessary for visual awareness, what then, are the minimal neural requirements to become aware of a single visual attribute?

I have discussed blindsight above in some detail, not only to introduce the Riddoch syndrome, but also to lay the groundwork for how I wanted to use this phenomenon, which is to look into whether there are any specific neural conditions that make conscious visual experience possible. The aim was to simply compare two different states, one in which patients can see the stimulus and one in which they cannot see it, but the investigation led us to unexpected territories, including that of conscious experience without stimulation, making the Riddoch syndrome an exceptionally powerful syndrome to study the neural correlates of visual consciousness.

REFERENCES

1. Felleman, D.J., and Van Essen, D.C. (1991). Distributed hierarchical processing in the primate cerebral cortex. Cerebral cortex *1*, 1–47. 10.1093/cercor/1.1.1-a.
2. Hubel, D.H., and Wiesel, T.N. (1977). Ferrier lecture - Functional architecture of macaque monkey visual cortex. Proc R Soc Lond B Biol Sci *198*, 1–59. 10.1098/rspb.1977.0085.
3. Hubel, D.H., and Wiesel, T.N. (1959). Receptive fields of single neurones in the cat's striate cortex. J Physiol *148*, 574–591. 10.1113/jphysiol.1959.sp006308.
4. Lissauer, H. (1890). Ein Fall von Seelenblindheit nebst einem Beitrage zur Theorie derselben. Arch Psychiatr Nervenkr *21*, 222–270.
5. Flechsig (1905). Brain physiology and theories of volition (Gehirnphysiologie und Willenstheorien), translated by von Bonin. In Some Papers on the Cerebral Cortex, pp. 181–200.
6. Kant, I. (1781). Kritik der reinen Vernunft, Transl. W.S. Pluhar (1996) as Critique of Pure Reason (Hackett Publishing).
7. Zeki, S. (1993). A vision of the brain (Blackwell scientific publications).
8. Clare, M.H., and Bishop, G.H. (1954). Responses from an association area secondarily activated from optic cortex. J Neurophysiol *17*, 271–277.
9. Henschen, S.E. (1890). Klinische und anatomische beiträge zur pathologie des gehirns (Almquist & Wiksells).
10. Glickstein, M., and Whitteridge, D. (1987). Tatsuji Inouye and the mapping of the visual fields on the human cerebral cortex. Trends Neurosci *10*, 350–353. 10.1016/0166-2236(87)90066-X.
11. Brewer, A.A., Liu, J., Wade, A.R., and Wandell, B.A. (2005). Visual field maps and stimulus selectivity in human ventral occipital cortex. Nat Neurosci *8*, 1102–1109. 10.1038/nn1507.
12. Inouye, T. (1909). Die Sehstörungen bei Schussverletzungen der kortikalen Sehsphäre: nach Beobachtungen an Verwundeten der letzten japanischen Kriege (W. Engelmann).
13. Holmes, G., and Lister, W.T. (1916). Disturbances of vision from cerebral lesions, with special reference to the cortical representation of the macula. Brain *39*, 34–73. 10.1093/brain/39.1-2.34.
14. Holmes, G. (1918). Disturbances of vision by cerebral lesions. British Journal of Ophthalmology *2*, 353–384. 10.1136/bjo.2.7.353.
15. Riddoch, G. (1917). Dissociation of visual perceptions due to occipital injuries, with especial reference to appreciation of movement. Brain *40*, 15–57. 10.1093/brain/40.1.15.
16. Holmes, G. (1945). Ferrier Lecture - The organization of the visual cortex in man. Proc R Soc Lond B Biol Sci *132*, 348–361. 10.1098/rspb.1945.0002.
17. Zeki, S. (1978). Functional specialisation in the visual cortex of the rhesus monkey. Nature *274*, 423–428. 10.1038/274423a0.
18. Livingstone, M., and Hubel, D. (1988). Segregation of form, color, movement, and depth: anatomy, physiology, and perception. Science (1979) *240*, 740–749. 10.1126/science.3283936.
19. Barlow, H.B. (1972). Single units and sensation: a neuron doctrine for perceptual psychology? Perception *1*, 371–394. 10.1068/p010371.

20. Fries, W. (1981). The projection from the lateral geniculate nucleus to the prestriate cortex of the macaque monkey. Proc R Soc Lond B Biol Sci *213*, 73–80. 10.1098/rspb.1981.0054.

21. Yukie, M., and Iwai, E. (1981). Direct projection from the dorsal lateral geniculate nucleus to the prestriate cortex in macaque monkeys. J Comp Neurol *201*, 81–97. 10.1002/cne.902010107.

22. Benevento, L.A., and Rezak, M. (1976). The cortical projections of the inferior pulvinar and adjacent lateral pulvinar in the rhesus monkey (Macaca mulatta): an autoradiographic study. Brain Res *108*, 1–24. 10.1016/0006-8993(76)90160-8.

23. Cragg, B.G. (1969). The topography of the afferent projections in the circumstriate visual cortex of the monkey studied by the nauta method. Vision Res *9*, 733–747. 10.1016/0042-6989(69)90011-X.

24. Pöppel, E., Held, R., and Frost, D. (1973). Residual visual function after brain wounds involving the central visual pathways in man. Nature *243*, 295–296. 10.1038/243295a0.

25. Weiskrantz, L., Warrington, E.K., Sanders, M.D., and Marshall, J. (1974). Visual capacity in the hemianopic field following a restricted occipital ablation. Brain *97*, 709–728. 10.1093/brain/97.1.709.

26. Barbur, J.L., Watson, J.D.G., Frackowiak, R.S.J., and Zeki, S. (1993). Conscious visual perception without VI. Brain *116*, 1293–1302. 10.1093/brain/116.6.1293.

27. Sanders, M.D., Warrington, E.K., Marshall, J., and Weiskrantz, L. (1974). "Blindsight": vision in a field defect. The Lancet *303*, 707–708. 10.1016/S0140-6736(74)92907-9.

28. Brent, P.J., Kennard, C., and Ruddock, K.H. (1994). Residual colour vision in a human hemianope: spectral responses and colour discrimination. Proc R Soc Lond B Biol Sci *256*, 219–225. 10.1098/rspb.1994.0073.

29. Stoerig, P., and Cowey, A. (1992). Wavelength discrimination in blindsight. Brain *115*, 425–444. 10.1093/brain/115.2.425.

30. Lamme, V.A.F. (2001). Blindsight: the role of feedforward and feedback corticocortical connections. Acta Psychol (Amst) *107*, 209–228. 10.1016/S0001-6918(01)00020-8.

31. Pascual-Leone, A., and Walsh, V. (2001). Fast backprojections from the motion to the primary visual area necessary for visual awareness. Science (1979) *292*, 510–512. 10.1126/science.1057099.

32. Zeki, S., and ffytche, D. (1998). The Riddoch syndrome: insights into the neurobiology of conscious vision. Brain *121*, 25–45. 10.1093/brain/121.1.25.

33. Weiskrantz, L. (1998). Blindsight: A Case Study and Implications (Clarendon).

34. Cowey, A. (2010). The blindsight saga. Exp Brain Res *200*, 3–24. 10.1007/s00221-009-1914-2.

35. Sahraie, A., Weiskrantz, L., Barbur, J.L., Simmons, A., Williams, S.C.R., and Brammer, M.J. (1997). Pattern of neuronal activity associated with conscious and unconscious processing of visual signals. Proceedings of the National Academy of Sciences *94*, 9406–9411. 10.1073/pnas.94.17.9406.

36. Stein, T., Kaiser, D., Fahrenfort, J.J., and van Gaal, S. (2021). The human visual system differentially represents subjectively and objectively invisible stimuli. PLoS Biol *19*, e3001241. 10.1371/journal.pbio.3001241.

37. Peters, M., and Lau, H. (2015). Human observers have optimal introspective access to perceptual processes even for visually masked stimuli. Elife *4*. 10.7554/eLife.09651.

38. Snodgrass, M., Bernat, E., and Shevrin, H. (2004). Unconscious perception: a model-based approach to method and evidence. Percept Psychophys *66*, 846–867. 10.3758/BF03194978.

39. Schmidt, T. (2015). Invisible stimuli, implicit thresholds: why invisibility judgments cannot be interpreted in isolation. Adv Cogn Psychol *11*, 31–41. 10.5709/acp-0169-3.

40. Overgaard, M., Fehl, K., Mouridsen, K., Bergholt, B., and Cleeremans, A. (2008). Seeing without seeing? Degraded conscious vision in a blindsight patient. PLoS One *3*, e3028. 10.1371/journal.pone.0003028.

41. Mazzi, C., Bagattini, C., and Savazzi, S. (2016). Blind-sight vs. degraded-sight: different measures tell a different story. Front Psychol *7*, 1–11. 10.3389/fpsyg.2016.00901.

42. Weiskrantz, L., Barbur, J.L., and Sahraie, A. (1995). Parameters affecting conscious versus unconscious visual discrimination with damage to the visual cortex (V1). Proceedings of the National Academy of Sciences *92*, 6122–6126. 10.1073/pnas.92.13.6122.

43. ffytche, D.H., and Zeki, S. (2011). The primary visual cortex, and feedback to it, are not necessary for conscious vision. Brain *134*, 247–257. 10.1093/brain/awq305.

44. Overgaard, M. (2011). Visual experience and blindsight: a methodological review. Exp Brain Res *209*, 473–479. 10.1007/s00221-011-2578-2.

45. Kentridge, R.W. (2015). What is it like to have type-2 blindsight? Drawing inferences from residual function in type-1 blindsight. Conscious Cogn *32*, 41–44. 10.1016/j.concog.2014.08.005.

46. Macpherson, F. (2015). The structure of experience, the nature of the visual, and type 2 blindsight. Conscious Cogn *32*, 104–128. 10.1016/j.concog.2014.10.011.

47. Phillips, I. (2021). Blindsight is qualitatively degraded conscious vision. Psychol Rev *128*, 558–584. 10.1037/rev0000254.

48. Mazzi, C., Savazzi, S., and Silvanto, J. (2019). On the "blindness" of blindsight: what is the evidence for phenomenal awareness in the absence of primary visual cortex (V1)? Neuropsychologia *128*, 103–108. 10.1016/j.neuropsychologia.2017.10.029.

49. Brogaard, B. (2011). Are there unconscious perceptual processes? Conscious Cogn *20*, 449–463. 10.1016/j.concog.2010.10.002.

50. Foley, R. (2015). The case for characterising type-2 blindsight as a genuinely visual phenomenon. Conscious Cogn *32*, 56–67. 10.1016/j.concog.2014.09.005.

51. Weiskrantz, L., Cowey, A., and Barbur, J.L. (1999). Differential pupillary constriction and awareness in the absence of striate cortex. Brain *122*, 1533–1538. 10.1093/brain/122.8.1533.

2.

Neural Patterns of Conscious Visual Awareness in the Riddoch Syndrome

The Riddoch syndrome refers to a phenomenon in which patients blinded by cortical lesions to their primary visual cortex (V1) can consciously perceive visual motion in their blind field. Previous brain imaging studies have shown that motion perception in such patients, whether conscious or not, always correlates with activity in V5, a cortical area known to process visual motion. The goal of this work was to establish whether neural patterns emerge in V5 specifically during conscious visual experience. We used psychophysics and multimodal magnetic resonance imaging in patient ST who was cortically blinded by a lesion in V1. Structural MRI and tractography confirmed that ST's V5 is intact and receives direct subcortical input. Using functional MRI, we found that decodable neural patterns emerge in V5 only during conscious visual motion perception. We also observed a phenomenon that is diametrically opposed to "blindsight", which we refer to as gnosanopsia, namely the presence of very high perceptual certainty despite chance performance in the discrimination of the direction of motion, a phenomenon accompanied by inferior frontal gyrus activity, and the appearance of post-stimulatory visual hallucinations in the patient's blind field, with hippocampal activity as a correlate. These results thus reveal experience-dependent neural networks and demonstrate the rich perceptual experiences that cortically 'blind' patients can have, which can inform us about multiple facets of consciousness.

This chapter overlaps significantly with published work:

Beyh, A.*, Rasche, S. E.*, Leff, A., ffytche, D., & Zeki, S. (2023). Neural patterns of conscious visual awareness in the Riddoch syndrome. *Journal of Neurology*, 1-12. https://doi.org/10.1007/s00415-023-11861-5

2.1 INTRODUCTION

The Riddoch syndrome refers to the phenomenon that patients blinded by lesions in their primary visual cortex (V1) can have a crude but conscious experience of some visual stimuli, prominent amongst which is visual motion. Imaging studies of such patients [1–4] led to two conclusions that form the basis of this chapter. The first is that the conscious experience of visual motion always correlates with activity in V5, an area of the visual brain that is specialised for the processing of visual motion [5,6]; but to be perceived consciously the moving visual stimuli must have certain characteristics, namely be fast moving, be of high contrast, and of low spatial frequency [1,7]. The second conclusion is that moving visual stimuli that are not perceived consciously also result in weaker but detectable activity within V5 [1,7].

This led to the question of what the minimal conditions are for conscious visual experience; what is it that dictates a quantitative difference in V5 activity between two states, one in which the patient is conscious of the visual stimulus and its direction of motion, and another in which they are not and can only discriminate motion direction at chance levels?

Two main possibilities, not necessarily exclusive of each other, presented themselves: that the heightened activity is due to the more intense response of cells that are engaged in the conscious perception of visual motion, or that the conscious perceptual state entails the recruitment of an additional population of cells; in the latter instance, the spatial arrangement of activity in V5 should be different in the conscious state. We favoured the latter hypothesis and conjectured that decodable patterns within V5 will only emerge during the conscious experience of visual motion.

This hypothesis was tested in patient ST (not his real initials) who developed an incomplete right homonymous hemianopia, denser in the lower field, following a left posterior cerebral artery stroke that damaged his V1; we assessed him using psychophysics, as well as structural, functional, and diffusion MRI. The results confirmed our main hypothesis – that patterns emerge in V5 only during conscious visual experience – and also led to a more detailed study of a phenomenon that is the opposite of "blindsight", namely the presence of high perceptual certainty despite chance performance [1], leading to the involvement of areas implicated in conflict resolution.

Equally important and previously unreported is the appearance of post-stimulatory visual hallucinations in a patient's blind field, with hippocampal activity as a correlate.

2.2 METHODS

2.2.1 Patient

ST was referred to the study via a specialist outpatient visual service run at the National Hospital for Neurology and Neurosurgery in London. He gave informed written consent to participate in the study, which had been approved by the Yorkshire & The Humber - South Yorkshire Research Ethics Committee (NHS Health Research Authority) and UCLH/UCL Joint Research Office (protocol number 137605).

2.2.2 Visual-motion task

To establish the characteristics of the visual stimulus that ST could perceive consciously, an achromatic checkerboard stimulus was used which varied in spatial frequency (0.3 or 1.4 cycles/°), contrast (20% or 80%) and speed (1 or 8 °/second), resulting in eight different stimuli. It moved either upward or downward on each trial. Blank trials during which no stimulus was presented were also included to assess ST's baseline response to the task. The checkerboard was confined to the lower right portion of his visual field (7° below the horizontal meridian and 7° to the right of the vertical meridian) and subtended 12° in width and 5° in height (Figure 2.1). Its edges were blurred to avoid a sharp boundary between it and the surrounding grey background, and its mean luminance was matched to that of the background. The task was programmed in PsychToolbox 3 [8], running in Matlab (MathWorks, Natick, MA).

2.2.3 Procedure for psychophysical testing

ST viewed the stimuli at a 60 cm distance while seated and resting his chin on a support. First, we confirmed the extent of the blind field as revealed by perimetry with the use of a laser pointer. ST was asked to indicate whether he saw a red dot appear on the screen while fixating on a cross at the centre of the screen. Next, we conducted a 2×2×2 design; he was presented with an achromatic checkerboard with either low or high speed (1 or 8 °/s), contrast (20% or 80%) and spatial frequency (0.3 or 1.4 cycles/°). Blank trials (no stimulus) were also included. Each run contained four trials of each combination and six

blanks. Six runs of 38 trials were completed, amounting to a total of 24 trials per condition and 36 blanks (228 total trials).

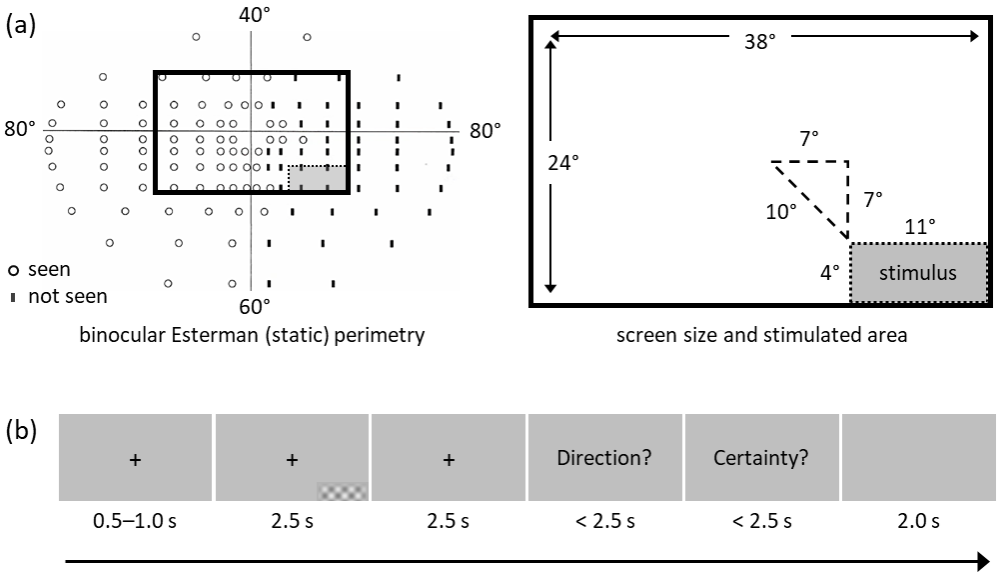

Figure 2.1. Visual field assessment and visual-motion task.
(a) Visual field assessment delineating ST's blind field, and the area in which the stimulus was displayed during the experiment. This part was chosen to ensure that the stimulus did not encroach on the spared parts of the field near the horizontal and vertical meridians. **(b)** The task that ST performed during the psychophysics and imaging experiments. After a short cue, a stimulus appeared for a maximum duration of 2.5 s in ST's blind field. The stimulus was a drifting achromatic checkerboard that varied in spatial frequency (0.3 or 1.4 cycles/°), contrast (20% or 80%), and speed (1 or 8 °/second), resulting in eight different stimuli. Blank trials, in which no stimulus was presented, were also included. The patient was then asked to indicate in which direction the checkerboard had moved (upward or downward) in a forced-choice manner, and to indicate his level of certainty about the answer on a three-point scale. The time under each frame indicates its duration.

Figure 2.1 shows a schematic of the task. Each trial started with a cue (fixation cross) that lasted for 0.5-1.0 s. Next, the stimulus appeared and lasted for a total duration of 2.5 s, including 0.5 s of fade-in and 0.5 s of fade-out, followed by a rest period of 2.5 s. Then, two questions were presented sequentially: the first asked ST to report the direction of motion and the second asked ST about his level of certainty. Using a keyboard, ST indicated the direction of motion in a two-alternative forced choice (2AFC, up or down) paradigm and his certainty (awareness) on a three-point scale, 1 corresponding to "complete guess", 2 to "I think I saw motion, but I am not sure of its direction", and 3 to "very certain of the direction". The maximum time allowed to respond to each question

was 2.5 s, but the task moved on as soon as a response was recorded. Finally, a blank screen (grey background without a fixation cross) was displayed for 2.0 s as a rest period between trials.

2.2.4 Statistical analysis

Performance

ST's accuracy on the motion direction discrimination task was calculated as the percentage of correct trials. For instance, for a given condition (e.g., low frequency, high speed, high contrast), accuracy, A, was calculated as:

$$A = \frac{N_{correct}}{N_{correct} + N_{incorrect}} \times 100 \qquad (eq. 1)$$

Given that the direction response had two possible outcomes only with equal probability (50% each), we used the binomial distribution based on the appropriate number of responses (trials) to determine whether accuracy was significantly above chance for a given task condition.

Certainty

To ease the interpretation of the certainty scores, which were collected on a three-point scale, each trial's certainty score was converted to a percentage value as follows:

$$C_{perc} = \frac{C - 1}{2} \times 100 \qquad (eq. 2)$$

where C is the original score obtained on the three-point scale (values between 1 and 3), and C_{perc} is the certainty score in percentage terms. Therefore, C_{perc} = 0% would indicate the lowest certainty possible (i.e., complete guess), C_{perc} = 50% would indicate moderate certainty, and C_{perc} = 100% would indicate the highest level of certainty.

Metacognitive Sensitivity

Finally, the degree of correspondence between certainty and performance (metacognitive sensitivity) on a trial-by-trial basis was calculated using a type 2 receiver operating characteristic (Type 2 ROC) analysis obtained from Fleming & Lau [9]. A value of 0.5 indicates chance performance, i.e., the certainty level of the patient does not discriminate between correct and incorrect trials. A higher value indicates greater

sensitivity, meaning that the patient is able to distinguish correct responses from incorrect ones.

2.2.5 Procedure for testing during the imaging session

Based on the results of the initial psychophysics session, ST performed the visual-motion task while undergoing brain imaging. The task was divided into four runs; during each, the eight stimuli were presented five times randomly, in addition to five blank trials. This amounted to 45 trials per run, or 180 trials in total, with each stimulus (including blanks) being presented 20 times. During each trial, ST indicated the direction of motion with his right hand and his certainty with his left hand using a customised button-box.

2.2.6 Imaging acquisition

Structural, functional, and diffusion MRI data was acquired on a 3T Siemens Prisma scanner (Siemens Healthcare GmbH, Erlangen, Germany) with a 64-channel head coil. The structural images were based on a 3D magnetisation-prepared accelerated gradient echo (MPRAGE) sequence: repetition time (TR) = 2.53 ms; echo time (TE) = 3.34 ms; flip angle = 7°; matrix of 256×256; field of view = 256 mm; voxel size = 1×1×1 mm^3.

fMRI data was based on the BOLD signal, measured with a 2D T2*-weighted Echo Planar Imaging (EPI) sequence: volume TR = 3360 ms; TE = 30 ms; flip angle = 90°; ascending acquisition; matrix of 64×64; voxel size = 3×3×3 mm^3; 48 slices. A total of four fMRI runs were acquired. Field mapping images were also acquired using a dual-echo gradient echo sequence to assist with susceptibility distortion correction.

Diffusion MRI data was based on a 2D spin-echo EPI sequence: TR = 3500 ms; TE = 61 ms; flip angle = 88°; matrix of 110×110; voxel size = 2×2×2 mm^3; 72 slices; multiband factor of 2; in-plane acceleration factor of 2. Images were acquired with three diffusion shells: 30 diffusion directions at b = 500 $s{\cdot}mm^{-2}$, 60 directions at b = 1500 $s{\cdot}mm^{-2}$, and 90 directions at b = 2500 $s{\cdot}mm^{-2}$. Additionally, 16 b = 0 $s{\cdot}mm^{-2}$ were interleaved throughout the acquisition, and seven b = 0 $s{\cdot}mm^{-2}$ volumes were acquired with the reverse phase encoding polarity to correct for susceptibility distortions.

2.2.7 T1w MRI pre-processing

The T1w image was skull-stripped using *optiBET* [10], bias field corrected using the *N4* tool [11], and rigidly aligned, using *flirt* [12], to the 1 mm MNI T1w brain template [13] as a substitute for AC-PC alignment. This aligned image served as the anatomical reference for subsequent pre-processing and analysis steps. Additionally, the T1w image was normalised to the MNI template through affine and diffeomorphic non-linear transformations (SyN algorithm) computed with ANTs [14]. A manually delineated lesion mask was used to exclude the lesioned tissue during the normalisation step.

2.2.9 fMRI pre-processing

The fMRI images were corrected for motion and slice-timing differences using *SPM12* (http://www.fil.ion.ucl.ac.uk/spm/software/). The corrected images were then simultaneously corrected for geometric distortions (based on the acquired field map) and aligned to the T1w image using FSL's *epireg* tool [12,15], while maintaining the voxel size at 3×3×3 mm^3. This produced the final fMRI time series images that were used in subsequent analyses.

2.2.8 Diffusion MRI pre-processing

Raw diffusion weighted imaging (DWI) data was first corrected for noise and Gibbs ringing artefacts [16,17]. A magnetic susceptibility field was then calculated using *topup* [18] based on b = 0 $s{\cdot}mm^{-2}$ images acquired with opposite phase-encoding. All images were subsequently corrected for motion and eddy current distortions using *eddy* [19] with outlier (signal dropout) slice replacement [20], incorporating the *topup* field into this step. The anisotropic power map was derived from the pre-processed data using StarTrack (www.mr-startrack.com) and used to calculate a rigid affine transformation (six degrees of freedom) to the T1w image with *flirt*. The rigid transformation was then applied to the diffusion data (kept at a 2 mm voxel size) with a spline interpolation to produce the final set of pre-processed images. The diffusion gradients were also rotated at this stage using the same transformation matrix.

2.2.10 Univariate fMRI analysis

Various categorical comparisons were performed to assess the activity related to different perceptual and certainty states. Each combination of factors of the 2×2×2 design

was considered as a separate condition. In addition, As ST reported moderate to high levels of certainty on nearly half the blank trials, indicating that he had seen something moving, we decided to divide the blank trials into two separate conditions: "low-certainty blanks" included trials receiving a rating of 1 (i.e., total guess), and "high-certainty blanks" included trials receiving a rating of 2 or 3 (i.e., somewhat to very certain).

For the univariate analysis, the BOLD time series images were spatially smoothed with a Gaussian kernel of a full width at half maximum (FWHM) of 4.5 mm. The time series were entered into a GLM in *SPM12* with a single task effect (stimulus presentation) and the six motion correction parameters as nuisance regressors. A contrast image was generated to compare each condition with the low-certainty blank condition, and this contrast was entered into a t-test to assess its statistical significance at each voxel. All resulting statistical images were thresholded at a voxelwise significance level of $p < .001$.

2.2.11 Representational similarity analysis

For the multivariate analysis, the BOLD time series were first entered into a GLM in *SPM12,* without any spatial smoothing, with a single task effect (stimulus presentation) and six motion correction parameters as nuisance regressors. Each trial was modelled as a separate condition, thereby generating a parameter estimate (beta image) for every trial.

To investigate whether certainty in perceiving the motion direction of a stimulus in the blind field was accompanied by specific spatial patterns of neural activity, we used representational similarity analysis (RSA) [21]. The 20 beta maps of each condition and the nine beta maps of the low-certainty blank trials were selected and a whole-brain searchlight analysis was performed using cubic regions of interest (ROI) of 3×3×3 voxels. For each searchlight ROI, the Pearson correlation distance, *d*, was calculated between the neural patterns associated with these trials, for each pair of trials, as follows:

$$d = \frac{1 - r}{2} \qquad (eq. 3)$$

where r is the Pearson correlation coefficient; the division by two was performed to rescale d to the range [0-1]. This was done to simplify the interpretation and visualisation of the metric: $d = 0.0$ corresponds to a full correlation between the neural patterns of two

trials (i.e., r = 1.0); d = 0.5 corresponds to the absence of any correlation (i.e., r = 0.0); and d = 1.0 corresponds to the two trials having opposed (anti-correlated) patterns (i.e., r = -1.0).

Once the Pearson distances were calculated for each pair of trials, neural representational dissimilarity matrices (RDMs) were generated to capture the (dis)similarity between pairs of trials in each searchlight ROI. The Pearson correlation distance is mainly sensitive to the spatial pattern of brain activity and is insensitive to the overall BOLD signal amplitude change in a given ROI [21]. Given that the aim here was to find a specific pattern of activity regardless of amplitude, the Pearson correlation distance is the preferred distance metric for our purposes (unlike, e.g., the Euclidean distance which would also record overall magnitude changes like the univariate framework) [21].

To test whether the similarity was significant only for the trials of a given condition (and not for those of the low-certainty blanks), the neural RDM of each searchlight ROI was compared with a model RDM (Figure 2.2). The correlation between the neural and model RDMs was assessed with the Spearman rank correlation, using only the elements in the lower triangle of the RDMs (excluding the diagonal).

For a given condition, the model RDM (Figure 2.2) assumed a high similarity in the activity patterns associated with the trials of that condition (i.e., d = 0.0), and no similarity for the trials of the low certainty blanks, or between the patterns of that condition and those of the low certainty blanks (i.e., d = 0.5). No pairs of trials were expected to have anti-correlated patterns (i.e., d = 1.0) as this would be a strong assumption to make. This type of model was chosen instead of one that contains all conditions simultaneously, as the latter makes more assumptions about the relationships between all conditions in each searchlight ROI.

The searchlight map was thresholded at $p < 0.001$. Clusters of interest in each condition as revealed by the searchlight analysis were selected for exploratory reasons to examine whether other conditions also showed pattern similarity in these areas.

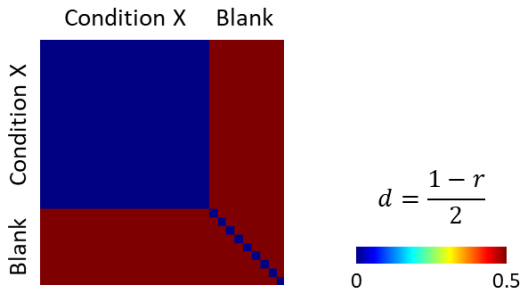

Figure 2.2. Model RDM for RSA.
The model representational dissimilarity matrix (RDM) used for the representational similarity analysis (RSA). The model, which represents the Pearson correlation distance shown on the right, assumes a similar spatial activity pattern for trials of a given condition and no similar pattern for the trials of the low-certainty blank condition, nor a similar pattern between the given condition *and* the low-certainty blank condition.

2.2.12 Tractographic reconstruction

The diffusion data was used to reconstruct the optic radiations connecting ST's lateral geniculate nucleus (LGN) to area V5 of his visual cortex. The data was modelled with spherical deconvolution based on the damped Richardson-Lucy algorithm [22,23] in StarTrack, according to the following parameters: fibre response $\alpha = 1.5$; number of iterations = 350; amplitude threshold $\eta = 0.0015$; geometric regularisation $\nu = 16$.

A probabilistic dispersion tractography approach was conducted to explore the full profile of the fibre orientation distribution function (fODF) in each voxel. This approach follows the principal fibre orientations indicated by the fODF local maxima, as well as the directions captured by other vertices of the fODF that convey information about various local fibre orientations [23]. Fibre tracking was performed according to the following parameters: minimum HMOA threshold = 0.0025; number of seeds per voxel = 2000; maximum angle threshold = 40°; minimum fibre length = 50 mm; maximum fibre length = 150 mm. This was done using a seed region of interest in the LGN obtained from a published atlas [24]. The resulting tractogram was imported into TrackVis (http://trackvis.org/) where manual cleaning was performed and streamlines terminating in V5 were selected. For the along-tract microstructural analysis, each streamline was divided into 100 equal segments between its LGN and V5 terminations, and the mean HMOA value of all streamlines was calculated for each segment along with the 95% confidence interval.

2.3 RESULTS

2.3.1 Visual assessment of patient ST

ST is a male in his early fifties who experienced a posterior cerebral artery ischaemic stroke resulting in partial loss of vision in his right visual field. Despite this, he showed signs of residual visual processing of motion in his blind field during clinical testing, suggesting that he fits the description of a Riddoch syndrome patient.

Automated, static, binocular Esterman perimetry confirmed that ST was blind in a large portion of his right visual field with sparing of some portions along the meridians (Figure 2.1). He described the visual disturbance not as a static blackness, but more like a persistent migraine aura that is permanently 'flickering' in his lower right visual field and he insisted that he could distinguish this flicker from motion. He reported seeing shapes and colours in an unclear and fuzzy manner, which he described as a 'flickering smudge'. We confirmed his report with psychophysical testing in the lab, where he was unable to detect static bright dots of various sizes presented in his perimetrically blind field but saw the same dots when they moved quickly.

2.3.2 Behavioural results

During the imaging session, ST was very good at discriminating the direction of motion when the checkerboard had specific properties, most prominently low spatial frequency (Figure 2.3 and Table 2.1). Specifically, he performed perfectly (100% accuracy) when contrast and speed were high and spatial frequency was low, but he also performed very well with other combinations of contrast and speed as long as the spatial frequency was low (84% accuracy with all low frequency conditions combined). Conversely, his performance was at chance level when presented with high spatial frequency checkerboards, although there were indications during the psychophysics session that he could occasionally reach above-chance levels of performance with such stimuli (Table 2.1). Notably, his certainty level was very high (83% ± 17%) whenever he was presented with a high speed, high contrast and high spatial frequency stimulus, despite performing at chance, which made this condition of special interest, because it suggested a conscious experience with poor discrimination, i.e., the reverse of blindsight. Another interesting results was that on about half of the blank trials (no stimulus) ST reported

moderate-to-high certainty in correctly discriminating the direction of motion of the absent visual stimulus (Figure 2.4 and Table 2.1).

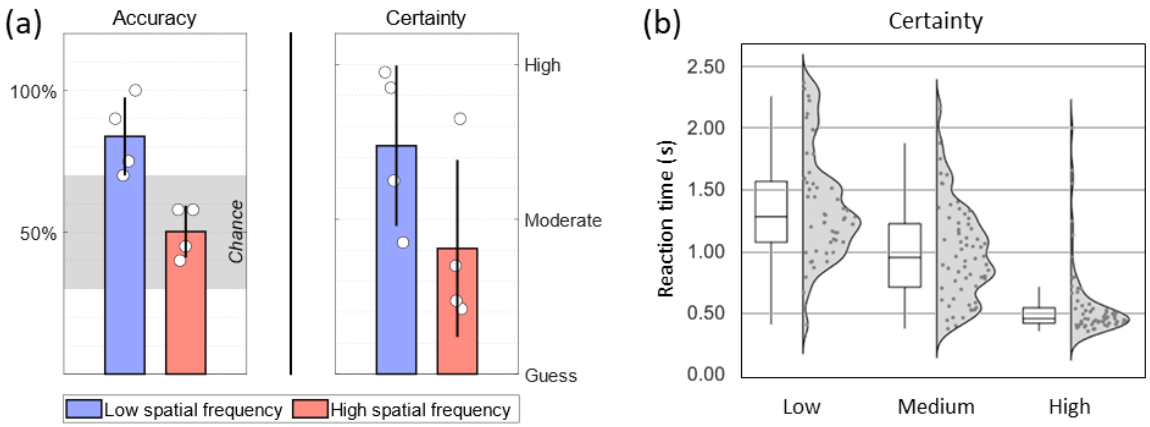

Figure 2.3. Behavioural results from the visual-motion task during the MRI session. **(a)** ST's performance was highly influenced by the spatial frequency of the checkerboard stimulus: he performed very well with low-frequency checkerboards but his performance was at chance with high frequency ones. The bars represent the mean accuracy and certainty scores separately for the low and high frequency conditions; the white dots represent the average scores of each condition. The shaded grey area in the accuracy plot indicates the 95% confidence interval of chance performance based on the binomial distribution for 20 trials. **(b)** ST's reaction time to report the direction of motion during the fMRI task. A Spearman rank correlation between reaction time and certainty was strong (r_s = -0.69, p < .0001), indicating that higher certainty correlated with faster responses.

Higher certainty also correlated with faster responses; we observed a strong negative correlation between certainty and reaction time (r_s = -0.69, p < .0001; Figure 2.3). This suggests that ST's subjective report of certainty was consistent with his experience and could therefore be used as a meaningful metric.

Behavioural results				
	Low spatial frequency (LF)		**High spatial frequency (HF)**	
Psychophysics session				
	Low contrast (LC)	**High contrast (HC)**	**Low contrast (LC)**	**High contrast (HC)**
Low speed (LS)	A: 75%*, C: 79%	A: 92%*, C: 92%	A: 50%, C: 48%	A: 83%*, C: 75%
High speed (HS)	A: 92%*, C: 94%	A: 96%*, C: 92%	A: 79%*, C: 52%	A: 63%, C: 84%

MRI session				
	Low contrast (LC)	**High contrast (HC)**	**Low contrast (LC)**	**High contrast (HC)**
Low speed (LS)	A: 70%*, C: 43%	A: 75%*, C: 63%	A: 55%, C: 21%	A: 40%, C: 35%
High speed (HS)	A: 90%*, C: 93%	A: 100%*, C: 98%	A: 55%, C: 24%	A: 45%, C: 83%

Table 2.1. Behavioural results during the psychophysics and MRI session.
Accuracy and certainty scores in visual motion direction discrimination for stimuli varying in contrast, speed and frequency. A represents accuracy and C represents the average certainty rating in percentages. For the blank condition, certainty was 30% on average for both sessions. *Significantly different from chance performance ($p < .05$) determined from the binomial distribution.

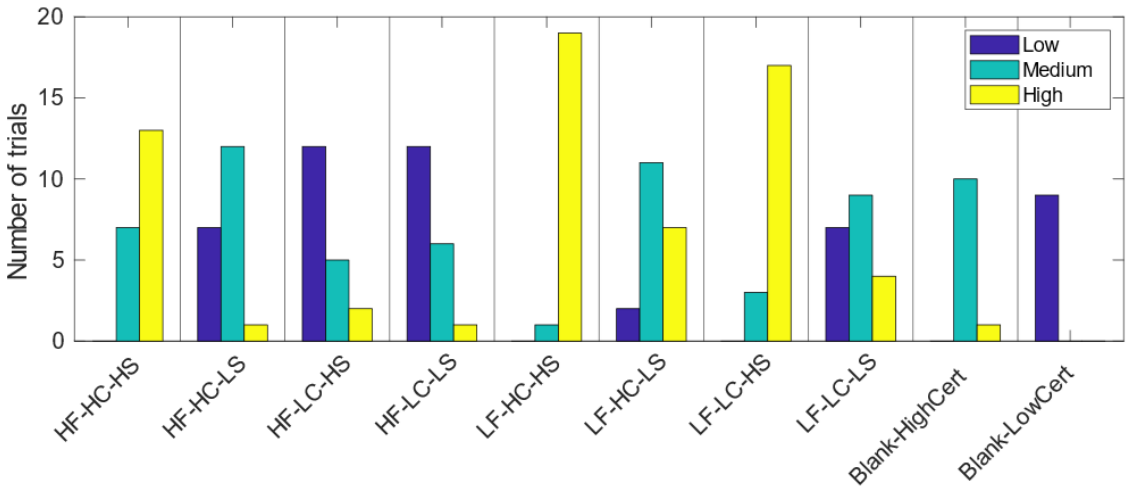

Figure 2.4. Certainty ratings across conditions.
The plots show the distribution of ST's certainty ratings for each condition. The names of the conditions along the x-axis describe the stimulus properties. For example, LF-HC-HS corresponds to stimuli with low spatial frequency (LF), high luminance contrast (HC), and high speed (HS). Blanks are shown here as two conditions to highlight the difference between high and low certainty blank trials, which was the basis of how we defined the *Hallucinated* condition and the true *Blank* condition.

Finally, the degree of correspondence between certainty and accuracy on individual trials (metacognitive sensitivity [9]) differed per condition. As expected, a type 2 ROC analysis revealed that metacognitive sensitivity was 0.50 when ST did not perceive the stimulus (high spatial frequency, low contrast, low speed condition), indicating that ST could not discriminate between correct and incorrect responses, thereby further supporting that he was completely blind to these stimuli. When ST perceived the stimulus, metacognitive sensitivity was 0.79, suggesting that although some information was lost, he was able to reliably distinguish between correct and incorrect judgements. His sensitivity was 0.68

for trials in which he was highly certain yet performance at chance (high spatial frequency, high contrast, and high speed condition), indicating that there was a degree of 'blind insight' [25], that is, in this condition he was more certain on correct trials and less so on incorrect ones, even though his performance was at chance.

When ST's performance is plotted on a psychophysical model adopted from Zeki and ffytche [1], it becomes apparent that his perceptual states, induced by the different stimuli, largely fall along the expected continuum between blindness and conscious vision. This further supports the observation that his experience (certainty) and accuracy are closely linked (Figure 2.5).

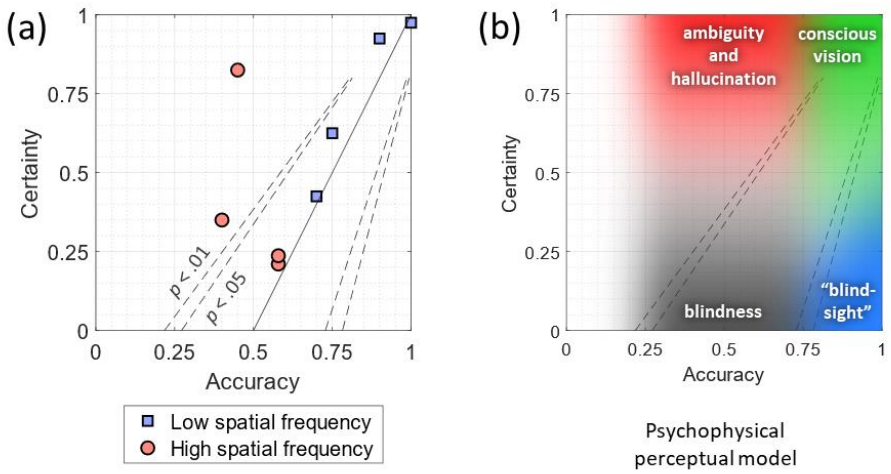

Figure 2.5. Psychophysical model and behavioural results.
(a) The solid line represents a psychophysical model that assumes that certainty and accuracy are strongly linked; the dashed lines represent the boundaries of the model under the binomial distribution at $p < .05$ and $p < .01$, calculated for 20 trials per condition. ST's certainty was congruent with accuracy, except for one strong departure from this trend where he thought he performed very well but was in fact performing at chance level. **(b)** Various perceptual states placed within the same psychophysical model, showing that ST's perceptual states largely follow the continuum between blindness and conscious vision, with occasional departures toward ambiguity and hallucination.

2.3.3 Lesion extent and white matter input to V5

Structural T1w images revealed that ST had a circumscribed lesion (7.27 millilitres in volume) confined to his medial occipital lobe, affecting the calcarine sulcus and pericalcarine grey and white matter (Figure 2.6). Area V1 was the most affected, but tissue near the occipital pole (subserving central vision) was spared. The surrounding area V2 may also have been affected in part. The lesion extended more into the cuneus than the lingual gyrus and did not approach the locations of areas V3 and V4 ventrally, nor that of V3 dorsally. Importantly, the lesion did not include area V5.

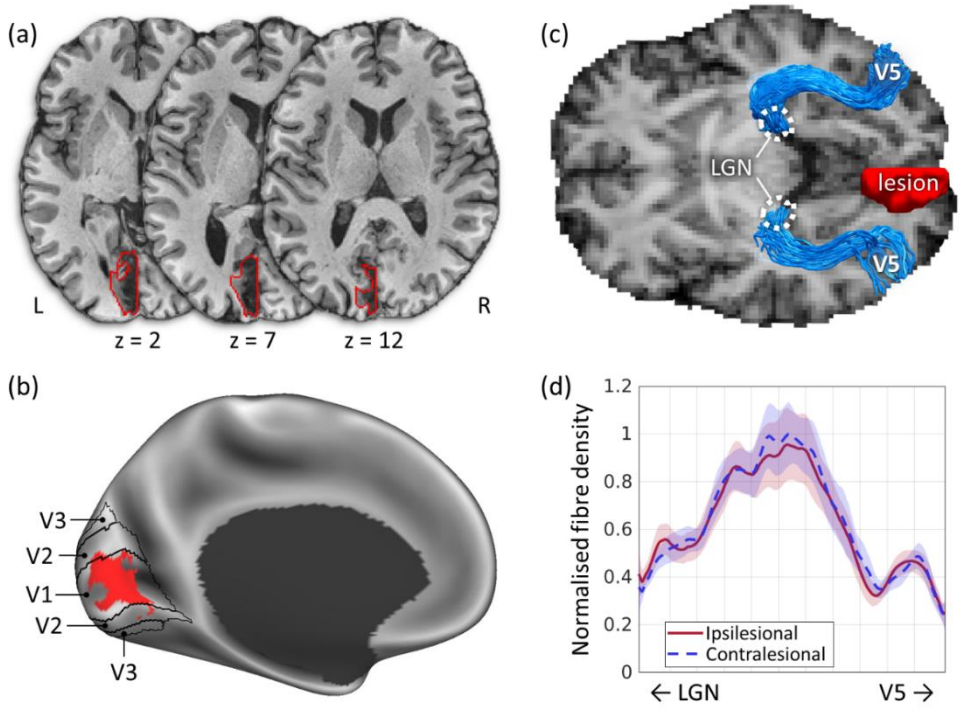

Figure 2.6. ST's lesion extent and reconstructed optic radiations terminating in V5. **(a)** Axial slices through ST's T1w structural image showing that the lesion (red contour) was confined to V1 and did not extend laterally to affect V5. **(b)** The lesion displayed on a canonical brain surface, showing the full extent of its cortical reach. The crescent shape within the posterior calcarine sulcus corresponds to the spared visual field along the horizontal meridian in the perimetry plot (Figure 2.1). **(c)** Tractographic reconstruction of the optic radiations connecting the lateral geniculate nucleus (LGN) with area V5, in both hemispheres, displayed against the anisotropic power map derived from the diffusion data. The location of V5 was determined from the fMRI task. **(d)** Microstructural comparison of the LGN-V5 connections in the ipsilesional and contralesional hemispheres based on the hindrance modulated orientational anisotropy (HMOA), a proxy for fibre density. No difference is observed between the two hemispheres, indicating that the direct input from the LGN to V5 has not been compromised in the lesioned hemisphere.

A tractographic reconstruction of the optic radiations confirmed that ST's V5 in the lesioned hemisphere remained directly connected with the lateral geniculate nucleus (LGN), and that the microstructure of these connections was indistinguishable from that in the contralesional hemisphere (Figure 2.6).

2.3.4 Functional imaging results

Various univariate and multivariate analyses were conducted to assess brain activity related to different perceptual states while ST performed the visual-motion fMRI task; here are the four conditions of main interest discussed.

The first condition (*Seen*) represents conscious vision (high accuracy and high certainty); here, the stimulus had a low spatial frequency, high contrast, and high speed. The second condition (*Not seen*) represents blindness, i.e., the inability to consciously perceive a stimulus presented in the blind field (chance discrimination and low certainty); the stimulus in this condition was of high spatial frequency, low contrast, and low speed. The third condition (*Ambiguous*) represents a false sense of confidence that is incongruent with performance (high certainty despite chance discrimination); in this case the stimulus had a high spatial frequency, high contrast, and high speed. Finally, the fourth condition (*Hallucinated*) represents imagined vision, i.e., the experience of seeing a moving stimulus despite none being presented; this condition consisted of blank trials for which ST reported moderate-to-high certainty in discriminating "motion" direction.

Thus, to conduct the univariate and multivariate analyses, the blank trials were divided into those with low and those with moderate-to-high certainty, as only the former can be used as a true 'blank' condition that does not elicit a conscious percept. The latter represented the *hallucinated* condition.

Univariate analyses

The univariate analysis, which compared activity produced by each condition with activity produced by low-certainty blanks (i.e. true blanks), revealed increased activity in V5 during the *Seen* condition. V5 was also active during the *Ambiguous* condition, along with the inferior frontal gyrus (IFG). There was weak but significant bilateral orbitofrontal activation when comparing the *Hallucinated* condition to low-certainty

blanks, and no significant activations for the *Not seen* condition. The univariate results are shown in Figure 2.7 and reported in detail in Table 2.2.

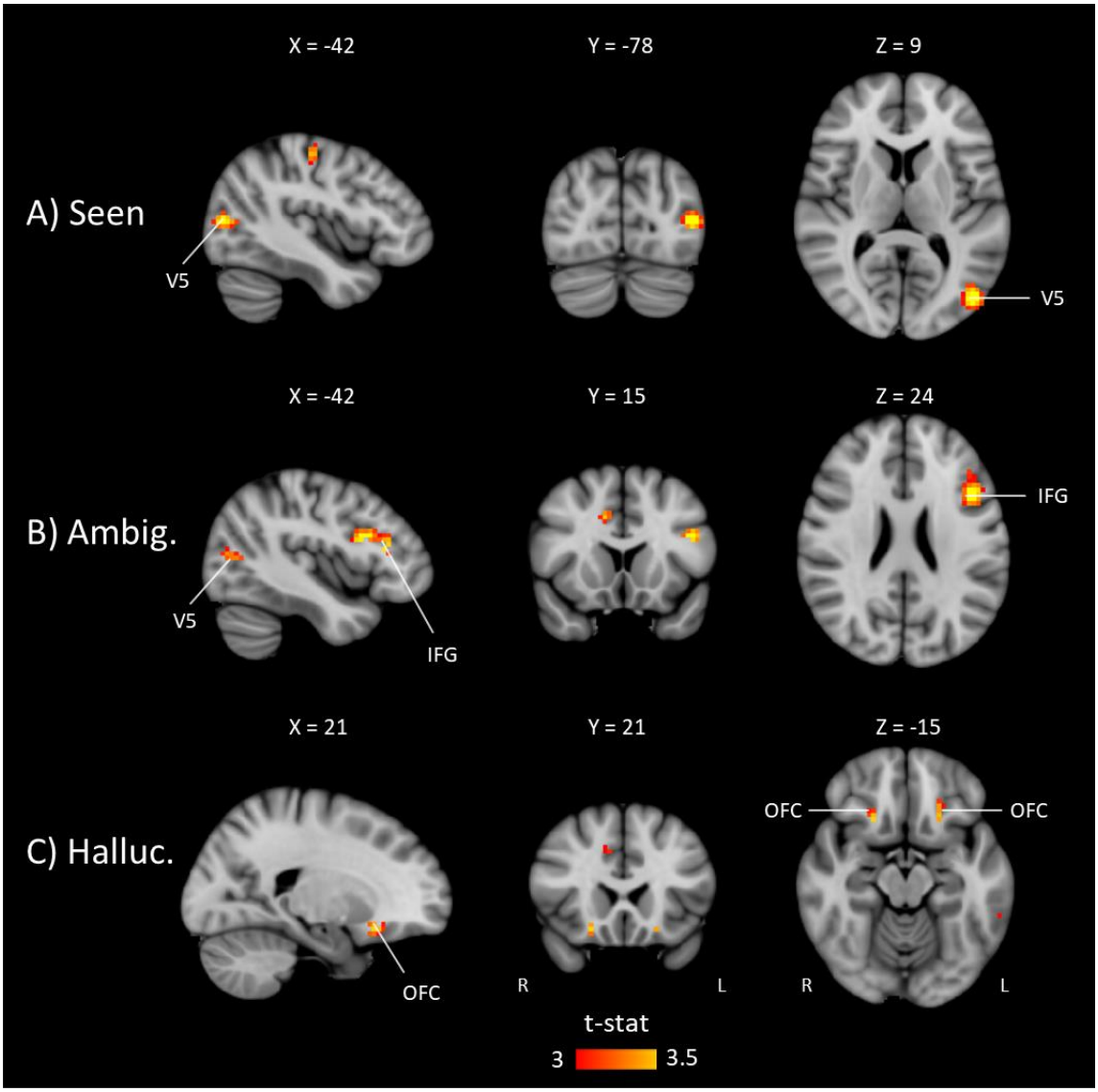

Figure 2.7. Univariate categorical results per condition.
Visual representation of the univariate categorical activations of the A) *Seen* (LF-HC-HS), B) *Ambiguous* (HF-HC-HS), and C) *Hallucinated* (High-certainty blanks) conditions compared with low-certainty blanks. Comparing the *Not Seen* (HF-LC-LS) condition with low-certainty blanks did not reveal any significant univariate activations. The clusters are reported in detail in table 2.2. All results are thresholded at $p < 0.001$ and displayed on the MNI template.

Cluster and/or region	# voxels	*p*	*t*	Coordinates (mm)		
				x	y	z
Low spatial frequency conditions > low-certainty blanks						
L V5	31	0.000	3.48	-48	-78	9
High spatial frequency conditions (not including HF-HC-HS) > low-certainty blanks						
No significant activations.						
LF-HC-HS (Seen condition) > low-certainty blanks						
L V5	38	0.000	3.67	-45	-78	9
L precentral gyrus	35	0.000	3.53	-36	-15	60
HF-LC-LS (Not seen condition) > low-certainty blanks						
No significant activations.						
HF-HC-HS (Ambiguous condition) > low-certainty blanks						
L inferior frontal gyrus (IFG)	66	0.000	3.64	-45	27	18
L IFG		0.000	3.63	-45	15	24
R cingulate gyrus mid-body	11	0.000	3.38	12	15	36
R precentral gyrus	9	0.001	3.31	45	6	33
V5	14	0.001	3.27	-42	-75	12
High-certainty blanks (Hallucinated condition) > low-certainty blanks						
R orbitofrontal cortex	8	0.000	3.41	21	21	-15
L orbitofrontal cortex	9	0.000	3.36	-21	24	-15
R cingulate gyrus mid-body	10	0.001	3.28	12	18	39

Table 2.2. Results of the univariate fMRI analysis.
Various univariate comparisons were performed; for each comparison, the clusters of significant activity are reported with their corresponding peak t-statistic and MNI coordinates. All results are thresholded at $p < 0.001$, and only clusters of five voxels or more are reported.

Multivariate analyses

For the RSA [21], the model assumed that neural patterns would be similar for trials of the same condition (e.g., *Seen*), and different from those of the low-certainty blank trials; it further assumed that the latter would not share a common pattern (Figure 2.2). According to this model, patterns emerged in V5 only when ST reported a high level of certainty, i.e., during the *Seen*, *Ambiguous*, and *Hallucinated* conditions, but not when he was unconscious of the visual stimuli and failed to discriminate motion direction (*Not seen*) (Figure 2.8 and Figure 2.9).

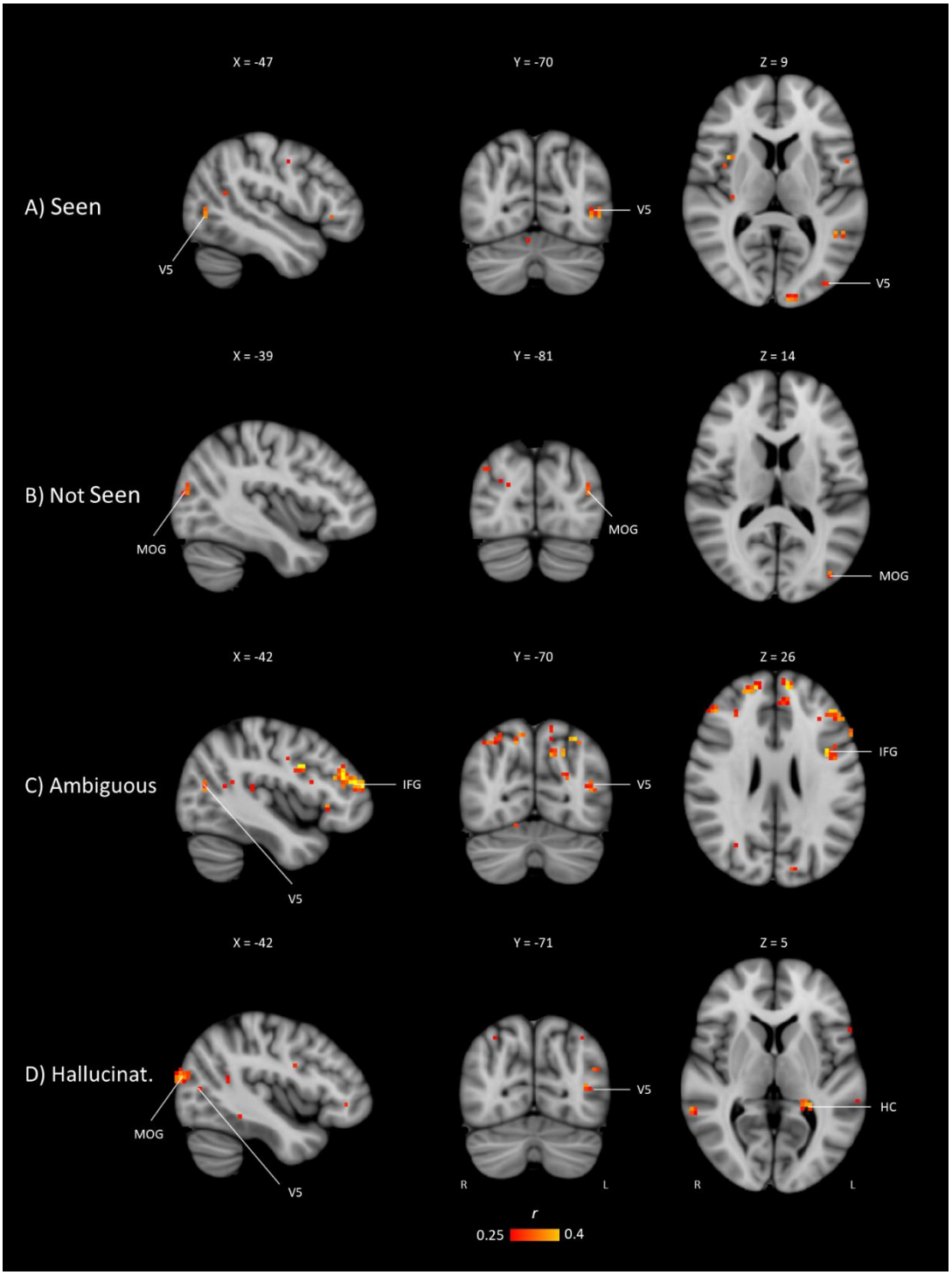

Figure 2.8. RSA searchlight results per condition.
The representational similarity analysis (RSA) searchlight revealed several areas with significant pattern similarity in each condition. In the A) *Seen* condition, there was pattern similarity in V5 and early visual cortex (EVC); B) *Not Seen* stimuli engaged the middle occipital gyrus (MOG) and EVC; C) *Ambiguous* stimuli engaged V5 and the prefrontal cortex, notably the inferior frontal gyrus (IFG); and D) the *Hallucinated* condition was associated with pattern similarity in V5, MOG and the hippocampus (HC). All results are thresholded at $p < 0.001$ and Spearman rank correlations of 0.25 or higher are shown. These searchlight maps were used to select ROIs. The results are shown on the MNI template, and the ipsilesional (left) hemisphere is presented on the right.

Although the main aim was to investigate activity patterns in V5, RSA revealed the involvement of several other regions of interest in the various conditions (Figure 2.8). We therefore also selected for exploratory purposes the early visual cortex (EVC, areas V2/V3), the middle occipital gyrus (MOG), the inferior frontal gyrus (IFG), and the hippocampus (HC) to investigate how similar the activity patterns were in these areas for each condition.

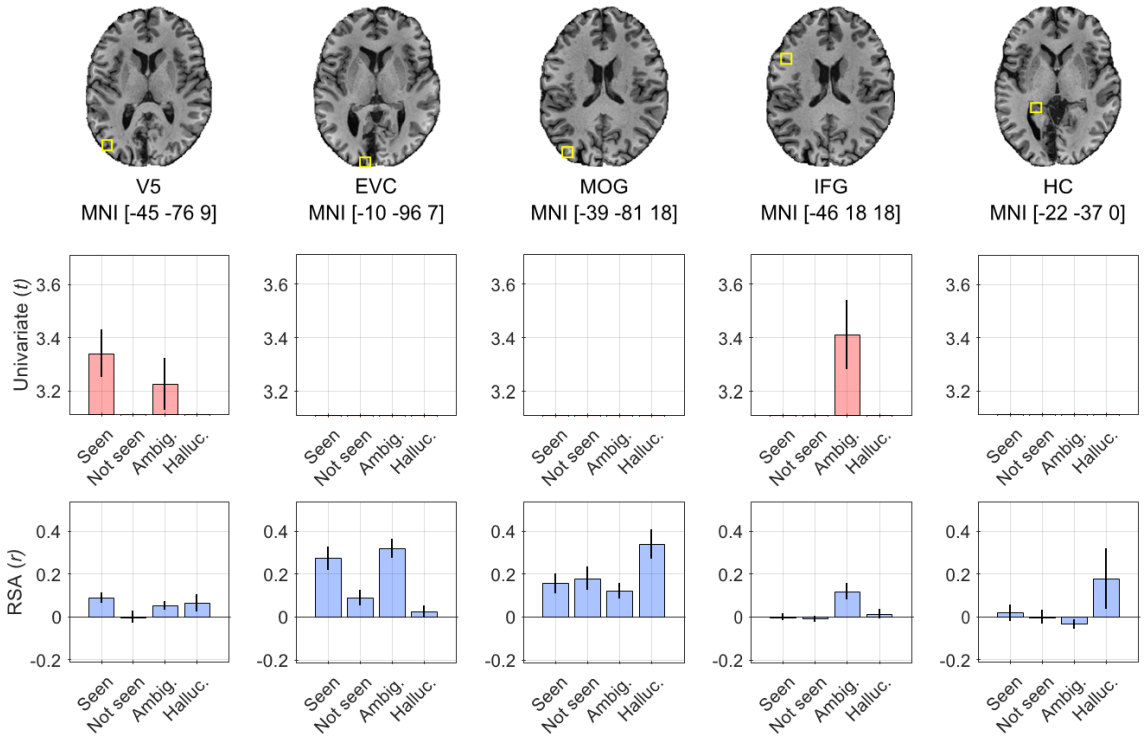

Figure 2.9. Univariate and multivariate activity during the visual-motion task.
Functional MRI during the visual motion task revealed various regions implicated in conscious or unconscious visual motion perception. **(a)** The location (yellow square) and MNI coordinates of each region of interest (ROI) are shown on an anatomical T1w image of ST's brain. The regions are V5, early visual cortex (EVC, V2/V3), middle occipital gyrus (MOG), inferior frontal gyrus (IFG), and the tail of the hippocampus (HC). **(b)** Each panel shows the t-statistic of the change in activity in the corresponding ROI in (a) relative to the 'low-certainty blank' condition from a univariate analysis. **(c)** Each panel here shows the pattern similarity (in Spearman rank correlations) in the same ROIs and for the same conditions as in (b).

We observed patterns in (a) EVC when a stimulus was present, i.e. in the *Seen*, *Not Seen* and *Ambiguous* conditions, regardless of ST's level of certainty; (b) patterns emerged in the MOG for all four conditions; (c) in the IFG only during the *Ambiguous* condition, which is in line with univariate activity in that region; (d) and in the tail of the HC, which showed

strong pattern similarity only during the *Hallucinated* condition (Figure 2.9). This indicates that activity in these regions was too weak to be detectable by the univariate analysis, but its involvement was nevertheless revealed be the pattern analysis. Importantly, these additional areas were only engaged during specific experiences; in other words, their functional connection was experience dependent.

2.4 DISCUSSION

This research began with a simple question and ended up, unexpectedly, on shores we had not intended to visit. We enquired into patient ST who fits the profile of a Riddoch syndrome patient in that, despite becoming hemianopic after a lesion to V1, he retained the ability to perceive visual motion consciously in his blind field. We assessed him using psychophysics and MRI, and obtained a complex set of results that speaks to the neural correlates of various experiential states in the Riddoch syndrome, including conscious visual perception, ambiguity and hallucination, as defined above. Above all, it speaks to the appearance of experience-dependent connections.

A lesion in V1 sparing subcortical input to V5

Structural imaging revealed that ST's lesion is confined to V1 in the left hemisphere, and tractography confirmed that V5 in the same hemisphere receives direct input from the LGN. These findings are in accordance with the expected anatomy of a Riddoch syndrome patient based on previous reports [1,26].

Behavioural determination of conscious awareness of visual motion in the blind field

The stimuli were specifically tailored to create conditions in which ST could discriminate visual-motion direction easily and consciously, and ones in which he is blind to visual motion. Our behavioural results showed that we successfully induced a spectrum of experiential states in ST; they are in agreement with those obtained by Zeki and ffytche [1], with perceptual states largely falling along the continuum between blindness and conscious vision, and with a tight link between performance and awareness (Figure 2.5). Thus, we find no evidence in ST of a dissociation between performance and awareness after V1 damage as described by "blindsight", where a patient can unconsciously discriminate visual-motion direction with high accuracy [27,28]. In fact, several reports have

since shown that such "blindsight" findings can be explained by a methodological bias in how patients are asked about their experience and that discrimination and conscious awareness are very closely related [1,29–32].

The variety of stimuli that we used did, however, induce experiential states associated with the Riddoch syndrome that have not been explored extensively, such as ambiguous and hallucinatory states (Figure 2.5). For example, when the stimulus was of high spatial frequency, high speed, and high contrast, ST reported a high level of certainty despite chance discrimination; and during some blank trials where no stimulus was presented, he reported being moderately to highly certain of discriminating the direction of motion of the non-existent visual stimuli.

Consciously seen motion correlates with decodable neural patterns in V5

When we used stimuli of low spatial frequency, high speed, and high contrast – stimuli associated with good discrimination and conscious awareness – the results of the univariate analysis were straightforward; they showed that there was heightened activity in V5, and the multivariate analysis revealed distinct neural patterns for these stimuli in V5. In addition, though absent in the univariate analysis, presumably because of relatively weak activity, pattern similarity was also found in EVC and the MOG. The patterns in EVC fell at the border between areas V2 and V3; although neither has been shown to be specifically or exclusively involved in visual motion, V2 has been called a "distributor" area because, among its compartments of specialised cells, is one where directionally selective cells are concentrated (the thick cytochrome oxidase stripes) and project anatomically to V5 [33,34]. Further, V3 is largely dominated by magnocellular input, responds to visual motion, and has good concentrations of directionally selective cells in it, ranging from 12% [35] to 40% [36] in the macaque, and has been observed in the human brain to respond to both first and second-order motion [37]. The MOG patterns, on the other hand, can be attributed to its role in categorising visual inputs in general, as has been demonstrated by previous reports [38,39].

V5 activity is an essential complement to consciously seen motion

When the stimulus was of high spatial frequency, low speed and low contrast, it was unperceivable to ST; he was unable to discriminate its motion direction and reported low certainty. These stimuli engage the magnocellular pathway weakly and the parvocellular

one strongly, and thus depend on a healthy V1 or early visual cortex for their perception, rather than on V5; it is therefore not surprising that ST, with his lesion in V1, was unable to perceive these stimuli. Consistent with this, there were no significant univariate activations anywhere in the brain compared with low-certainty blanks. However, we did find some (weak) evidence for pattern similarity for this type of stimulus in the MOG and EVC. Although the role of the MOG may be seen as an attempt to categorise even the weakest visual input, spared EVC, which receives direct subcortical input [40–43], can exhibit very weak but decodable activity that is not sufficient to evoke a conscious percept [44]. Therefore, moving stimuli may give rise to neural activity in medial visual areas, but unless this is associated with V5 activity, they remain unseen by Riddoch syndrome patients.

Furthermore, previous reports on patients [1] and healthy subjects [45,46] have demonstrated that visual motion that is not perceived consciously can activate V5, though to a lesser extent than motion that is seen consciously. Our results do not contradict this; in fact, when the stimulus was of high spatial frequency, low speed but high contrast, it was not consciously perceived by ST and his performance was at chance during the fMRI experiment (Table 2.1), but this condition nevertheless showed univariate V5 activity; however, there were no decodable patterns in it. Therefore, we only observe patterns in V5 in association with consciously perceived motion, even if univariate activity can be detected in it.

High certainty with chance discrimination correlates with activity in the inferior frontal gyrus

A stimulus of high spatial frequency, high speed and high contrast evoked a false sense of certainty in ST; that is, he reported being highly confident in perceiving and correctly discriminating the direction of motion despite his ability to do so remaining at chance. An assessment of metacognitive sensitivity [9] revealed that ST exhibited 'blind insight' [25] during these trials; despite chance performance, he was able to introspectively distinguish between correct and incorrect judgements with greater accuracy than one would expect from chance. We refer to this condition as ambiguous, because there was a certainty which only he perceived [47]; it is a phenomenon strongly reminiscent of *gnosanopsia* [1], i.e., awareness without discrimination. Note that ST's performance was at chance level, indicating that he was not consistent in his imperception; he was not, for

example, consistently reporting the opposite of the correct motion direction, as has been reported in a case of akinetopsia [48], nor was he consistently responding with a single motion direction (e.g., upward on all trials). It would therefore be more accurate to label this as a directionally "bistable" percept, which is well supported by the neuroimaging results: there was increased activity, as well as decodable patterns, in the IFG, which has been shown to play a crucial role in resolving perceptual conflict and stabilizing visual awareness when different interpretations are equally valid [49–51]. Additional areas also showed distinct neural patterns for this type of stimulus, namely V5, EVC, and the MOG. This indicates that these visual stimuli were indeed perceived as moving, but that their direction of motion was ambiguous, requiring input from the IFG to reach a resolution.

Hallucinatory motion in the Riddoch syndrome correlates with hippocampal activity

Another interesting finding is that, during blank trials where no stimulus was presented, ST occasionally reported having moderate-to-high certainty of having seen a moving stimulus and discriminating its direction of motion. We consider these occurrences to be hallucinations or imagery of visual motion, though they may not necessarily be clear or vivid; therefore, they may be regarded as minor rather than complex hallucinations [52]. This is supported by the imaging results, which showed univariate activity in bilateral orbitofrontal cortex (Table 2.2), and multivariate patterns in V5, the MOG, and the tail of the hippocampus. The fact that there were patterns in V5 is a strong indication that these trials were associated with a visual-motion percept, as previous work has shown that the content of a hallucination correlates with activity in the visual areas specialised for the processing of that type of content [53]. Additionally, the MOG and hippocampus have been implicated in imagery and the retrieval of visual perceptual information from recent memory [54,55]. Although we did not explicitly address this question, we suspect that the hallucinations observed here are task-induced, in that they may be brought upon by strong expectations about encountering visual motion immediately after the cue at the start of each trial [56]. In fact, several recent reports have proposed that hippocampal neural representations generate cued predictions about upcoming sensory events, modulating activity in sensory cortex in a predominantly top-down fashion [57–60].

2.5 Concluding remarks

Only experiential states in which ST reported some degree of awareness of motion direction showed distinct neural patterns in V5. One possible criticism may be that the neural activity associated with each experiential state is driven by low-level stimulus properties and is difficult to disentangle from activity associated with conscious experience. However, the fact that neural patterns emerged in V5 only during conditions with conscious experience, be it driven by a clear, ambiguous, or hallucinated percept, speaks to a common thread connecting these conditions despite the differences in low-level features.

On the other hand, the various experiential states engaged different sets of areas along with V5, some of which are more generally involved in conscious perceptual processing and not necessarily restricted to visual motion. The activity in these areas, which was relatively weak and therefore not easily demonstrable by the univariate analysis, could be decoded through to the multivariate analysis. Moreover, the recruitment of these additional areas, along with V5, only happened during specific experiences. This finding emphasises the central idea in this thesis, namely that certain connections in the brain become demonstrable through certain experiences, and highlights the importance of tackling patient cases and group studies with multiple analytical tools, as this may reveal mechanisms of conscious perception that otherwise remain occult. These results also highlight the complex continuum of perceptual experiences in patients 'blinded' by cortical lesions, and their ability to tell us about the neural mechanisms of conscious perception, within and beyond visual cortex.

REFERENCES

1. Zeki, S., and ffytche, D.H. (1998). The Riddoch syndrome: insights into the neurobiology of conscious vision. Brain *121*, 25–45. 10.1093/brain/121.1.25.

2. Arcaro, M.J., Thaler, L., Quinlan, D.J., Monaco, S., Khan, S., Valyear, K.F., Goebel, R., Dutton, G.N., Goodale, M.A., Kastner, S., et al. (2019). Psychophysical and neuroimaging responses to moving stimuli in a patient with the Riddoch phenomenon due to bilateral visual cortex lesions. Neuropsychologia *128*, 150–165. 10.1016/j.neuropsychologia.2018.05.008.

3. Ajina, S., Kennard, C., Rees, G., and Bridge, H. (2015). Motion area V5/MT+ response to global motion in the absence of V1 resembles early visual cortex. Brain *138*, 164–178. 10.1093/brain/awu328.

4. Barbur, J.L., Watson, J.D.G., Frackowiak, R.S.J., and Zeki, S. (1993). Conscious visual perception without V1. Brain *116*, 1293–1302. 10.1093/BRAIN/116.6.1293.

5. Watson, J.D.G., Myers, R., Frackowiak, R.S.J., Hajnal, J. V., Woods, R.P., Mazziotta, J.C., Shipp, S., and Zeki, S. (1993). Area V5 of the human brain: evidence from a combined study using positron emission tomography and magnetic resonance imaging. Cerebral Cortex *3*, 79–94. 10.1093/CERCOR/3.2.79.

6. Zeki, S.M. (1974). Functional organization of a visual area in the posterior bank of the superior temporal sulcus of the rhesus monkey. J Physiol *236*, 549–573. 10.1113/JPHYSIOL.1974.SP010452.

7. Barbur, J.L., Harlow, A.J., and Weiskrantz, L. (1994). Spatial and temporal response properties of residual vision in a case of hemianopia. Philos Trans R Soc Lond B Biol Sci *343*, 157–166. 10.1098/rstb.1994.0018.

8. Brainard, D.H. (1997). The Psychophysics Toolbox. Spat Vis *10*, 433–436. 10.1163/156856897X00357.

9. Fleming, S.M., and Lau, H.C. (2014). How to measure metacognition. Front Hum Neurosci *8*, 443. 10.3389/fnhum.2014.00443.

10. Lutkenhoff, E.S., Rosenberg, M., Chiang, J., Zhang, K., Pickard, J.D., Owen, A.M., and Monti, M.M. (2014). Optimized brain extraction for pathological brains (optiBET). PLoS One *9*, e115551. 10.1371/journal.pone.0115551.

11. Tustison, N.J., Avants, B.B., Cook, P.A., Zheng, Y., Egan, A., Yushkevich, P.A., and Gee, J.C. (2010). N4ITK: Improved N3 bias correction. IEEE Trans Med Imaging *29*, 1310–1320. 10.1109/TMI.2010.2046908.

12. Jenkinson, M., Bannister, P., Brady, M., and Smith, S. (2002). Improved optimization for the robust and accurate linear registration and motion correction of brain images. Neuroimage *17*, 825–841. 10.1006/NIMG.2002.1132.

13. Fonov, V., Evans, A.C., Botteron, K., Almli, C.R., McKinstry, R.C., and Collins, D.L. (2011). Unbiased average age-appropriate atlases for pediatric studies. Neuroimage *54*, 313–327. 10.1016/J.NEUROIMAGE.2010.07.033.

14. Avants, B.B., Tustison, N.J., Song, G., Cook, P.A., Klein, A., and Gee, J.C. (2011). A reproducible evaluation of ANTs similarity metric performance in brain image registration. Neuroimage *54*, 2033–2044. 10.1016/J.NEUROIMAGE.2010.09.025.

15. Greve, D.N., and Fischl, B. (2009). Accurate and robust brain image alignment using boundary-based registration. Neuroimage *48*, 63–72. 10.1016/J.NEUROIMAGE.2009.06.060.

16. Veraart, J., Fieremans, E., and Novikov, D.S. (2016). Diffusion MRI noise mapping using random matrix theory. Magn Reson Med *76*, 1582–1593. 10.1002/mrm.26059.

17. Kellner, E., Dhital, B., Kiselev, V.G., and Reisert, M. (2016). Gibbs-ringing artifact removal based on local subvoxel-shifts. Magn Reson Med *76*, 1574–1581. 10.1002/mrm.26054.

18. Andersson, J.L.R., Skare, S., and Ashburner, J. (2003). How to correct susceptibility distortions in spin-echo echo-planar images: Application to diffusion tensor imaging. Neuroimage *20*, 870–888. 10.1016/S1053-8119(03)00336-7.

19. Andersson, J.L.R., and Sotiropoulos, S.N. (2016). An integrated approach to correction for off-resonance effects and subject movement in diffusion MR imaging. Neuroimage *125*, 1063–1078. 10.1016/j.neuroimage.2015.10.019.

20. Andersson, J.L.R., Graham, M.S., Zsoldos, E., and Sotiropoulos, S.N. (2016). Incorporating outlier detection and replacement into a non-parametric framework for movement and distortion correction of diffusion MR images. Neuroimage *141*, 556–572. 10.1016/j.neuroimage.2016.06.058.

21. Kriegeskorte, N., Mur, M., and Bandettini, P. (2008). Representational similarity analysis – connecting the branches of systems neuroscience. Front Syst Neurosci *2*. 10.3389/neuro.06.004.2008.

22. Dell'Acqua, F., Scifo, P., Rizzo, G., Catani, M., Simmons, A., Scotti, G., and Fazio, F. (2010). A modified damped Richardson-Lucy algorithm to reduce isotropic background effects in spherical deconvolution. Neuroimage *49*, 1446–1458. 10.1016/j.neuroimage.2009.09.033.

23. Dell'Acqua, F., Simmons, A., Williams, S.C.R., and Catani, M. (2013). Can spherical deconvolution provide more information than fiber orientations? Hindrance modulated orientational anisotropy, a true-tract specific index to characterize white matter diffusion. Hum Brain Mapp *34*, 2464–2483. 10.1002/hbm.22080.

24. Müller-Axt, C., Eichner, C., Rusch, H., Kauffmann, L., Bazin, P.L., Anwander, A., Morawski, M., and von Kriegstein, K. (2021). Mapping the human lateral geniculate nucleus and its cytoarchitectonic subdivisions using quantitative MRI. Neuroimage *244*, 118559. 10.1016/J.NEUROIMAGE.2021.118559.

25. Scott, R.B., Dienes, Z., Barrett, A.B., Bor, D., and Seth, A.K. (2014). Blind insight: metacognitive discrimination despite chance task performance. Psychol Sci *25*, 2199–2208. 10.1177/0956797614553944.

26. Ajina, S., Pestilli, F., Rokem, A., Kennard, C., and Bridge, H. (2015). Human blindsight is mediated by an intact geniculo-extrastriate pathway. Elife *4*, e08935. 10.7554/eLife.08935.

27. Sahraie, A., Weiskrantz, L., Barbur, J.L., Simmons, A., Williams, S.C.R., and Brammer, M.J. (1997). Pattern of neuronal activity associated with conscious and unconscious processing of visual signals. Proc Natl Acad Sci U S A *94*, 9406–9411. 10.1073/pnas.94.17.9406.

28. Weiskrantz, L., Barbur, J.L., and Sahraie, A. (1995). Parameters affecting conscious versus unconscious visual discrimination with damage to the visual cortex (V1). Proceedings of the National Academy of Sciences *92*, 6122–6126. 10.1073/pnas.92.13.6122.

29. Overgaard, M., Fehl, K., Mouridsen, K., Bergholt, B., and Cleeremans, A. (2008). Seeing without seeing? Degraded conscious vision in a blindsight patient. PLoS One *3*, e3028. 10.1371/JOURNAL.PONE.0003028.

30. Mazzi, C., Bagattini, C., and Savazzi, S. (2016). Blind-sight vs. degraded-sight: different measures tell a different story. Front Psychol *7*, 901. 10.3389/FPSYG.2016.00901/BIBTEX.

31. Peters, M.A.K., and Lau, H. (2015). Human observers have optimal introspective access to perceptual processes even for visually masked stimuli. Elife *4*, e09651. 10.7554/ELIFE.09651.

32. Phillips, I. (2021). Blindsight is qualitatively degraded conscious vision. Psychol Rev *128*, 558–584. 10.1037/REV0000254.

33. DeYoe, E.A., and Van Essen, D.C. (1985). Segregation of efferent connections and receptive field properties in visual area V2 of the macaque. Nature *317*, 58–61. 10.1038/317058a0.

34. Shipp, S., and Zeki, S. (1985). Segregation of pathways leading from area V2 to areas V4 and V5 of macaque monkey visual cortex. Nature *315*, 322–324. 10.1038/315322a0.

35. Zeki, S.M. (1978). Uniformity and diversity of structure and function in rhesus monkey prestriate visual cortex. J Physiol *277*, 273–290. 10.1113/jphysiol.1978.sp012272.

36. Gegenfurtner, K.R., Kiper, D.C., and Levitt, J.B. (1997). Functional properties of neurons in macaque area V3. J Neurophysiol *77*, 1906–1923. 10.1152/jn.1997.77.4.1906.

37. Smith, A.T., Greenlee, M.W., Singh, K.D., Kraemer, F.M., and Hennig, J. (1998). The processing of first- and second-order motion in human visual cortex assessed by functional magnetic resonance imaging (fMRI). Journal of Neuroscience *18*, 3816–3830. 10.1523/JNEUROSCI.18-10-03816.1998.

38. Van de Nieuwenhuijzen, M.E., Backus, A.R., Bahramisharif, A., Doeller, C.F., Jensen, O., and van Gerven, M.A.J. (2013). MEG-based decoding of the spatiotemporal dynamics of visual category perception. Neuroimage *83*, 1063–1073. 10.1016/J.NEUROIMAGE.2013.07.075.

39. Lorenc, E.S., Lee, T.G., Chen, A.J.W., and D'Esposito, M. (2015). The effect of disruption of prefrontal cortical function with transcranial magnetic stimulation on visual working memory. Front Syst Neurosci *9*, 169. 10.3389/FNSYS.2015.00169/BIBTEX.

40. Yukie, M., and Iwai, E. (1981). Direct projection from the dorsal lateral geniculate nucleus to the prestriate cortex in macaque monkeys. J Comp Neurol *201*, 81–97. 10.1002/cne.902010107.

41. Benevento, L.A., and Rezak, M. (1976). The cortical projections of the inferior pulvinar and adjacent lateral pulvinar in the rhesus monkey (Macaca mulatta): an autoradiographic study. Brain Res *108*, 1–24. 10.1016/0006-8993(76)90160-8.

42. Fries, W. (1981). The projection from the lateral geniculate nucleus to the prestriate cortex of the macaque monkey. Proc R Soc Lond B Biol Sci *213*, 73–80. 10.1098/rspb.1981.0054.

43. Cragg, B.G. (1969). The topography of the afferent projections in the circumstriate visual cortex of the monkey studied by the nauta method. Vision Res *9*, 733–747. 10.1016/0042-6989(69)90011-X.

44. Rees, G. (2007). Neural correlates of the contents of visual awareness in humans. Philosophical Transactions of the Royal Society B: Biological Sciences *362*, 877–886. 10.1098/RSTB.2007.2094.

45. Moutoussis, K., and Zeki, S. (2006). Seeing invisible motion: A human fMRI study. Current Biology *16*, 574–579. 10.1016/j.cub.2006.01.062.

46. Itoh, K., Fujii, Y., Kwee, I.L., and Nakada, T. (2005). MT+/V5 activation without conscious motion perception: a high-field fMRI study. Magnetic Resonance in Medical Sciences *4*, 69–74. 10.2463/mrms.4.69.

47. Zeki, S. (2004). The neurology of ambiguity. Conscious Cogn *13*, 173–196. 10.1016/J.CONCOG.2003.10.003.

48. Heutink, J., de Haan, G., Marsman, J.B., van Dijk, M., and Cordes, C. (2019). The effect of target speed on perception of visual motion direction in a patient with akinetopsia. Cortex *119*, 511–518. 10.1016/J.CORTEX.2018.12.002.

49. Ishizu, T., and Zeki, S. (2014). Varieties of perceptual instability and their neural correlates. Neuroimage *91*, 203–209. 10.1016/j.neuroimage.2014.01.040.

50. Bartels, A. (2021). Consciousness: What is the role of prefrontal cortex? Current Biology *31*, R853–R856. 10.1016/J.CUB.2021.05.012.

51. Weilnhammer, V., Fritsch, M., Chikermane, M., Eckert, A.L., Kanthak, K., Stuke, H., Kaminski, J., and Sterzer, P. (2021). An active role of inferior frontal cortex in conscious experience. Current Biology *31*, 2868-2880.e8. 10.1016/J.CUB.2021.04.043.

52. Weil, R.S., and Lees, A.J. (2021). Visual hallucinations. Pract Neurol *21*, 327–332. 10.1136/practneurol-2021-003016.

53. ffytche, D.H., Howard, R.J., Brammer, M.J., David, A., Woodruff, P., and Williams, S. (1998). The anatomy of conscious vision: an fMRI study of visual hallucinations. Nat Neurosci *1*, 738–742. 10.1038/3738.

54. Lifanov, J., Griffiths, B.J., Linde-Domingo, J., Ferreira, C.S., Wilson, M., Mayhew, S.D., Charest, I., and Wimber, M. (2022). Reconstructing spatio-temporal trajectories of visual object memories in the human brain. bioRxiv. 10.1101/2022.12.15.520591.

55. Oertel, V., Rotarska-Jagiela, A., van de Ven, V.G., Haenschel, C., Maurer, K., and Linden, D.E.J. (2007). Visual hallucinations in schizophrenia investigated with functional magnetic resonance imaging. Psychiatry Res Neuroimaging *156*, 269–273. 10.1016/J.PSCYCHRESNS.2007.09.004.

56. Zarkali, A., Adams, R.A., Psarras, S., Leyland, L.A., Rees, G., and Weil, R.S. (2019). Increased weighting on prior knowledge in Lewy body-associated visual hallucinations. Brain Commun *1*. 10.1093/BRAINCOMMS/FCZ007.

57. Kok, P., and Turk-Browne, N.B. (2018). Associative prediction of visual shape in the hippocampus. Journal of Neuroscience *38*, 6888–6899. 10.1523/JNEUROSCI.0163-18.2018.

58. Ekman, M., Kusch, S., and de Lange, F.P. (2023). Successor-like representation guides the prediction of future events in human visual cortex and hippocampus. Elife *12*, e78904. 10.7554/ELIFE.78904.

59. Clarke, A., Crivelli-Decker, J., and Ranganath, C. (2022). Contextual expectations shape cortical reinstatement of sensory representations. Journal of Neuroscience *42*, 5956–5965. 10.1523/JNEUROSCI.2045-21.2022.

60. Biane, J.S., Ladow, M.A., Stefanini, F., Boddu, S.P., Fan, A., Hassan, S., Dundar, N., Apodaca-Montano, D.L., Zhou, L.Z., Fayner, V., et al. (2023). Neural dynamics underlying associative learning in the dorsal and ventral hippocampus. Nat Neurosci. 10.1038/s41593-023-01296-6.

3.

Spectral Composition Discrimination in the Riddoch Syndrome

So far, the Riddoch syndrome has been related to awareness of visual motion, but research in "blindsight" suggests a possible sensitivity to colour and orientation. Could it be that Riddoch syndrome patients, besides visual motion, can be aware of other visual features? If so, is this awareness accompanied by a decodable pattern in the visual area specialised for the processing of it? To answer these questions, ST was presented with (a)chromatic checkerboards while measuring his brain activity with fMRI. He was able to discriminate checkerboards that were coloured (red-green or blue-yellow) from those that were achromatic (black-white) but could not discriminate the colours contained within them. Nevertheless, using RSA, we found specific neural patterns in V4 complex when he was presented with red-green or blue-yellow checkerboards. Blue-yellow stimuli also activated V5, supporting previous descriptions. These findings suggest that, despite cortical blindness, V1-damaged patients may still be able to consciously discriminate coloured checkerboards from those that are "achromatic", and that the perception of chromatic stimuli correlates with engagement of colour-sensitive brain regions.

3.1 INTRODUCTION

The investigation in the previous chapter demonstrated that a patient blinded by lesions in V1 can be conscious of visual motion and only during the conscious state are there decodable patterns in the specialised area for motion processing, i.e., V5. Moreover, we discovered another, previously unreported, manifestation of the syndrome, namely that of hallucinations of motion, which we refer to as gnosanopsia. This unexpected finding motivated us to look at other aspects of ST's vision.

Although the patients described by Riddoch [1] reported not perceiving any other visual attributes, research in "blindsight" has demonstrated residual discriminatory capacities for different attributes, such as orientation, form and colour [2–6]. Of course, it was claimed that this ability occurred without any awareness of the patient, but some indications of coloured stimuli inducing a conscious experience can be deduced from early reports. For example, Weiskrantz et al. [3] described that the patient reported a 'stronger feeling of something being there' with the presentation of a green stimulus compared to a red one. And indeed, direct subcortical projections to the visual area specialised for processing colour, i.e., V4, were subsequently described [7,8]. Nevertheless, these indications are merely hints suggesting that there is awareness of colour after V1 damage. Some have argued that although there is wavelength discrimination in patients with a damaged V1, they do not experience any colour qualia, such as hue, saturation or brightness [5,9]. One interpretation has been that the experience of these patients is a mere non-visual 'feeling' or thought without any phenomenological content; this leads to the same discredited conclusion that activity in V1 is essential for visual consciousness [9].

We therefore investigated whether patient ST, whom I have described in the previous chapter, can discriminate between achromatic and chromatic stimuli; this was especially relevant because he declared that he could. Since we know that ST has an intact and responsive V5 that receives direct, V1-bypassing, input, and that V5 input from the LGN is predominantly koniocellular (K) input [10], a short-wavelength (S) cone isolating stimulus was included to investigate whether this may lead to a differential response in awareness and behavioural performance. Furthermore, we examined his brain activity in response to these stimuli to ascertain whether decodable neural patterns emerge in visual areas specialised for the processing of such stimuli, such as in V4 complex and V5.

This is therefore another instance in which one can determine whether there are experience-dependent connections; does this crude but conscious experience, which is different from the conscious experience of motion, reveal any significant neural networks that are demonstrable only through these specific experiences?

3.2 METHOD

3.2.1 Procedure

Patient ST (described in chapter 2.3.1) performed a slightly different task while undergoing MRI scanning. Again, he was presented with a checkerboard in the lower right corner of his blind field (see chapter 2.2.2 and Figure 2.1 for the exact location); this time however, the spatial frequency of the checkerboard was always 0.5 cycles/° and presented statically or at a fixed speed of 16 °/second. It also varied in colour; the checks were "achromatic" (black-white), red-green, or blue-yellow (S-cone isolating stimulus). The latter colour combination was created using a technique adapted from Cavanagh et al. [11]. Specifically, the 'blue' checks were overlaid onto a yellow image; this yellow image exhibited full saturation for red and green, but no saturation of blue, thereby representing the 'blue-off' aspect. On the other hand, the 'blue-on' checks were fully saturated across all three colour channels. Consequently, the sole distinction between these two colours rested in the presence or absence of blue, effectively causing S-cones to respond differentially to the information in the image, which in turn engage the K system [12]. Perceptually, this made the checkerboard appear white-yellow instead of blue-yellow.

In total, there were seven different conditions: three different (a)chromatic checkerboards presented statically or in motion, plus blank trials. Each condition was presented 30 times, amounting to 210 trials in total. The task had the same procedure as described in chapter 2.2.3 and Figure 2.1, except for one change; instead of asking for a certainty rating about motion, we asked ST to indicate on a three-point scale whether he saw something of colour appear in his blind field while he fixated on a cross in the centre of the screen. The three-point scale that assessed his subjective experience consisted of the following options: 1 meant "I did not see any colour", 2 meant "I think I saw a coloured stimulus, but I am not sure" and 3 meant "I saw a coloured stimulus". Direction

discrimination and colour detection performance were again calculated in percentages as described in chapter 2.2.4.

After scanning, ST was led to a separate psychophysics room to test his ability to correctly identify the specific colour of a stimulus presented in his blind field. Squares and checkerboards of various colours (Table 3.2) were presented while he fixated on a cross in the centre. His task was to verbally report the colour of the stimulus. A total of 26 trials, including blanks, were collected.

3.2.2 Image acquisition and pre-processing

Structural and functional MRI data was acquired on the same 3T Siemens Prisma scanner (Siemens Healthcare GmbH, Erlangen, Germany) with a 64-channel head coil. The sequences had the same parameters as described in chapter 2.2.6. Six runs of fMRI data were collected, each consisting of 35 trials. The T1w image and functional images were pre-processed in the same manner as described in 2.2.7 and 2.2.9, respectively.

3.2.3 Univariate analysis

We conducted several categorical comparisons to determine the brain activity associated with the perception of the various stimuli. The conditions were compared to one another and to the blank condition. The BOLD time series images were smoothed and entered into a GLM as described in 2.2.10. The resulting statistical images were thresholded at a voxelwise significance level of $p < .001$.

3.2.4 Multivariate analysis

A whole-brain searchlight RSA analysis was performed in similar fashion as in the previous chapter (2.2.11), but this time surface-based, to determine whether specific neural activity patterns emerge when perceiving each type of stimulus. First, a first-level GLM that considered each trial as an independent condition was run. Next, we grouped the 30 resulting beta maps of each condition together and added a separate group of 30 beta maps of the blank trials. The beta images (parameter estimates) were projected to ST's cortical surface (obtained from *FreeSurfer*). The surface-based beta maps were then used for the multivariate analysis; the similarity between each pair of trials was calculated in each searchlight ROI, using the Pearson correlation distance metric.

The resulting neural RDMs were compared to the model RDM, which assumed a high similarity in activity patterns associated with the trials of that condition (i.e., d = 0.0) and no similarity for the trials of the blanks, or between the patterns of that condition and those of the blanks (i.e., d = 0.5). The correlation between the neural and model RDMs was assessed using the Spearman rank correlation and statistical significance was determined by means of permutation testing. For each ROI of the searchlight, 5000 random permutations of the trial labels were generated to estimate the null distribution of the distance, d, and obtain a robust measure of statistical significance. Final results were thresholded at $p < .001$ and at a minimum cluster size of 36 mm^2 (chosen as the rough equivalent of 2×2 voxels with a size of 3 mm, which is the original resolution of the fMRI data) to reveal meaningful clusters, as that the multivariate data was not smoothed.

3.3 RESULTS

3.3.1 Behavioural results

To our surprise, ST was unable during the MRI session to correctly discriminate the direction of motion of all the checkerboards; performance was at chance level with achromatic stimuli (p = 0.10), red-green stimuli (p = 0.29) and blue-yellow stimuli (p = 0.43) (Figure 3.1). The chance performance could possibly be due to the spatial frequency of the stimulus being too high, although previous psychophysical testing suggested that he would be able to distinguish the motion direction at this frequency (see chapter 2). This indicates that there can be variability or fluctuations in his perception, although it should be noted that performance in the achromatic condition is numerically above chance (60%). Chance discrimination in this case may reflect a type-2 error, and increasing the number of trials (and thereby the power) may bring performance significantly above chance.

Nevertheless, ST was highly accurate in detecting the presence of chromatic stimuli in his blind field; he very rarely reported perceiving colour when there was no stimulus (blank) or when the stimulus was achromatic (only 12% of trials of these conditions combined received a score of '2' or '3'), and almost always reported perceiving colour when the stimulus was chromatic (only 7.5% of all trials containing a coloured stimulus received a

score of '1', i.e., no colour); this was regardless of whether the stimulus was moving or static (Figure 3.1).

Yet, psychophysical testing revealed that ST rarely attributed the correct colour to the stimulus (Table 3.1), despite his claim to see colour and his usage of terms indicative of colour perception, such as 'I see something orange'. This inability to attribute the correct colour to a stimulus indicates that he may not be able to see colour. Instead, the fact that he could discriminate broadly between chromatic and achromatic stimuli may simply be driven by the ability to distinguish between different wavelength compositions [13]. He was clearly aware of something, but what he was aware of is difficult to ascertain.

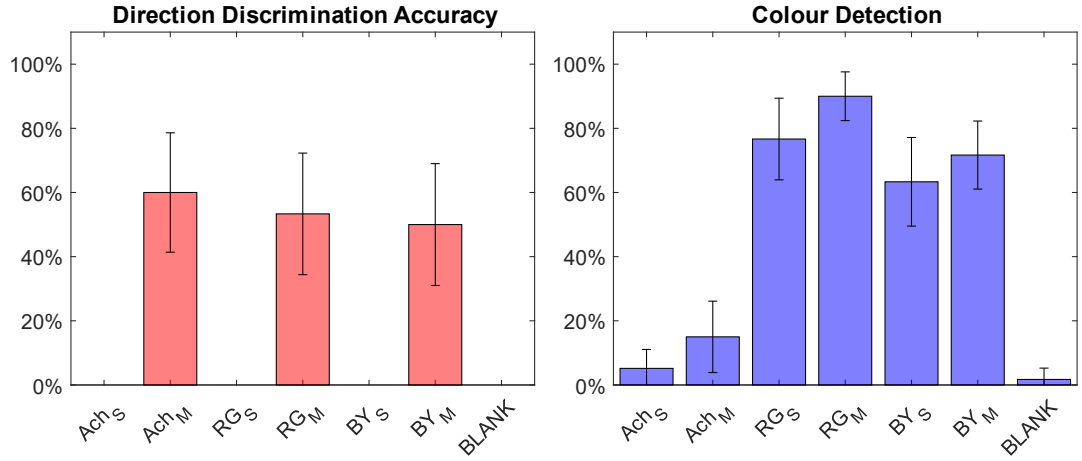

Figure 3.1. Performance on the motion-colour task during the MRI session.
ST's accuracy in detecting the direction of motion and presence of colour. His performance on direction discrimination did not differ significantly from chance (50%), indicating that he did not perceive the direction of motion. However, ST was very accurate in detecting the presence of colour; he almost always reported seeing colour with coloured stimuli and rarely reported seeing colour with blanks or achromatic stimuli. A score of 100% indicates correctly identifying the direction of motion and reporting perceiving colour on all trials of a given condition, whereas a score of 0% indicates incorrectly identifying the direction of motion and reporting not seeing colour on any trials of a given condition. Direction discrimination is not applicable for static stimuli, as there was no motion-direction to perceive. Abbreviations: Ach – achromatic, RG – red/green, BY – blue/yellow (S-cone isolating), M – moving, S – static.

Trial	Colour of the presented stimulus	ST's verbal response
1.	Red	Warm colour; yellow or orange.
2.	Blank	It's still there.
3.	Blue	Something darker; I don't know, orange?
4.	Blank	Is there anything there?
5.	Green	No colour; nothing there.
6.	Blank	Still no colour.
7.	Red	Something orange.
8.	Green	I think there is colour, orange?
9.	Blue	Something darker appeared.
10.	Yellow	Orange.
11.	Blue	Grey or a dark colour.
12.	Green	No colour, a shade of grey.
13.	Red	Something is there, something warmer.
14.	Black	Grey.
15.	White	Something bright, white.
16.	Black	Darker again, no colour.
17.	Blue-yellow	Nothing.
18.	Red-green	I think there is something grey, but I'm not sure.
19.	Blue-yellow	A grey smudge.
20.	Red-green	Something green or yellow.
21.	Blue-yellow	Nothing.
22.	Blue-yellow	A smudge appeared, but no colour.
23.	Red-green	Something dark, but no colour.
24.	Red-green	Something brighter appeared, but no colour.
25.	Blue-yellow	Purple or blue.
26.	Red-green	I have a vague sense of something bright, perhaps yellow?

Table 3.1. Phenomenological assessment of ST's experience of colour in his blind field. ST reported verbally the colour that he perceived when presented with static squares and checkerboards of various colours in his blind field. Although inaccurate on most trials, he often reported that there was something coloured.

3.3.2 fMRI results

Based on previous studies on patients with lesions in V1, we expected that the stimuli presented in his blind field would significantly engage the prestriate cortex; chromatic stimuli were expected to engage the V4 complex [14] and moving stimuli were expected to engage motion area V5 [14–19], although our confidence in finding this latter result was diminished by the fact that ST was not always able to discriminate the direction of motion.

Univariate results

When we compared the activity induced by chromatic stimuli with achromatic stimuli, no significant activations were found in ST's brain. In fact, engagement of colour-sensitive visual areas, such as V4 and V4α [20–22], was not revealed by any univariate comparison. Achromatic stimuli were associated with increased activity in V2, the lateral occipital cortex (LOC) and the motor cortex when compared with chromatic ones (Table 3.2).

Comparing moving stimuli with static ones did not reveal significant activations of V5. Nevertheless, there was increased activity in ipsilesional V5 when comparing achromatic moving stimuli and S-cone isolating (blue-yellow) moving stimuli with blanks (Table 3.2). Moreover, the static S-cone isolating checkerboards also activated ipsilesional V5. This is not a surprising result, given that V5 receives direct K input from the LGN [10]. The red-green moving stimuli failed to elicit increased activity in V5. In fact, Comparing the red-green checkerboards to blanks or achromatic stimuli did not yield any significant univariate activations in visual cortex.

Cluster and/or region	**# voxels**	***p***	***t***	**MNI Coordinates (mm)**		
				x	**y**	**z**
Chromatic stimuli > achromatic stimuli						
No significant activations.						
Moving stimuli > static stimuli						
R inferior frontal gyrus (IFG)	13	0.000	3.92	-48	-75	12
Achromatic stimuli > chromatic stimuli						
R postcentral gyrus	308	0.000	4.11	15	-45	66
R postcentral gyrus		0.000	3.72	12	-33	72
R precentral gyrus		0.000	3.65	12	-18	75

L V2	12	0.000	3.64	-6	-93	-18
L cerebellum	15	0.000	3.46	-15	-45	-18
L lateral occipital cortex (LOC)	13	0.000	3.41	-12	-60	63
L LOC		0.001	3.22	-21	-66	60
Red-green moving stimuli > blanks						
L precentral gyrus	99	0.000	3.96	-42	-18	57
Red-green static stimuli > blanks						
No significant activations.						
Blue-yellow moving stimuli > blanks						
L V5	42	0.000	3.74	-51	-75	9
Blue-yellow static stimuli > blanks						
L V5	40	0.000	3.87	-48	-75	12
Moving stimuli > static stimuli						
R inferior frontal gyrus (IFG)	13	0.000	3.92	-48	-75	12
Achromatic moving stimuli > blanks						
L V5	400	0.000	4.45	-51	-72	9
L supramarginal gyrus		0.000	3.97	-48	-42	24
L postcentral gyrus	265	0.000	4.21	-54	-21	36
L postcentral gyrus		0.000	4.01	-54	-27	51
L postcentral gyrus		0.000	3.80	-45	-39	57
R inferior frontal gyrus (IFG)	104	0.000	3.92	51	12	24
R V5	105	0.000	3.88	48	-60	3
R postcentral gyrus	130	0.000	3.70	60	-15	27
R postcentral gyrus		0.000	3.68	51	-21	30
R middle frontal gyrus	56	0.000	3.59	39	3	57
R middle frontal gyrus		0.000	3.43	33	-3	48
L cerebellum	14	0.000	3.47	-12	-45	-18
R precentral gyrus	45	0.000	3.47	12	-18	75
R postcentral gyrus		0.001	3.31	12	-39	66
R PHC1	17	0.000	3.37	24	-60	-15
L inferior frontal gyrus (IFG)	25	0.000	3.35	-51	6	27

Table 3.2. Results of the univariate fMRI analysis.
The clusters of significant activity with their corresponding peak t-statistic and MNI coordinates for various comparisons. All results are thresholded at $p < .001$ and only clusters of 10 voxels or more are reported.

Multivariate results

The aim of the representational similarity analysis (RSA) was to answer the following question: given that with conscious perception of motion a pattern appears in the visual

area specialised in motion processing, i.e., V5 [19], does such a pattern appear in the visual area specialised for colour processing, i.e., V4 [20–22], with the conscious detection of chromatic stimuli? Given that ST was highly accurate and confident in detecting the presence of chromatic stimuli in his blind field, even with static ones, I chose to focus on static trials, since additional visual attributes, such as motion, may influence brain activity and may therefore cause a confound in the interpretation.

Indeed, significant pattern similarity was found for both static chromatic conditions (red-green and blue-yellow) in V4 complex (V4 and V4α) and extended into V3, whereas the static achromatic condition elicited patterns in V2/V3 (Figure 3.2). Additional visual areas also showed distinct neural patterns for these static stimuli; PHC1 and PHC2, two parahippocampal areas with a retinotopic organisation that respond to visual scenes [23], showed activity patterns for both achromatic and red-green static stimuli. The blue-yellow stimulus elicited activity patterns in V5, which is in accordance with previous studies demonstrating that cells in V5 respond to S-cone isolating stimuli, even in the absence of V1 [24].

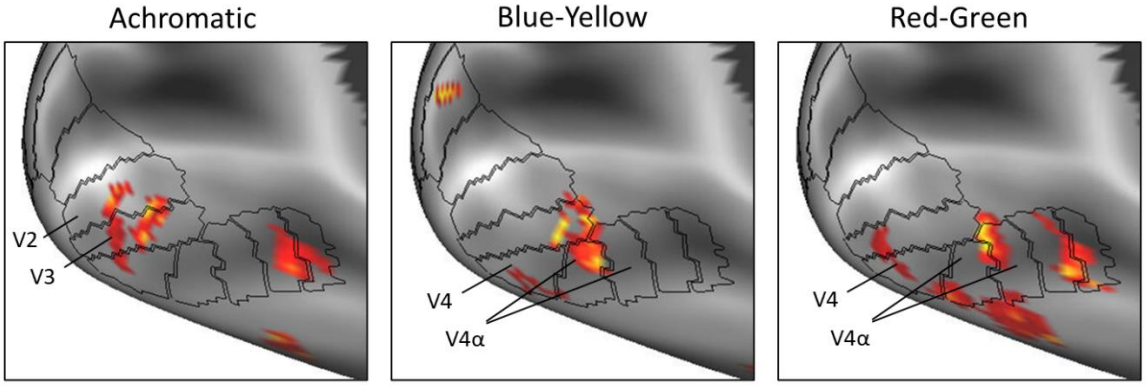

Figure 3.2. Results of the multivariate analysis.
Significant pattern similarity in visual areas for the various conditions. For the static blue-yellow (S-cone isolating) stimulus, activity patterns emerged in: V3, V4, VO1 (V4α), VO2 (V4α), and V5 (not shown). For the static red-green condition, patterns were found in the following visual areas: V3, V4, VO1 (V4α), VO2 (V4α), PHC1 and PHC2. The achromatic condition elicited similar patterns in V2, V3, PHC1 and PHC2. These results are based on permutation testing with a vertex-wise p-value threshold of .001 and a minimum cluster size of 36 mm². The clusters are labelled according to the visual cortex atlas by Wang et al. [25]

3.4 DISCUSSION

After establishing in the previous chapter that patient ST, despite a lesion in V1, was able to consciously perceive motion, we wanted to determine whether ST had other residual visual capacities. Despite his blindness, ST claimed to be able to see colour; we therefore presented him with chromatic and achromatic checkerboards in his blind field. He was very good at indicating whether the stimulus was chromatic (red-green or blue-yellow) or achromatic (black-white). Yet, phenomenological assessments provided little support for colour perception; when asked to report the colour of various static squares and checkerboards, he attributed incorrect colours to the stimuli, or none at all. This observation has been reported in other V1-damaged patients as well; studies have described such patients who are able to consciously detect wavelength changes of stimuli but are unable to report their colour [5,14]. Despite the inability to report the correct colour, he nonetheless had a conscious experience that allowed him to differentiate between these two broad categories of chromatic and achromatic stimuli. This conscious experience was most likely visual in nature, based on the terms he used to describe his percept. We can thus conclude that Riddoch syndrome patients can be conscious of the presence of chromatic visual stimuli in their blind field, but what precisely this conscious experience consists of is difficult to decipher.

fMRI revealed that static chromatic stimuli elicited distinct neural activity patterns in areas important for colour processing, namely V4 and V4α [20–22]. Heightened (univariate) activity in these areas was not found, but, as we saw in the previous chapter on visual motion awareness, univariate activity may not always be a good indication of conscious perception; there may be no sign of increased activity despite awareness, or there may be increased activity but no awareness of the visual attribute [15,26,27]. Additionally, the use of an event-related fMRI design in this study may lend itself better to a multivariate analysis where sensitivity to single trials is of interest, and less so to univariate analyses that would benefit more from a block-design that maximises BOLD signal changes over longer epochs. In fact, others have reported increased activity in V4 when V1-damaged patients were presented with chromatic stimuli using such a block-design [14].

Significant increased activity and distinct patterns were found in ST's ipsilesional V5 when he was presented with S-cone isolating stimuli. This finding is in accordance with

previous reports; it has been shown with fMRI that such stimuli activate V1 and V5 [28], and, even in the absence of V1, cells in V5 respond to S-cone isolating stimuli [24]. This is not surprising, given that V5 receives direct, V1-bypassing, input from the koniocellular pathways [10], and these pathways are very effectively engaged by this type of stimulus [12,29]. This result can be contrasted with the red-green stimulus, which did not show any involvement of V5 in ST. A likely explanation for this observation is that this type of stimulus engages the parvocellular system, which is sensitive to colour. While V5 input is largely dominated by magnocellular and koniocellular input [10,30,31], there are indications of parvocellular input into V5 [31,32]. Nevertheless, this information is thought to be relayed via V1 [32], which is absent in this case. Given that these two types of stimuli engaged a distinct neural network, it may very well be the case that they also evoke a different sensation in ST. It would therefore be interesting to investigate in future studies whether ST experiences these two stimuli as visually different.

In conclusion, after V1 damage, the ability to consciously discriminate between two broad categories of chromatic and achromatic stimuli may persist and the perception of chromatic ones correlates with specific neural activity patterns in the relevant specialised sensory areas, namely in the V4 complex. This conclusion is similar to the one drawn for motion awareness in the Riddoch syndrome; with motion, there are decodable patterns in motion area V5. It is therefore another demonstration of experience-dependent connections; depending upon the stimulus that is perceived, different visual areas become involved and specific neural patterns appear in it. It is also another demonstration of conscious residual abilities that are retained after V1 damage, and that engagement of prestriate areas is enough to support crude and degraded, yet conscious, visual perception.

REFERENCES

1. Riddoch, G. (1917). Dissociation of visual perceptions due to occipital injuries, with especial reference to appreciation of movement. Brain *40*, 15–57. 10.1093/brain/40.1.15.
2. Perenin, M.T. (1978). Visual function within the hemianopic field following early cerebral hemidecortication in man — II. Pattern discrimination. Neuropsychologia *16*, 697–708. 10.1016/0028-3932(78)90004-0.
3. Weiskrantz, L., Warrington, E.K., Sanders, M.D., and Marshall, J. (1974). Visual capacity in the hemianopic field following a restricted occipital ablation. Brain *97*, 709–728. 10.1093/brain/97.1.709.
4. Stoerig, P., and Cowey, A. (1992). Wavelength discrimination in blindsight. Brain *115*, 425–444. 10.1093/brain/115.2.425.
5. Brent, P.J., Kennard, C., and Ruddock, K.H. (1994). Residual colour vision in a human hemianope: spectral responses and colour discrimination. Proc R Soc Lond B Biol Sci *256*, 219–225. 10.1098/rspb.1994.0073.
6. Boyer, J.L., Harrison, S., and Ro, T. (2005). Unconscious processing of orientation and color without primary visual cortex. Proceedings of the National Academy of Sciences *102*, 16875–16879. 10.1073/pnas.0505332102.
7. Yukie, M., and Iwai, E. (1981). Direct projection from the dorsal lateral geniculate nucleus to the prestriate cortex in macaque monkeys. J Comp Neurol *201*, 81–97. 10.1002/cne.902010107.
8. Fries, W. (1981). The projection from the lateral geniculate nucleus to the prestriate cortex of the macaque monkey. Proc R Soc Lond B Biol Sci *213*, 73–80. 10.1098/rspb.1981.0054.
9. Brogaard, B. (2011). Color experience in blindsight? Philos Psychol *24*, 767–786. 10.1080/09515089.2011.562641.
10. Sincich, L.C., Park, K.F., Wohlgemuth, M.J., and Horton, J.C. (2004). Bypassing V1: a direct geniculate input to area MT. Nat Neurosci *7*, 1123–1128. 10.1038/nn1318.
11. Cavanagh, P., Adelson, E.H., and Heard, P. (1992). Vision with equiluminant colour contrast: 2. A large-scale technique and observations. Perception *21*, 219–226. 10.1068/p210219.
12. Dacey, D.M., and Lee, B.B. (1994). The “blue-on” opponent pathway in primate retina originates from a distinct bistratified ganglion cell type. Nature *367*, 731–735. 10.1038/367731a0.
13. Zeki, S. (2022). The Paton prize lecture 2021: a colourful experience leading to a reassessment of colour vision and its theories. Exp Physiol *107*, 1189–1208. 10.1113/EP089760.
14. Schoenfeld, M.A., Noesselt, T., Poggel, D., Tempelmann, C., Hopf, J.-M., Woldorff, M.G., Heinze, H.-J., and Hillyard, S.A. (2002). Analysis of pathways mediating preserved vision after striate cortex lesions. Ann Neurol *52*, 814–824. 10.1002/ana.10394.
15. Zeki, S., and ffytche, D. (1998). The Riddoch syndrome: insights into the neurobiology of conscious vision. Brain *121*, 25–45. 10.1093/brain/121.1.25.
16. Barbur, J.L., Watson, J.D.G., Frackowiak, R.S.J., and Zeki, S. (1993). Conscious visual perception without VI. Brain *116*, 1293–1302. 10.1093/brain/116.6.1293.

17. Ajina, S., Kennard, C., Rees, G., and Bridge, H. (2015). Motion area V5/MT+ response to global motion in the absence of V1 resembles early visual cortex. Brain *138*, 164–178. 10.1093/brain/awu328.

18. Arcaro, M.J., Thaler, L., Quinlan, D.J., Monaco, S., Khan, S., Valyear, K.F., Goebel, R., Dutton, G.N., Goodale, M.A., Kastner, S., et al. (2019). Psychophysical and neuroimaging responses to moving stimuli in a patient with the Riddoch phenomenon due to bilateral visual cortex lesions. Neuropsychologia *128*, 150–165. 10.1016/j.neuropsychologia.2018.05.008.

19. Beyh, A., Rasche, S.E., Leff, A., ffytche, D., and Zeki, S. (2023). Neural patterns of conscious visual awareness in the Riddoch syndrome. J Neurol, 1–12. 10.1007/s00415-023-11861-5.

20. Zeki, S. (1980). The representation of colours in the cerebral cortex. Nature *284*, 412–418. 10.1038/284412a0.

21. Zeki, S., and Bartels, A. (1999). The clinical and functional measurement of cortical (in)activity in the visual brain, with special reference to the two subdivisions (V4 and V4α) of the human colour centre. Philos Trans R Soc Lond B Biol Sci *354*, 1371–1382. 10.1098/rstb.1999.0485.

22. Brewer, A.A., Liu, J., Wade, A.R., and Wandell, B.A. (2005). Visual field maps and stimulus selectivity in human ventral occipital cortex. Nat Neurosci *8*, 1102–1109. 10.1038/nn1507.

23. Arcaro, M.J., McMains, S.A., Singer, B.D., and Kastner, S. (2009). Retinotopic organization of human ventral visual cortex. The Journal of Neuroscience *29*, 10638–10652. 10.1523/JNEUROSCI.2807-09.2009.

24. Jayakumar, J., Roy, S., Dreher, B., Martin, P.R., and Vidyasagar, T.R. (2013). Multiple pathways carry signals from short-wavelength-sensitive ('blue') cones to the middle temporal area of the macaque. J Physiol *591*, 339–352. 10.1113/jphysiol.2012.241117.

25. Wang, L., Mruczek, R.E.B., Arcaro, M.J., and Kastner, S. (2015). Probabilistic maps of visual topography in human cortex. Cerebral Cortex *25*, 3911–3931. 10.1093/cercor/bhu277.

26. Moutoussis, K., and Zeki, S. (2006). Seeing invisible motion: a human fMRI study. Current Biology *16*, 574–579. 10.1016/j.cub.2006.01.062.

27. Itoh, K., Fujii, Y., Kwee, I.L., and Nakada, T. (2005). MT+/V5 activation without conscious motion perception: a high-field fMRI study. Magnetic Resonance in Medical Sciences *4*, 69–74. 10.2463/mrms.4.69.

28. Wandell, B.A., Poirson, A.B., Newsome, W.T., Baseler, H.A., Boynton, G.M., Huk, A., Gandhi, S., and Sharpe, L.T. (1999). Color signals in human motion-selective cortex. Neuron *24*, 901–909. 10.1016/S0896-6273(00)81037-5.

29. Morand, S., Thut, G., de Peralta, R.G., Clarke, S., Khateb, A., Landis, T., and Michel, C.M. (2000). Electrophysiological evidence for fast visual processing through the human koniocellular pathway when stimuli move. Cerebral Cortex *10*, 817–825. 10.1093/cercor/10.8.817.

30. Livingstone, M., and Hubel, D. (1988). Segregation of form, color, movement, and depth: anatomy, physiology, and perception. Science (1979) *240*, 740–749. 10.1126/science.3283936.

31. Maunsell, J., Nealey, T., and DePriest, D. (1990). Magnocellular and parvocellular contributions to responses in the middle temporal visual area (MT) of the macaque monkey. The Journal of Neuroscience *10*, 3323–3334. 10.1523/JNEUROSCI.10-10-03323.1990.

32. Nassi, J.J., Lyon, D.C., and Callaway, E.M. (2006). The parvocellular LGN provides a robust disynaptic input to the visual motion area MT. Neuron *50*, 319–327. 10.1016/j.neuron.2006.03.019.

4.

A Case of the Riddoch Syndrome With an Intact V1

The Riddoch syndrome, characterized by the ability to perceive, consciously, moving visual stimuli but not static ones, has been associated with lesions in primary visual cortex (V1). I present here the case of patient YL who, after a tumour resection surgery that spared his V1, nevertheless showed symptoms of the Riddoch syndrome. Diffusion MRI tractography revealed that YL's optic radiation is partially damaged but not severed. He was presented with static and moving checkerboards in his blind field while undergoing functional magnetic resonance imaging (fMRI). We found extensive activity in his visual cortex for moving, but not for static, visual stimuli, while our psychophysical tests revealed that only low spatial frequency moving checkerboards were perceived. We therefore postulated that the magnocellular (M) and the parvocellular (P) inputs to his V1 may be differentially affected. High-resolution (7T) fMRI studies revealed strong responses in YL's V1 to M stimuli and very weak ones to P stimuli, indicating a functional P lesion affecting V1. In addition, YL frequently reported seeing moving stimuli and discriminating their direction of motion in the absence of visual stimulation, suggesting that he was experiencing visual hallucinations, which we refer to as gnosanopsia. Overall, this study highlights the possibility of a selective loss of P inputs to V1 resulting in the Riddoch syndrome and in hallucinations of visual motion.

4.1 INTRODUCTION

George Riddoch's description [1] of patients, blinded by damage to their primary visual cortex, who could perceive moving visual stimuli consciously opened a Pandora's box of interesting observations; not only about consciousness, but also about the anatomico-physiological basis of the syndrome. Although normally associated with lesions in V1, I shall describe here a particularly interesting case of the Riddoch syndrome with an intact V1. Namely, the syndrome can result from a specific damage to a functional subdivision of the visual input to V1 (in this instance the parvocellular input) in an otherwise physically intact optic radiation.

As described in chapter two, studies of Riddoch syndrome patients using brain imaging techniques have shown that the cortical motion area V5 is activated when visual motion is perceived in their blind field [2–5]. In the macaque brain, V5 receives direct input from the LGN and the pulvinar of the thalamus [6] and, in humans, signals from very fast-moving visual stimuli can reach V5 up to 40 milliseconds before reaching V1 [7], indicating that the inputs to the two visual areas are anatomically, functionally and temporally segregated. Experimental ablation studies in the macaque [8] and tractography studies in humans [9] have shown that direct input to V5 from the LGN is the anatomical substrate underlying residual motion perception after V1 damage. Thus, V5 can support a crude and impoverished but conscious visual motion perception in the absence of V1.

The case presented here is that of patient YL (not his real initials) whose psychophysical profile matches that of the Riddoch syndrome but who has no direct injury to V1, which is instead partially deafferented. This raises puzzling questions, of how such a lesion can selectively destroy a patient's ability to see static objects but spare their sensitivity to visual motion, and what cortical mechanisms might be involved in producing those selective deficits. Given that V1 receives input from the magnocellular (M) pathways, which are specialised in transmitting information about low spatial frequencies and fast motion, and the parvocellular (P) pathways, which transmit information related to high spatial frequencies, we hypothesised that the M and P input from the optic radiations may be differentially affected [10]. By presenting YL with stimuli that recruit mainly the M or the P visual pathways, we determined that indeed the P input to his V1 is selectively affected. We also observed that YL has a strong tendency to report perceiving visual motion during

the experiment in the absence of visual stimulation (hallucination of motion) and thus this Riddoch syndrome patient showed signs of gnosanopsia as well.

4.2 METHODS

4.2.1 Patient

YL is a right-handed male in his late twenties. He underwent an operation for a left hemispheric, low-grade intraventricular tumour and became hemianopic after surgery, three years prior to this study. Subsequent clinical testing revealed signs of residual visual motion perception in his blind (right) hemifield. He was referred to our study via a specialist outpatient visual service run at the National Hospital for Neurology and Neurosurgery in London. He gave informed written consent to participate in our study, which had been approved by the Yorkshire & The Humber - South Yorkshire Research Ethics Committee (NHS Health Research Authority) and UCLH/UCL Joint Research Office (protocol number 137605).

4.2.2 Experiment 1

The aim of this experiment was to establish whether YL could consciously perceive visual motion in his blind field and to determine his neural responses to this stimulation. We assessed the former with psychophysics and the latter with fMRI.

Psychophysical testing

We used achromatic random checkerboards (40% contrast) that were either static or drifted upward or downward at a speed of 20°/s. The stimuli subtended 12° in width and 22° in height and were confined to YL's blind (right) field, namely 6° to the right of the vertical meridian. During this initial psychophysics session, YL was asked to indicate the motion direction of the stimulus after each presentation, following a two-alternative forced choice (2AFC) approach, and to indicate his certainty of the response on a three-point scale, one indicating "complete guess", two "I think I saw motion, but I'm not sure of its direction", and three "I definitely saw the stimulus moving up (or down)". Performance, certainty and metacognitive sensitivity was calculated in the same manner as described in chapter 2.2.4.

Image acquisition

Based on the results of the psychophysics studies, YL underwent MRI scanning. We collected data on the 3T Siemens Megnetom Prisma scanner (Siemens Healthcare GmbH, Erlangen, Germany). To assess the extent of his lesion, we acquired a structural scan. Multishell diffusion MRI was also acquired to reconstruct his optic radiations with tractography and, finally, two runs of fMRI data were collected to assess brain activity in response to visual motion. All the sequences were the same as described in 2.2.6.

Data pre-processing

The structural data was pre-processed in the exact same way as in chapter 2.2.7, with one minor difference; YL's T1w image was not normalised to the MNI template, because the size of his lesion made this particularly difficult. Diffusion and functional data were also pre-processed in the same way as previously described (chapter 2.2.8 and 2.2.9, respectively).

Tractographic reconstruction

The diffusion data was used to reconstruct the optic radiations connecting YL's lateral geniculate nucleus (LGN) to his visual cortex. Data from the two highest shells (b = 2500 and 6000 $s \cdot mm^{-2}$) were modelled with spherical deconvolution based on the damped Richardson-Lucy algorithm in StarTrack, with the following parameters: fibre response $\alpha = 1.5$; number of iterations = 200; amplitude threshold $\eta = 0.001$; geometric regularisation $\nu = 16$. A probabilistic dispersion tractography approach was followed to explore the full profile of the fibre orientation distribution function (fODF) in each voxel according to the following parameters: minimum HMOA threshold = 0.0015; number of seeds per voxel = 2500; maximum angle threshold = 60°; minimum fibre length = 50 mm; maximum fibre length = 175 mm. This was done using a manually defined seed region of interest in the LGN. The resulting tractogram was imported into TrackVis (http://trackvis.org/) where manual cleaning was performed and streamlines terminating in visual cortex were selected.

fMRI procedure and univariate analysis

To assess visual-motion responses, two runs of fMRI data were collected during which we presented YL with the same random checkerboard stimulus in his blind field, either stationary or in motion, as well as a 'blank' condition during which no stimulus was

shown. Each of the three conditions was presented eight times in blocks of approximately 20 s. To ensure that YL was fixating the screen's centre, he engaged in a fixation task by pressing a button in response to a brief (300 ms) colour change in the fixation cross that occurred at random throughout the acquisition.

The BOLD time series images were first spatially smoothed with a Gaussian kernel of a FWHM of 4.5 mm. A standard GLM was then fitted to the time series, with a task effect (stimulus presentation) for each of the moving and static conditions, and six motion correction parameters as nuisance regressors. Categorical comparisons were performed to identify the brain regions in which activity increased in response to the presentation of the moving and static random checkerboards. All resulting statistical images were thresholded at a voxelwise significance level of $p < .001$. This was done in *SPM12*.

4.2.3 Experiment 2

The first experiment revealed that YL can perceive motion in his blind field consciously, that his visual cortex is responsive to moving but not static visual stimuli, and that his optic radiations, though damaged, still connect his visual cortex with the thalamus. This led us to hypothesise that the M and P systems are differentially affected in his brain; we therefore conducted additional experiments to address this question.

Psychophysical testing

We used the same visual-motion task with the 2×2×2 design as described in the previous chapter (Figure 2.1): YL was presented with an achromatic sine wave checkerboards that varied in spatial frequency (0.3 or 1.4 cycles/°), contrast (20% or 80%), and speed (1 or 8 °/s), and he reported the direction of motion and his certainty in perceiving it. We collected a total of 224 trials over seven task runs, which included 28 trials per condition. The stimuli were confined to the same location in his blind field as in experiment 1.

7T structural and functional imaging

We acquired high-resolution MRI data on a Siemens Magnetom Terra 7T scanner (Siemens Healthcare GmbH, Erlangen, Germany) with an 8-channel head coil for localised transmission with a 32-channel receive head coil insert (Nova Medical, Wilmington, USA).

A T1w structural scan was acquired based on a 3D fast low angle shot (FLASH) sequence with the following parameters: TR = 19.5 ms; TE = 2.3 ms; flip angle = 24°; field of

view = 364×426×288 mm^3; voxel size = 0.6×0.6×0.6 mm^3. The image was aligned with the structural image from the 3T session for ease of comparison, and served as the reference for the 7T fMRI pre-processing steps.

Two fMRI runs were acquired and were based on the BOLD signal, measured with a 3D T2*-weighted EPI sequence: volume acquisition time = 2332 ms; TR = 53 ms; TE = 20 ms; flip angle = 15°; field of view = 192×192×88 mm^3; voxel size = 1×1×1 mm^3; PAT acceleration factor of 8; partial Fourier 6/8 in the phase-encoded direction. Four additional EPI volumes were acquired with the opposite phase encoding to be used later for distortion correction.

The fMRI images were first denoised using NORDIC [11]. Then, the first two volumes of the first run were combined with their opposite phase encoding counterparts and passed to *topup* to calculate the susceptibility distortion field [12]. Afterwards, the images from both fMRI runs were concatenated and passed to *eddy* [13] where motion correction and susceptibility distortion correction (based on the *topup* field) were simultaneously applied, accounting for the effect of motion on these distortions [14]. The corrected images from both task runs, all of which were in alignment at this stage, were then aligned to the structural T1w image by way of a rigid body alignment performed in *flirt* [15] using the mutual information cost function and spline interpolation. Finally, the images were spatially smoothed with a Gaussian kernel of a FWHM of 1.0 mm.

During the two fMRI runs we presented YL with P- and M-type stimuli, as well as blank trials. The P stimulus was a sine wave checkerboard with a spatial frequency of 1.4 cycles/°, 90% contrast, and drifting at a speed of 1.5 °/s. The M stimulus had a spatial frequency of 0.35 cycles/°, 30% contrast, and a speed of 16 °/s. Each stimulus was presented eight times in blocks of approximately 24 s, interleaved by blank blocks of approximately 12 s. The stimulus subtended 20° in width and 10° in height due to the limited screen size at 7T, simultaneously targeting both hemifields, and was masked with a grey disk (3° in diameter) in the centre to ensure that the fixation cross remained visible. Here, again, YL engaged in a fixation task. A standard GLM was fitted to the data with a task effect (stimulus presentation) for each of the M- and P-type conditions, and six motion correction parameters as nuisance regressors. The two conditions were

directly compared to each other. All resulting statistical images were thresholded at a voxelwise significance level of $p < .001$. This was done in *SPM12*.

4.3 RESULTS

4.3.1 Experiment 1

Static Humphrey perimetry (30-2) revealed that YL had a dense homonymous right hemianopia (Figure 4.1). During psychophysical testing, he was very accurate in discriminating the direction of motion of drifting random checkerboards presented in his blind field (81% accuracy, $p < .001$) and was aware of them (71% certainty).

Structural imaging revealed a large lesion covering a sizeable portion of the left temporal lobe, with significant gliosis extending into the inferior parietal lobe. Prior to surgery, the intraventricular tumour had substantially expanded, compressing the white matter of the temporal lobe, and displacing subcortical structures such as the thalamus and basal ganglia. Despite this, using tractography, we were able to successfully track white matter connections between the thalamus and visual cortex, including V1 and V5 (Figure 4.1).

fMRI revealed that YL's visual cortex in general is highly responsive to moving random checkerboards (Figure 4.1). The BOLD signal change associated with these stimuli was highly significant in a large portion of visual cortex, spanning medial, dorsal, and lateral visual cortical areas, including V2, V3 and V5. In contrast, the same random checkerboards failed to elicit any significant activations when they were presented statically.

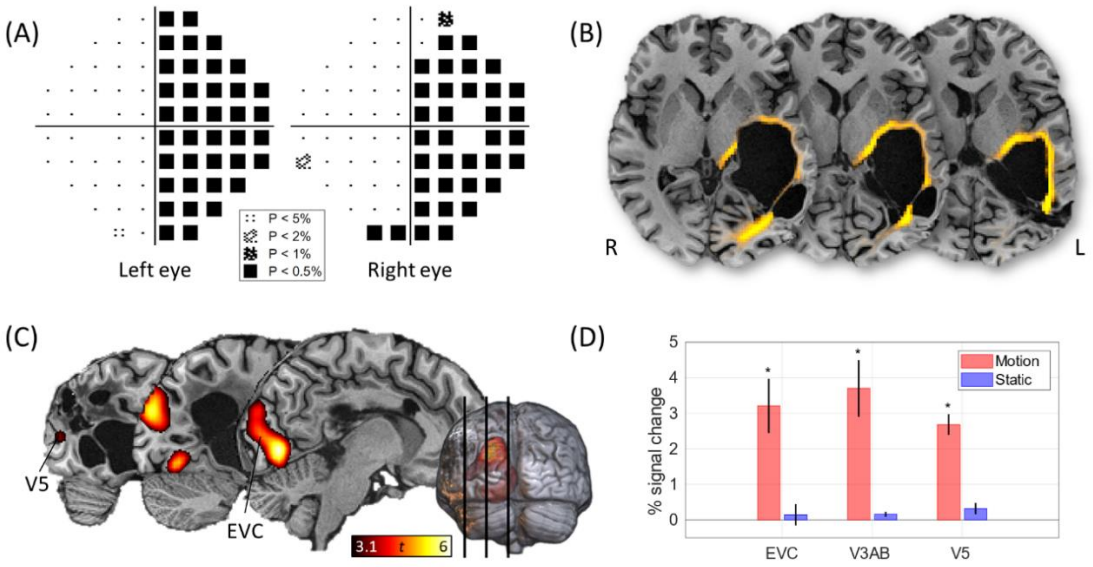

Figure 4.1. Strong responses to visual motion in the blind field in YL's brain driven by direct thalamic input.
(A) Perimetry results revealed that YL has a dense homonymous right hemianopia. The plots shown here are statistical displays that correspond to pattern deviation, i.e., the percentage of the normal population who measure below the patient's value at each retinal point, corrected for optical impairments that affect the eye. The black squares indicate that YL is unable to detect bright flashes of light presented in his right visual field, while the small dots show that his vision is normal in the left visual field. **(B)** The tractographic reconstruction of the optic radiations connecting the LGN with visual cortex, including V5 and V1, in YL's brain. **(C)** fMRI activity in visual cortex in response to fast-moving random checkerboards presented in YL's blind field ($p < .001$). **(D)** fMRI BOLD signal changes in early visual cortex (EVC), V3A and V3B, and V5 were strong in response to drifting random checkerboards, but absent when the same checkerboards were static.

4.3.2 Experiment 2

In the first experiment, there was a very strong response in early visual cortex, including visual areas V2 and V3, to moving stimuli but an insignificant response to their static counterparts, despite a direct subcortical input to visual cortex in general [16,17]. This led us to hypothesise that the M and P visual pathways may have been affected differentially by the lesion. It was also difficult, due to the limited resolution of the 3T fMRI data, to ascertain whether V1 in and around the calcarine sulcus was active, or whether we were instead measuring the partially overlapping signal from neighbouring V2. Therefore, we extended our studies by using high-resolution fMRI at 7T to determine whether the P and M inputs had been differentially compromised.

Psychophysical testing confirmed that YL's ability to consciously perceive moving stimuli and accurately discriminate their direction of motion is very much dependent on the spatial frequency of the stimuli (Table 4.1); his performance was very good with low frequency checkerboards (93% accuracy, $p < .001$) but at chance for high frequency ones (52% accuracy, $p = .286$) (Figure 4.2).

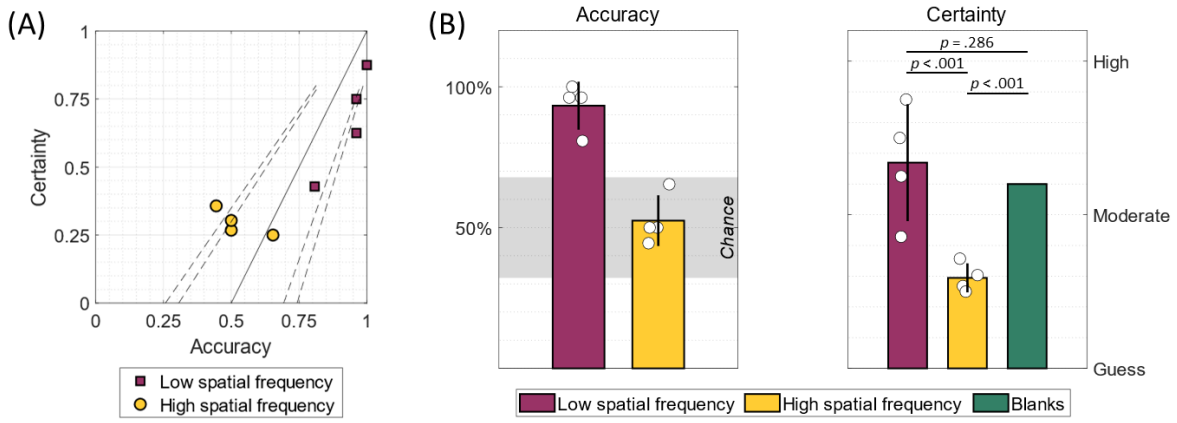

Figure 4.2. Different responses to spatial frequency.
(A) YL's accuracy and certainty per condition during the visual-motion task, in which he had to discriminate the direction of motion of a stimulus presented in his blind field. YL's performance was highly influenced by the spatial frequency of the stimulus. The solid line represents a psychophysical model that assumes that certainty and accuracy are strongly linked; the dashed lines represent the boundaries of the model under the binomial distribution at $p < .05$ and $p < .01$, calculated for 28 trials per condition. The points represent the eight different conditions. **(B)** The same data from the first plot grouped by spatial frequency, with the addition of the mean certainty rating that YL gave in response to blank trials that did not contain a stimulus, indicating that he was likely hallucinating visual motion.

YL's certainty ratings in this experiment were interesting. Expectedly and in line with his performance, he reported high certainty (67% ± 19%) for low frequency trials, and lower certainty (29% ± 5%) for high frequency ones. Consistent with the latter result, a type 2 ROC analysis revealed that metacognitive sensitivity was 0.50 on high frequency trials, indicating that ST could not discriminate between correct and incorrect responses, further supporting that he did not consciously perceive these stimuli. However, a type 2 ROC analysis also revealed that his sensitivity was 0.53 on low frequency trials, that is, trials in which he indicated perceiving the stimulus. This suggests that his confidence does not discriminate between correct and incorrect trials on these trials either,

indicating a curious instance of failure or lack of metacognition, which has been observed in another case of the Riddoch syndrome as well [18].

Moreover, his certainty ratings for the blank trials, during which there was no visual stimulation, were remarkably high (60% ± 38%) and comparable to his ratings for low frequency trials ($t(130) = 0.82$, $p = .416$, *n.s.*); they were in fact much higher than his responses to high frequency stimuli ($t(130) = 3.89$, $p < .001$). This suggested that, when a stimulus is expected but not presented, YL could be hallucinating visual motion. To explore this further, we presented him with a blank screen for 2m30s (grey background with a fixation cross) and asked him to verbally respond whenever he detected motion in his blind field. He frequently reported seeing motion, and his experience varied in intensity, e.g., he occasionally described this hallucinated motion by exclaiming "oh, this was a big one!"

	Low spatial frequency (LF)		**High spatial frequency (HF)**	
	Low contrast (LC)	**High contrast (HC)**	**Low contrast (LC)**	**High contrast (HC)**
Low speed (LS)	A: 81%*, C: 43%	A: 96%*, C: 75%	A: 50%, C: 27%	A: 50%, C: 30%
High speed (HS)	A: 96%*, C: 63%	A: 100%*, C: 88%	A: 65%, C: 25%	A: 44%, C: 36%

Table 4.1. Behavioural results from the second psychophysics session.
Accuracy and certainty scores in visual motion direction discrimination for stimuli varying in contrast, speed, and frequency. *A* represents accuracy in percentages and *C* represents certainty in percentages. For the blank condition, certainty was 60%. *Significantly different from chance performance ($p < .05$) determined from the binomial distribution for 28 trials.

High-resolution fMRI data showed that in the contralesional hemisphere, P activity was stronger than M activity within V1 (Figure 4.3); this was expected based on previously reported fMRI results [19]. In contrast, ipsilesional V1 responses to M stimuli were much stronger than those to P stimuli (Figure 4.3 and Table 4.2). This indicates that neural responses in ipsilesional V1 are selectively impaired for P stimuli, which explains why YL is perimetrically blind to static visual input presented in his right visual field.

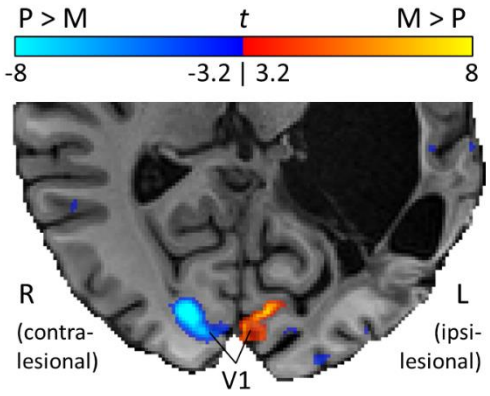

Figure 4.3. Comparison of neural responses to M and P stimuli in YL's visual cortex. YL performed an fMRI experiment at 7T in which two visual stimuli were presented bilaterally, one that preferentially engages the magnocellular visual pathway, M, and the other the parvocellular pathway, P. A direct comparison of the responses to the M and P stimuli revealed that contralesional V1 activity is much stronger for P compared to M stimuli, as expected. However, the reverse trend is true for ipsilesional V1, with much stronger responses to M compared to P stimuli.

Cluster and/or region	Voxels	$P_{Clust-FWE}$	T	Coordinates (mm)		
				x	y	z
M-type stimuli > P-type stimuli						
R V3	61	0.000	7.15	12	-71	0
L V1	2	0.014	5.88	-7	-81	6

Table 4.2. Results of the univariate 7T fMRI analysis.
Significant activations when comparing the magnocellular-stimulus condition with the parvocellular-stimulus condition. Reported are their corresponding peak t-statistic and coordinates in native space. The results in this table are stringently thresholded at FWE < 0.05.

4.4 DISCUSSION

Through our inquiry into patient YL, who is hemianopic but can see motion, we have demonstrated that the Riddoch syndrome can arise through a disconnection mechanism. In line with YL's visual impairment and spared motion perception, neural responses to static stimuli in his visual cortex are absent, while visual motion of low spatial frequency stimuli elicits strong, widespread activity. Yet, tractography showed that his optic radiations, although damaged, still connect his LGN with his visual cortex, including V1. We reconstructed these connections using diffusion MRI data acquired with a very high diffusion weighting value (b = 6000 s/mm^2), which is mainly sensitive to intra-axonal

diffusion [20], rendering the connections anatomically plausible despite their unusual shape due to the tumour's expansion. So, our findings in patient YL are puzzling: how could V1 receive direct subcortical input, just like prestriate cortex and V5, yet remain unresponsive under certain conditions which should otherwise strongly engage it?

We suspected that YL's P and M systems were differentially affected by the injury. The two systems arise from different populations of retinal ganglion cells; the P system carries information about high spatial frequencies (high resolution) and requires high luminance contrast, while the M system is mainly responsive to low spatial frequencies (low resolution) and fast motion [10]. Therefore, an impaired P system would result in blindness according to static perimetry assessments, while a spared M system would be sufficient for the perception of visual motion. Indeed, psychophysical testing using stimuli of high and low spatial frequencies confirmed that YL's ability to discriminate visual motion direction requires low frequency inputs. Also, upon further investigation using high-resolution fMRI, we observed that the response properties of his ipsilesional V1 were unusual in that they were much stronger for M stimuli compared with P stimuli, which is the opposite trend of contralesional V1. The detected M signal in V1 is unlikely to be the simple result of feedback from other areas such as V5 because, if this were the case, one would also expect to measure strong feedback signals for P inputs in V1 from areas such as V2. We therefore propose that in patient YL, thalamic P input to V1 is compromised.

A possible explanation for this differential functional response could be that that M system is more resilient to injury than the P system. Anatomically, M neurons have larger axonal diameters and thicker myelin sheaths, and they can be preferentially spared in the pre-geniculate optic pathway in autoimmune diseases like multiple sclerosis [21]. Curiously, Zappia et al. [22] wrote about two patients who exhibited symptoms of the Riddoch phenomenon and attributed their symptoms to non-cortical origins elsewhere in the visual pathway, such as the optic nerve and optic radiations, though without imaging data to rule out cortical involvement. The reverse trend of M and P responses in ipsilesional V1 could be caused by a more localised injury to fibres of the optic radiations that project to V1 but not to other visual areas. This is difficult to assess with imaging, especially given the very narrow anatomical passage that these fibres cross in the compressed white matter of the temporal lobe in YL's brain.

Alternatively, V1 could be particularly susceptible to any perturbation of the P system. V1 is the largest recipient of LGN input and the largest cortical distributor of visual signals to prestriate visual cortex [23,24]; the processing that occurs within V1 prior to its communication with these areas may be strongly dependent on the quality of thalamic input, which is compromised in YL's brain. This dependence may be more important for the P system, which is used to extract fine stimulus features such as contours and colour, whereas the M system may be more resilient to such disturbances as it is mainly interested in coarser features of the visual stimulus. Of course, these propositions remain speculative and are difficult to directly address with imaging data.

One very interesting finding is that YL has a high tendency to report seeing moving stimuli and is certain of correctly discriminating their direction of motion even when none are presented. In fact, YL's mean certainty score for blank trials (60%) is comparable to his score for low frequency stimuli (67%), and much higher than that for high frequency ones (29%). So, his certainty responses generally follow the psychophysical model in Figure 4.2, in which performance and certainty are tightly linked, but strongly deviate from the model only in the absence of visual stimulation. In the latter case, his high certainty reports suggest that these trials are accompanied by visual hallucinations and are an example of gnosanopsia, or awareness without discrimination [2,5], a phenomenon that we also observed in patient ST (described in the previous chapter). However, the hallucinations may possibly arise through a different mechanism; given the partial deafferentation of YL's visual cortex, a link can be drawn between his hallucinations and those described in the Charles Bonnet syndrome, which can arise following a mere reduction of visual input that leads to increased cortical excitability [25–28]. In YL's case, his lower confidence on high frequency trials can be explained by the fact that they are accompanied by a visual input that can regulate visual cortex even if YL cannot use this information to perform the task.

In conclusion, a partial disconnection of the optic radiations can lead to a selective loss of visual function where a patient can retain the ability to consciously perceive visual motion despite being blind to static visual stimuli. A differential resilience to injury in the M and P systems may lie at the origin of this anatomical variant of the Riddoch syndrome, in which V1 responses to P stimuli may be selectively impaired after injury to the optic

radiations. Therefore, these results raise important questions about the mechanisms that make the M and P systems differentially susceptible to such damage.

In addition, a further issue we wanted to address was the emergence of neural patterns in response to his different experiential states, a study bearing resemblance to the one conducted in the previous chapter. Unfortunately, we could not examine YL further, because he was suffering from frequent epileptic seizures. Nevertheless, this study has been an important contribution, because it has demonstrated that the Riddoch syndrome, including the manifestation of gnosanopsia, can occur with an intact V1.

REFERENCES

1. Riddoch, G. (1917). Dissociation of visual perceptions due to occipital injuries, with especial reference to appreciation of movement. Brain *40*, 15–57. 10.1093/BRAIN/40.1.15.

2. Zeki, S., and ffytche, D.H. (1998). The Riddoch syndrome: insights into the neurobiology of conscious vision. Brain *121*, 25–45. 10.1093/brain/121.1.25.

3. Ajina, S., Kennard, C., Rees, G., and Bridge, H. (2015). Motion area V5/MT+ response to global motion in the absence of V1 resembles early visual cortex. Brain *138*, 164–178. 10.1093/brain/awu328.

4. Arcaro, M.J., Thaler, L., Quinlan, D.J., Monaco, S., Khan, S., Valyear, K.F., Goebel, R., Dutton, G.N., Goodale, M.A., Kastner, S., et al. (2019). Psychophysical and neuroimaging responses to moving stimuli in a patient with the Riddoch phenomenon due to bilateral visual cortex lesions. Neuropsychologia *128*, 150–165. 10.1016/j.neuropsychologia.2018.05.008.

5. Beyh, A., Rasche, S.E., Leff, A., Ffytche, D., and Zeki, S. (2023). Neural patterns of conscious visual awareness in the Riddoch syndrome. J Neurol. 10.1007/S00415-023-11861-5.

6. Sincich, L.C., Park, K.F., Wohlgemuth, M.J., and Horton, J.C. (2004). Bypassing V1: A direct geniculate input to area MT. Nat Neurosci *7*, 1123–1128. 10.1038/nn1318.

7. ffytche, D.H., Guy, C.N., and Zeki, S. (1995). The parallel visual motion inputs into areas V1 and V5 of human cerebral cortex. Brain *118*, 1375–1394. 10.1093/brain/118.6.1375.

8. Schmid, M.C., Mrowka, S.W., Turchi, J., Saunders, R.C., Wilke, M., Peters, A.J., Ye, F.Q., and Leopold, D.A. (2010). Blindsight depends on the lateral geniculate nucleus. Nature *466*, 373–377. 10.1038/nature09179.

9. Ajina, S., Pestilli, F., Rokem, A., Kennard, C., and Bridge, H. (2015). Human blindsight is mediated by an intact geniculo-extrastriate pathway. Elife *4*, e08935. 10.7554/eLife.08935.

10. Kaplan, E. (2014). The M, P and K Pathways of the Primate Visual System Revisited. In The New Visual Neurosciences, J. S. Werner and L. M. Chalupa, eds. (MIT Press), pp. 215–226.

11. Vizioli, L., Moeller, S., Dowdle, L., Akçakaya, M., De Martino, F., Yacoub, E., and Uğurbil, K. (2021). Lowering the thermal noise barrier in functional brain mapping with magnetic resonance imaging. Nat Commun *12*, 5181. 10.1038/s41467-021-25431-8.

12. Andersson, J.L.R., Skare, S., and Ashburner, J. (2003). How to correct susceptibility distortions in spin-echo echo-planar images: application to diffusion tensor imaging. Neuroimage *20*, 870–888. 10.1016/S1053-8119(03)00336-7.

13. Andersson, J.L.R., and Sotiropoulos, S.N. (2016). An integrated approach to correction for off-resonance effects and subject movement in diffusion MR imaging. Neuroimage *125*, 1063–1078. 10.1016/j.neuroimage.2015.10.019.

14. Andersson, J.L.R., Graham, M.S., Drobnjak, I., Zhang, H., and Campbell, J. (2018). Susceptibility-induced distortion that varies due to motion: Correction in diffusion MR without acquiring additional data. Neuroimage *171*, 277–295. 10.1016/J.NEUROIMAGE.2017.12.040.

15. Jenkinson, M., Bannister, P., Brady, M., and Smith, S. (2002). Improved optimization for the robust and accurate linear registration and motion correction of brain images. Neuroimage *17*, 825–841. 10.1006/NIMG.2002.1132.

16. Cragg, B.G. (1969). The topography of the afferent projections in the circumstriate visual cortex of the monkey studied by the nauta method. Vision Res *9*, 733–747. 10.1016/0042-6989(69)90011-x.

17. Benevento, L.A., and Rezak, M. (1976). The cortical projections of the inferior pulvinar and adjacent lateral pulvinar in the rhesus monkey (macaca mulatta): An autoradiographic study. Brain Res *108*, 1–24. 10.1016/0006-8993(76)90160-8.

18. Persaud, N., Davidson, M., Maniscalco, B., Mobbs, D., Passingham, R.E., Cowey, A., and Lau, H. (2011). Awareness-related activity in prefrontal and parietal cortices in blindsight reflects more than superior visual performance. Neuroimage *58*, 605–611. 10.1016/j.neuroimage.2011.06.081.

19. Liu, C.S.J., Bryan, R.N., Miki, A., Woo, J.H., Liu, G.T., and Elliott, M.A. (2006). Magnocellular and parvocellular visual pathways have different blood oxygen level-dependent signal time courses in human primary visual cortex. American Journal of Neuroradiology *27*, 1628–1634.

20. Veraart, J., Fieremans, E., and Novikov, D.S. (2019). On the scaling behavior of water diffusion in human brain white matter. Neuroimage *185*, 379–387. 10.1016/J.NEUROIMAGE.2018.09.075.

21. Evangelou, N., Konz, D., Esiri, M.M., Smith, S., Palace, J., and Matthews, P.M. (2001). Size-selective neuronal changes in the anterior optic pathways suggest a differential susceptibility to injury in multiple sclerosis. Brain *124*, 1813–1820. 10.1093/BRAIN/124.9.1813.

22. Zappia, R.J., Enoch, J.M., Stamper, R., Winkelman, J.Z., and Gay, A.J. (1971). The Riddoch phenomenon revealed in non-occipital lobe lesions. Br J Ophthalmol *55*, 420. 10.1136/BJO.55.6.416.

23. Felleman, D.J., and Van Essen, D.C. (1991). Distributed hierarchical processing in the primate cerebral cortex. Cerebral Cortex *1*, 1–47. 10.1093/cercor/1.1.1.

24. Zeki, S. (2015). A massively asynchronous, parallel brain. Philosophical Transactions of the Royal Society B: Biological Sciences *370*, 20140174. 10.1098/rstb.2014.0174.

25. Braun, C.M.J., Dumont, M., Duval, J., Hamel-Hébert, I., and Godbout, L. (2003). Brain modules of hallucination: an analysis of multiple patients with brain lesions. Journal of Psychiatry and Neuroscience *28*, 432–449.

26. Boroojerdi, B., Bushara, K.O., Corwell, B., Immisch, I., Battaglia, F., Muellbacher, W., and Cohen, L.G. (2000). Enhanced excitability of the human visual cortex induced by short-term light deprivation. Cerebral Cortex *10*, 529–534. 10.1093/CERCOR/10.5.529.

27. Burke, W. (2002). The neural basis of Charles Bonnet hallucinations: a hypothesis. J Neurol Neurosurg Psychiatry *73*, 535–541. 10.1136/JNNP.73.5.535.

28. ffytche, D.H. (2005). Visual hallucinations and the Charles Bonnet syndrome. Curr Psychiatry Rep *7*, 168–179. 10.1007/S11920-005-0050-3/METRICS.

5.

The Sliding Consciousness Theory

The experiments presented thus far on the Riddoch syndrome challenge the conventional notion of a dissociation between performance and conscious awareness, as posited by "blindsight". Instead, discrimination and awareness appear to be tightly linked. There are, however, digressions from this. The sliding consciousness theory therefore proposes that in the Riddoch syndrome, the tight link between discrimination and awareness has been loosened. The Riddoch syndrome appears to consists of three different perceptual states; agnosopsia, i.e., discrimination without awareness, gnosanopsia, i.e., awareness without discrimination, and gnosopsia, in which discrimination and awareness are aligned. Moreover, conscious awareness of single visual attributes in the Riddoch syndrome correlates with neural activity patterns in the visual areas specialised for the processing of it, without the necessity of V1. This suggests that V1 is not a correlate of conscious visual awareness, which has implications for theories of consciousness. The emergence of activity patterns in relation to awareness of single visual attributes further raises the question of the presence of such patterns in other cognitive processes, especially more complex ones.

5.1 CONCLUDING REMARKS ON THE RIDDOCH SYNDROME

The Riddoch syndrome patients described in this thesis, as well as patients with lesions in V1 described by others [1–3], show that the ability to discriminate visual features and the awareness of these features are tightly linked. Therefore, there does not seem to be a dissociation between discriminatory performance and awareness, as suggested by "blindsight". However, there can be situations in which performance and awareness do not overlap. Zeki and ffytche [1] were the first to explicitly describe different perceptual states in a single Riddoch syndrome patient, and referred to these states as gnosopsia, gnosanopsia and agnosopsia.

5.1.1 Gnosopsia

Gnosopsia (derived from Greek, *gnosis* = knowledge and *opsia* = sight) is the most common state; this is the capacity to discriminate when aware. As can be gathered from both ST and YL, performance and awareness correlate strongly; when performance is high, certainty or confidence is also high, whereas with poor performance, certainty is low (Figure 2.5 and Figure 4.2). This is also observed in healthy individuals [4].

5.1.2 Gnosanopsia

Gnosanopsia (derived from Greek, *gnosis* = knowledge and *anopsia* = without sight) refers to awareness without discrimination. Zeki and ffytche [1] coined the term as they observed that patient GY occasionally was aware of something in his blind field, despite not being able to discriminate it. Another recent study further emphasised this point: a number of patients reported some degree of awareness, despite performing at chance levels [5]. The patients described here demonstrate this manifestation even more clearly; ST consistently indicated being highly certain of the direction of motion of a stimulus when it was of high spatial frequency, high speed and high contrast, despite his performance being at chance; he was thus aware of a stimulus, but failed to discriminate it correctly. This awareness is further demonstrated by ST's metacognitive sensitivity on these trials; as opposed to conditions where the patient is completely blind and has no metacognitive sensitivity (i.e., is unconscious), in the case of gnosanopsic ambiguity there was higher sensitivity than one would expect by chance, indicating that ST showed signs of 'blind insight' [6]; despite his chance performance, he had knowledge about which trials he had been correct on. This suggests that in this phenomenon there exists some degree of

conscious introspective, or metacognitive, insight about the judgements that have been made. Moreover, ST and YL have added another, previously unreported, key feature to gnosanopsia, namely that of visual hallucinations. Both patients, one more frequently than the other, reported being certain of perceiving motion, despite not being presented with any; in this case there is awareness without any "objective" performance. Thus, the state of gnosanopsia has increased significance with the present findings. Furthermore, we have been able to chart the neural correlates of this specific manifestation of the Riddoch syndrome. Whereas Zeki and ffytche [1] did not attribute any activity outside of V5 to it, we have found that depending on whether gnosanopsia occurred with or without stimulation, the inferior frontal gyrus or the hippocampus became involved in the conscious experience. This is therefore an instance of experience-dependent connections; the 'silent' connection between these areas and V5 only became demonstrable through these specific experiences.

5.1.3 Agnosopsia

Finally, there is agnosopsia (derived from Greek, *agnosia* = no knowledge and *opsia* = sight), or discrimination without awareness. One may object that this refers to the same condition as blindsight, which indeed it does; however, it is important to emphasize that agnosopsia, along with the other states, are all manifestations of a single condition, namely that of the Riddoch syndrome. "Blindsight" is therefore one aspect of a larger syndrome and thus not a separate disorder; nor are type-1 and type-2 categorically distinct. The occurrence of agnosopsia was not observed in the patients described here, but has been described by others [1,7,8]. Interestingly, we did observe chance metacognitive sensitivity with above chance performance in YL. This could possibly be interpreted as an instance of discrimination without awareness [9], given that metacognition can be used as an index of consciousness [10]. It is, however, important to keep in mind that the vision of these patients is very degraded; it is obviously challenging to discriminate stimuli that are presented near the threshold of visibility. In fact, 'blindsight-like' states can also be induced in healthy subjects [4,11]. Given that awareness and discrimination are not perfectly correlated, it remains possible that conditions may occur in which performance is better than chance, despite the disbelief of the subject. However, awareness and discrimination are nevertheless strongly linked, and therefore a near perfect performance on discrimination tasks without any awareness is improbable.

5.1.4 The sliding theory of consciousness

Thus, in both the Riddoch syndrome and healthy subjects, discrimination and awareness are tightly coupled. However, after damage to V1, in contrast to healthy individuals, it seems that this coupling is loosened. The uncoupling between discrimination and awareness may lead on the one hand to agnosopsia and on the other to gnosanopsia (Figure 5.1). This uncoupling is also illustrated by the metacognitive sensitivity of these patients; as we have seen, there are instances of chance performance with higher than chance metacognitive sensitivity, and the reverse, that is, above chance performance with chance metacognitive sensitivity. This is not to say that these states of agnosopsia and gnosanopsia do not occur in healthy subjects; hallucinations, blind insight and blindsight-like states can be experimentally induced in them [4,6,11]. However, it appears to be more prevalent or easily induced in the Riddoch syndrome. We therefore refer to this uncoupling as the 'sliding theory of consciousness'.

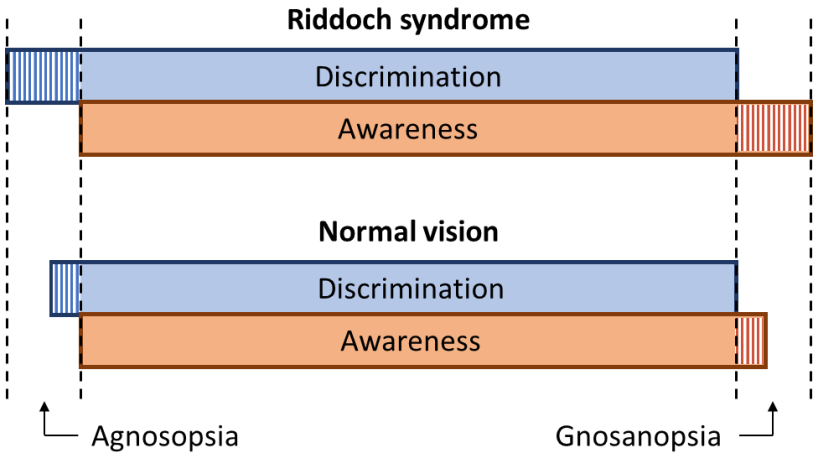

Figure 5.1. The sliding theory of consciousness.
In normal vision, awareness and discrimination typically go hand in hand, and departures from this, i.e. discrimination without awareness (agnosopsia) or awareness without discrimination (gnosanopsia), rarely occur. In the Riddoch syndrome too, awareness and discrimination are tightly linked. However, departures from this state seem to occur more often, or are at least more easily induced. This figure has been adopted from Zeki and ffytche [1].

5.2 MICRO-CONSCIOUSNESS

Another conclusion that we can draw from these studies on the Riddoch syndrome is that the conscious perception of a specific visual feature dictated the emergence of activity

patterns in prestriate visual areas that are responsible for the processing of it. Can this finding be linked to any theories of consciousness?

Many theories have been proposed to explain how consciousness arises in the brain; one of these theories, not quite as grand as others, is the theory of micro-consciousness, which argues that phenomenal consciousness consists of many micro-consciousnesses that are distributed in space and time [12]. This was proposed because different phenomenal components are processed in different locations and at different temporalities [13,14]. The theory implies that there is no unity of consciousness at the level of phenomenal consciousness. This is, however, not noticeable in day to day life – the several micro-conscious components that occur together are perceived as one on a macroscale, i.e., in macro-consciousness [15].

Various empirical observations led to the formulation of this theory. First is the fact that different parts of the visual brain perform different functions, that is, there is functional specialisation within the brain. This is clearly demonstrated by both physiological and human imaging studies [14,16,17], which show that different cardinal visual features are processed in anatomically different parts.

Second, there is the phenomenon of perceptual asynchrony. Functional specialisation raises the question of how the various features are bound together to give the experience of the world as a unified whole. Some theories of consciousness posit that binding between visual features is the prelude to conscious experience of the visual stimulus [18]. But psychophysical experiments have demonstrated that we do not see all visual features at the exact same time. Consequently, subjects mis-bind visual features that occur together in real time [13,19–22]. This demonstrates that the brain processes information asynchronously, that is, brain regions do not wait for other brain regions to complete the information processing [23].

Third, the processing regions of sensory information also appear to be perceptual regions. This argument is demonstrated by clinical evidence showing that lesions in V5 lead to akinetopsia (the inability to perceive motion) [24,25], whereas achromatopsia (the inability to perceive colour) is produced by lesions in V4 [26]. The studies on the Riddoch syndrome presented here further accentuate this point; as we saw in chapter 2, when V5

is disconnected from V1, following lesions in V1, the subject may still be able to perceive visual motion consciously, and this perception correlates with a distinct neural pattern in V5. In chapter 3 it was shown that the conscious discrimination between coloured and non-coloured stimuli was accompanied by a specific decodable activity pattern in V4 complex. Thus, these clinical observations show that the conscious experience of a particular visual feature is disrupted when there is damage to the relevant, specialised area, whereas conscious vision is preserved when the area is uninjured but other visual areas of the cortex are damaged, including V1, as long as the connections between the subcortex and the specialised region remain intact.

Importantly, although the theory of micro-consciousness argues that different regions can acquire a conscious correlate, it does not claim that no other regions are involved; putting V5 in a petri dish and exposing it to motion should not lead to awareness of visual motion. Instead, the theory proposes that if, for example, most of the visual cortex is damaged but V5 is intact, connected to the rest of the brain and receiving direct subcortical visual input, it is likely that this hypothetical subject would be able to perceive visual motion. Therefore, certain propositions can be eliminated, such as the proposal that conscious experience of visual motion requires return input from V5 to V1 [27]. Furthermore, the studies presented here on the Riddoch syndrome, in addition to the studies demonstrating perceptual asynchrony, undermine the idea that binding is a necessary prerequisite for conscious visual experience [18], since subjects can be conscious of a single visual feature in an 'unbound' state. Instead, the results described in this thesis support the theory of micro-consciousness, but other theories may be supported by these results as well.

5.3 DECODING 'HIGHER' COGNITIVE FUNCTIONS

In summary, I hope to have provided convincing evidence demonstrating that V1 is not necessary for visual consciousness; visual awareness of a specific visual attribute can be sustained if the relevant visual sensory area and subcortical pathways are intact. The studies described in this thesis add another important insight, namely that when there is awareness of a specific visual attribute, a distinct neural pattern emerges in the specialised visual area as a correlate.

Another conclusion that we can draw from these studies on the Riddoch syndrome is that the multivariate approach can reveal neural correlates which otherwise remain occult. For example, we found that neural activity patterns emerged in V5 during the hallucination of motion, yet there was no increased univariate activity in this region. Another example is the detection of red-green stimuli in the Riddoch syndrome; such stimuli did not lead to significant increased univariate activity in any region of the brain, but patterns did emerge in prestriate areas. Thus, if we had solely relied on the univariate analysis, we would not have concluded that these regions were involved in any significant way, and significant experience-dependent brain connections would not have been revealed. However, it should be pointed out that we designed these studies in such a way that the multivariate analysis could be carried out effectively; we opted for an event-related design, rather than a block-design. This experimental design may be more suitable for the multivariate approach instead of the univariate one, since a proper parameter estimate of single trials is critical [28]. This could explain discrepancies between our results and those of others. For example, using a block-design, others have found increased univariate activity in V4 when Riddoch patients were presented with chromatic stimuli in the blind field [29].

Importantly, the multivariate approach is not necessarily superior to the univariate one; although it may have increased sensitivity in certain situations and reveal significant multidimensional differences which the univariate approach cannot detect, it should be emphasised that it constitutes a different way of looking at the data, which does not mean that it is necessarily a better way. For example, it could be the case that distinct voxels of a given region of interest are activated by each stimulus, therefore not amounting to a high correlation between patterns. Yet, when taking the average activity of the voxels in this region of interest, there can be a significant increase in activity. In this situation, the univariate approach would be able to detect its involvement. The two methods thus reveal different aspects [30], which makes it desirable to combine both types of analyses, as this would lead to a more holistic understanding of the underlying neural mechanisms.

By combining both approaches, we have found that different perceptual states in the Riddoch syndrome engage different neural networks; when the patient consciously discriminated motion, V5 was involved, whereas with the discrimination of coloured stimuli V4 was involved. We did not find patterns in these areas when these attributes

were not consciously perceived. Involvement of additional areas was also revealed, depending on the experience, and neural activity patterns emerged in them. Having thus established the presence of such patterns in correlation with the conscious perception of single visual attributes (sometimes referred to as "low-level" features), such as motion and colour, a natural question arises: do specific activity patterns emerge with the perception of more complex attributes, such as aesthetic experiences? These "higher-level" experiences are not simply processed in a dedicated visual sensory area. Instead, they correlate with recruitment of additional, often frontal [31], brain areas, because additional cognitive processes are involved. For example, the experience of beauty includes judgement, emotion and reward, and needs to be orchestrated with one's internal goals. Therefore, such an experience requires more than the processing of incoming sensory input and may not be as purely perceptual as orientation, form and colour are. In fact, it has repeatedly been shown that field A1 of the medial orbitofrontal cortex is involved in the experience of beauty, regardless of its source [32,33]. This part of the brain has been implicated in reward [34], emotion [35] and decision-making [36].

Nevertheless, the same analytical approach that was used to study the perception of "low-level" features in the Riddoch syndrome can be used to study "high-level" perceptual processes [37]. Therefore, to answer this question that had emerged, we investigated whether aesthetic experiences, namely those of abstract beauty and facial ugliness, correlate with neural activity patterns and, if so, in which brain areas. By enquiring into the neural activity involved in these experiences, including its spatial arrangement, experience-dependent connections may be revealed.

REFERENCES

1. Zeki, S., and ffytche, D. (1998). The Riddoch syndrome: insights into the neurobiology of conscious vision. Brain *121*, 25–45. 10.1093/brain/121.1.25.

2. Overgaard, M., Fehl, K., Mouridsen, K., Bergholt, B., and Cleeremans, A. (2008). Seeing without seeing? Degraded conscious vision in a blindsight patient. PLoS One *3*, e3028. 10.1371/journal.pone.0003028.

3. Mazzi, C., Bagattini, C., and Savazzi, S. (2016). Blind-sight vs. degraded-sight: different measures tell a different story. Front Psychol *7*, 1–11. 10.3389/fpsyg.2016.00901.

4. Stein, T., Kaiser, D., Fahrenfort, J.J., and van Gaal, S. (2021). The human visual system differentially represents subjectively and objectively invisible stimuli. PLoS Biol *19*, e3001241. 10.1371/journal.pbio.3001241.

5. Garric, C., Sebaa, A., Caetta, F., Perez, C., Savatovsky, J., Sergent, C., and Chokron, S. (2019). Dissociation between objective and subjective perceptual experiences in a population of hemianopic patients: A new form of blindsight? Cortex *117*, 299–310. 10.1016/j.cortex.2019.05.006.

6. Scott, R.B., Dienes, Z., Barrett, A.B., Bor, D., and Seth, A.K. (2014). Blind insight: metacognitive discrimination despite chance task performance. Psychol Sci *25*, 2199–2208. 10.1177/0956797614553944.

7. Weiskrantz, L., Barbur, J.L., and Sahraie, A. (1995). Parameters affecting conscious versus unconscious visual discrimination with damage to the visual cortex (V1). Proceedings of the National Academy of Sciences *92*, 6122–6126. 10.1073/pnas.92.13.6122.

8. Sahraie, A., Weiskrantz, L., Barbur, J.L., Simmons, A., Williams, S.C.R., and Brammer, M.J. (1997). Pattern of neuronal activity associated with conscious and unconscious processing of visual signals. Proceedings of the National Academy of Sciences *94*, 9406–9411. 10.1073/pnas.94.17.9406.

9. Persaud, N., Davidson, M., Maniscalco, B., Mobbs, D., Passingham, R.E., Cowey, A., and Lau, H. (2011). Awareness-related activity in prefrontal and parietal cortices in blindsight reflects more than superior visual performance. Neuroimage *58*, 605–611. 10.1016/j.neuroimage.2011.06.081.

10. Michel, M. (2023). Confidence in consciousness research. WIREs Cognitive Science *14*, e1628. 10.1002/wcs.1628.

11. Hesselmann, G., Hebart, M., and Malach, R. (2011). Differential BOLD Activity Associated with Subjective and Objective Reports during "Blindsight" in Normal Observers. The Journal of Neuroscience *31*, 12936–12944. 10.1523/JNEUROSCI.1556-11.2011.

12. Zeki, S., and Bartels, A. (1999). Toward a theory of visual consciousness. Conscious Cogn *8*, 225–259. 10.1006/ccog.1999.0390.

13. Moutoussis, K., and Zeki, S. (1997). A direct demonstration of perceptual asynchrony in vision. Proc R Soc Lond B Biol Sci *264*, 393–399. 10.1098/rspb.1997.0056.

14. Zeki, S., Watson, J., Lueck, C., Friston, K., Kennard, C., and Frackowiak, R. (1991). A direct demonstration of functional specialization in human visual cortex. The Journal of Neuroscience *11*, 641–649. 10.1523/JNEUROSCI.11-03-00641.1991.

15. Zeki, S. (2003). The disunity of consciousness. Trends Cogn Sci *7*, 214–218. 10.1016/S1364-6613(03)00081-0.

16. Zeki, S.M. (1978). Functional specialisation in the visual cortex of the rhesus monkey. Nature *274*, 423–428. 10.1038/274423a0.

17. Livingstone, M., and Hubel, D. (1988). Segregation of form, color, movement, and depth: anatomy, physiology, and perception. Science (1979) *240*, 740–749. 10.1126/science.3283936.

18. Crick, F., and Koch, C. (1990). Towards a neurobiological theory of consciousness. Seminars in the Neurosciences *2*, 263–275.

19. Holcombe, A.O. (2009). Temporal binding favours the early phase of colour changes, but not of motion changes, yielding the colour–motion asynchrony illusion. Vis cogn *17*, 232–253. 10.1080/13506280802340653.

20. Lo, Y.T., and Zeki, S. (2014). Perceptual asynchrony for motion. Front Hum Neurosci *8*, 108. 10.3389/fnhum.2014.00108.

21. Viviani, P., and Aymoz, C. (2001). Colour, form, and movement are not perceived simultaneously. Vision Res *41*, 2909–2918. 10.1016/S0042-6989(01)00160-2.

22. Arnold, D.H., Clifford, C.W.G., and Wenderoth, P. (2001). Asynchronous processing in vision: color leads motion. Current Biology *11*, 596–600.

23. Zeki, S. (2015). A massively asynchronous, parallel brain. Philosophical Transactions of the Royal Society B: Biological Sciences *370*, 20140174. 10.1098/rstb.2014.0174.

24. Zihl, J., Von Cramon, D., and Mai, N. (1983). Selective disturbance of movement vision after bilateral brain damage. Brain *106*, 313–340. 10.1093/brain/106.2.313.

25. Zeki, S. (1991). Cerebral akinetopsia (visual motion blindness): a review. Brain *114*, 811–824. 10.1093/brain/114.2.811.

26. Zeki, S. (1990). A century of cerebral achromatopsia. Brain *113*, 1721–1777. 10.1093/brain/113.6.1721.

27. Lamme, V.A.F. (2001). Blindsight: the role of feedforward and feedback corticocortical connections. Acta Psychol (Amst) *107*, 209–228. 10.1016/S0001-6918(01)00020-8.

28. Kriegeskorte, N. (2008). Representational similarity analysis – connecting the branches of systems neuroscience. Front Syst Neurosci *4*. 10.3389/neuro.06.004.2008.

29. Schoenfeld, M.A., Noesselt, T., Poggel, D., Tempelmann, C., Hopf, J.-M., Woldorff, M.G., Heinze, H.-J., and Hillyard, S.A. (2002). Analysis of pathways mediating preserved vision after striate cortex lesions. Ann Neurol *52*, 814–824. 10.1002/ana.10394.

30. Davis, T., LaRocque, K.F., Mumford, J.A., Norman, K.A., Wagner, A.D., and Poldrack, R.A. (2014). What do differences between multi-voxel and univariate analysis mean? How subject-, voxel-, and trial-level variance impact fMRI analysis. Neuroimage *97*, 271–283. 10.1016/j.neuroimage.2014.04.037.

31. Frith, C., and Dolan, R. (1996). The role of the prefrontal cortex in higher cognitive functions. Cognitive Brain Research *5*, 175–181. 10.1016/S0926-6410(96)00054-7.

32. Zeki, S., Romaya, J.P., Benincasa, D.M.T., and Atiyah, M.F. (2014). The experience of mathematical beauty and its neural correlates. Front Hum Neurosci *8*. 10.3389/fnhum.2014.00068.

33. Ishizu, T., and Zeki, S. (2011). Toward a brain-based theory of beauty. PLoS One *6*, e21852. 10.1371/journal.pone.0021852.

34. Fliessbach, K., Rohe, T., Linder, N.S., Trautner, P., Elger, C.E., and Weber, B. (2010). Retest reliability of reward-related BOLD signals. Neuroimage *50*, 1168–1176. 10.1016/j.neuroimage.2010.01.036.

35. D'Argembeau, A., Jedidi, H., Balteau, E., Bahri, M., Phillips, C., and Salmon, E. (2012). Valuing one's self: medial prefrontal involvement in epistemic and emotive investments in self-views. Cerebral Cortex *22*, 659–667. 10.1093/cercor/bhr144.

36. Klein-Flügge, M.C., Bongioanni, A., and Rushworth, M.F.S. (2022). Medial and orbital frontal cortex in decision-making and flexible behavior. Neuron *110*, 2743–2770. 10.1016/j.neuron.2022.05.022.

37. Haynes, J.-D., and Rees, G. (2006). Decoding mental states from brain activity in humans. Nat Rev Neurosci *7*, 523–534. 10.1038/nrn1931.

Part II

6.

Neural Correlates of the Experience of Abstract Beauty

We enquired into the neural activity that correlates with the experience of beauty aroused by abstract paintings. During the brain imaging experiments, subjects rated abstract paintings according to aesthetic appeal. There was low agreement on the aesthetic classification of these paintings among participants. Univariate analyses revealed higher activity with higher declared aesthetic appeal in both the visual areas and the medial frontal cortex. Additionally, representational similarity analysis (RSA) revealed that the experience of beauty correlated with decodable patterns of activity in visual sensory areas. These results are broadly similar to those obtained in previous studies on facial beauty. With abstract art, it was the involvement of visual areas implicated in the processing of lines and colours, while with faces it was of visual areas implicated in the processing of faces. Both categories of aesthetic experience correlated with increased activity in medial frontal cortex. We conclude that the sensory areas participate in the selection of stimuli according to aesthetic appeal and that it is the co-operative activity between the sensory areas and the medial frontal cortex that is the basis for the experience of abstract visual beauty. Further, this co-operation is enabled by experience-dependent functional connections, in the sense that currently the existence and high specificity of these connections can only be demonstrated during certain experiences.

This chapter overlaps significantly with published work:
Rasche, S. E.*, Beyh, A.*, Paolini, M., & Zeki, S. (2023). The neural determinants of abstract beauty. *European Journal of Neuroscience, 57*(4), 633-645. https://doi.org/10.1111/ejn.15912

6.1 INTRODUCTION

What are the qualities in an object that arouse the sense of beauty, or what Clive Bell [1] termed the "aesthetic emotion"? Yang et al. [2] addressed this question by enquiring into the determinants of one of the most common sources of beauty, namely facial beauty. Features such as symmetry, proportion, and mathematically defined precise relationships between its constituent parts, have been posited by many, including leading artists such as Polykleitos and Leonardo Da Vinci, to be fundamental determinants of facial beauty, in the sense that without these biologically determined and inherited characteristics a face cannot be qualified as beautiful [3,4]. But even though essential, these characteristics are not in themselves necessarily sufficient to render a face beautiful; there is, in addition, another, or other, unknown and mysterious characteristics that do so. Whereas the viewing of faces is known to elicit activity in sensory face-perceptive areas [5–8], the study by Yang et al. [2] revealed that when a face is perceived as beautiful and only then, decodable activity patterns emerge not only in these face-processing areas of the visual brain, but parallel decodable activity also emerges in the medial orbitofrontal cortex, a region of the brain in which activity correlates with the experience of beauty, regardless of the source [9–13]. For faces at least, it is seemingly the joint activity of both components – the sensory on the one hand and the emotional on the other – that lies at the basis of the experience of beauty. This is thus an instance of an experience-dependent connection; it is only when a face is perceived as beautiful, that the connection between the sensory face-perceptive areas and the medial orbitofrontal cortex becomes evident.

Facial beauty has been classified as belonging to the biological category of beauty [4]. In the present study, we ask the same question of artifactual beauty, that is, beauty generated by human agency. Many artists, including those belonging to the schools of Abstract Expressionism, Neo-Plasticism and Russian Constructivism, considered that particular arrangements of lines and colours result in aesthetic experiences and consequently made such arrangements central to their art. The English art critic, Clive Bell, believed that "…lines and colours combined in a particular way [to produce] certain forms and relations of forms, stir our aesthetic emotions"; he did not specify what these particular combinations may be but argued that, "It need be agreed only that forms arranged and combined according to some unknown and mysterious laws do move us in a particular way and that it is the business of the artist to combine and arrange them that they shall

move us" [1]. Thus, there is in abstract paintings that arouse the aesthetic emotion, a mysterious and ineffable quality, just as there is in faces. Could that mysterious element also be represented in the form of decodable patterns in sensory areas of the visual brain that process lines and colours, just as happens in sensory face-processing areas when faces that arouse the aesthetic emotion are viewed? And would the emergence of decodable patterns in these sensory areas also correlate with the parallel emergence of decodable activity in medial frontal cortex, thus mirroring the network of brain activity during the experience of facial beauty? If so, an overall plausible interpretation would be that, whatever the mysterious qualities that endow stimuli, irrespective of their provenance, with the capacities of arousing the aesthetic emotion of beauty, they are represented in detectable patterns within the sensory areas that are specialised in the processing of those stimuli, as well as decodable activity within the medial frontal cortex.

For this study, given that the stimuli consisted of arbitrary assemblies of lines and colours, we expected that for stimuli experienced as beautiful, visual areas reported to have large concentrations of orientation-selective and colour selective cells will be active, namely, V1-V4 (including areas V3A and V3B) as well as areas in the intraparietal sulcus [14–21]. Moreover, we also expected to find increased activity in the medial frontal cortex, as this region is shown to be involved in beauty, regardless of the source. It would therefore be the co-operative emergence of activity in both sensory areas and in the medial frontal cortex that would lead to the experience of beauty derived from abstract art.

To avoid confusion, a brief terminological guide to the area of activation in medial prefrontal cortex will be given here. Although involving a common area, the exact location of activations there has varied across studies of the neural correlates of beauty, and different anatomical terms have been used to refer to the location in the literature, including medial orbitofrontal cortex (mOFC), medial prefrontal cortex (mPFC), ventromedial prefrontal cortex (vmPFC), and anterior cingulate cortex (aCC). Ishizu and Zeki [10] addressed this point and suggested that the region of medial frontal activations related to aesthetic experiences be labelled 'Field A1', a functionally defined region which does not necessarily obey anatomical or cytoarchitectonic boundaries; field A1 has its centre at Montreal Neurological Institute (MNI) coordinates [-3 41 -8] mm and a

diameter of 15-17 mm. Therefore, any activations within the medial frontal cortex that fall within mOFC, mPFC, vmPFC, and aCC will here be referred to as field A1.

6.2 METHODS

6.2.1 Participants

Eighteen healthy subjects (11 females, 7 males; ages 20-31 years, mean age 26.5 ± 3.2) participated in the study; all were right-handed and had normal or corrected-to-normal vision, all gave informed consent, and none was an artist or had art expertise. The experiment was approved by the ethical committee of Ludwig-Maximilians-Universität Munich (LMU), where the imaging experiments were conducted.

6.2.2 Stimuli

The stimuli consisted of 120 images of abstract paintings consisting of arbitrary assemblies of lines and colours. The images were obtained from a previous study [22] and additional paintings were selected from stock image websites. The stimuli were scaled to 500×500 pixels, presented in their original colour, and were not cropped or modified. The task was programmed in the *Presentation* software package (Neurobehavioral Systems, Inc., Albany, CA). Iconic paintings and schools were excluded, and no painting had faces or objects portrayed.

6.2.3 Procedure

Participants were presented with images of abstract paintings inside the MRI scanner and were asked to rate them on a scale from one to seven, one corresponding to not 'beautiful at all' and seven to 'very beautiful'. Pressing the left button on a customised button box shifted the pointer on the scale to a lower rating, while pressing the right button shifted it to a higher one, starting at the middle (rating of four) on each trial. The task followed an event-related design in which the stimulus was presented for a duration of 2 s and participants had 4.5 s to respond (Figure 6.1). The scanning consisted of five functional magnetic resonance imaging (fMRI) runs, each containing 24 trials. This, in addition to structural scans, amounted to a total scan time of 45 minutes for each subject.

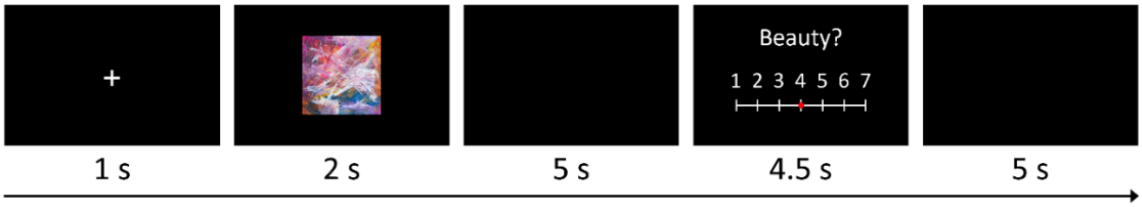

Figure 6.1. Experimental design.
Each trial started with a 1 s fixation cross, followed by a 2 s stimulus presentation, which was followed by a 5 s blank screen. Subjects then rated the stimulus on aesthetic appeal within 4.5 s on a scale from 1 to 7 (1 – not beautiful at all, 7 – very beautiful). Responses were followed by a 5 s blank screen, amounting to a total trial time of 17.5 s. Each fMRI run consisted of 24 trials, yielding to a total of 120 trials.

6.2.4 Image acquisition

Brain images were collected at the University Hospital of the LMU on a 3.0 T Philips Ingenia scanner (Philips Healthcare, Best, The Netherlands). Structural images were acquired with a T1-weighted scan: repetition time (TR) = 9.74 ms; echo time (TE) = 5.66 ms; flip angle = 8°; matrix of 256×256; field of view = 256 mm; voxel size = 1×1×1 mm^3.

The blood oxygen level dependent (BOLD) signal was measured with a T2*-weighted Echo Planar Imaging (EPI) sequence: TR = 2500 ms; TE = 30 ms; flip angle = 90°; ascending acquisition; matrix of 80×80; voxel size = 3×3×3 mm^3. A total of five fMRI runs were acquired. Field mapping data was also acquired using a dual-echo GRE sequence to assist with susceptibility distortion correction.

6.2.5 Image pre-processing

The pre-processing pipeline was similar to that of previous chapters; each subject's T1 weighted underwent skull-stripping using *optiBET* [23], bias field correction with the *N4* tool [24] and was rigidly aligned to the 1mm MNI T1w brain template [25] using *flirt* [26]. This aligned image was then used as the anatomical reference for the pre-processing of functional images that followed. In addition, the T1w image was normalised to the MNI template through affine and non-linear transformations (SyN algorithm) using ANTs [27].

The rigidly aligned T1w image was transferred to *FreeSurfer* [28] to obtain a model of each subject's cortical surface. Additional steps using tools from Connectome Workbench (https://www.humanconnectome.org/software) were applied to remap the surface of

each subject to the common space of the '32k_FS_LR' template. We specifically used these surfaces for each subject because they have the advantage of maintaining the native anatomy of the brain while offering a vertex-level matching between subjects. As a result, we were able to directly compare subjects at each vertex of the brain surface. These surfaces were used for the multivariate analysis.

The first six volumes of the functional series were discarded to allow the scanner to reach steady state. This short period (15 s) was used to display instructions to remind the participants of the task details. The remaining functional images were first corrected for motion and slice-timing differences using *SPM12*. The corrected images were then simultaneously corrected for geometric distortions (based on the acquired field map) and aligned to the T1w image using FSL's *epireg* tool [26,29], while maintaining the voxel size at 3×3×3 mm^3. This produced the final fMRI time series images that were used in subsequent analyses.

6.2.6 Image space and spatial smoothing

The data was analysed with both univariate and multivariate frameworks; both rely, in the first instance, on a subject-level (first-level) model fitting using the general linear model (GLM). For the univariate analysis, the fMRI series of each subject were normalised to MNI space (at 3 mm) and spatially smoothed with a Gaussian kernel of a FWHM of 6 mm before running the first-level GLM.

For the multivariate analysis, the first-level GLM was performed on each subject's data in native space without smoothing and the beta images (parameter estimates) were projected to the subject's cortical surface (obtained from *FreeSurfer*). The surface-based beta maps were then used for the multivariate analysis. These steps were done to maintain the spatial specificity of the parameter estimates, which is crucial for the multivariate framework.

6.2.7 Univariate analysis

Parametric analyses were performed to identify the brain regions in which activity increased with beauty ratings. A standard GLM was fitted to the time series of each subject, with a single task effect (stimulus presentation), regressors that modelled the responses and rest periods, and six motion correction parameters as nuisance regressors.

The beauty score given at each trial was used as an additional regressor to account for any variability in the BOLD signal that was not explained by the other regressors.

The parametric analyses were conducted according to three models (Figure 6.6). The first was the classical linear parametric model which assumes a linear increase in BOLD signal with increasing beauty ratings. In this model, 'not beautiful' stimuli would be associated with the weakest activations and 'very beautiful' stimuli with the strongest. The second model assumed a V-shaped relationship between beauty ratings and brain activity, whereby 'very beautiful' and 'not beautiful' stimuli would lead to a similar level of activity, and 'neutral' stimuli would be associated with the weakest activity. The third model assumed a 'checkmark-shaped' relationship between beauty ratings and brain activity, whereby 'very beautiful' stimuli are associated with the highest activity, followed by 'not beautiful' stimuli, and finally by 'neutral' stimuli.

Categorical analyses comparing the 'very beautiful' condition (ratings of 6 and 7) to both 'neutral' (rating of 4) and 'not-beautiful' (ratings of 1 and 2) conditions were also performed to examine the brain activity related to each condition. All the trials of a given condition were selected to conduct a robust GLM.

After processing each subject's time series at the first-level in *SPM12*, second-level modelling was performed through non-parametric permutation testing using the *SnPM* toolbox [30,31], as this type of group-level modelling for univariate analyses has been shown to be the most robust to false positives [32]. The first-level contrast images from all subjects were submitted to a one sample t-test and 5000 sign flipping permutations were performed to estimate the null distribution of the t-statistic at each voxel. The final statistical maps were created with a cluster-forming threshold of $p < .001$ and cluster-level FWE correction threshold of $p < .05$.

Finally, for control purposes, a categorical analysis was conducted to compare baseline activity versus three categories – 'not beautiful' (bottom 15 ratings), 'neutral' (all ratings of 4) and 'very beautiful' (top 15 ratings). Again, a GLM was fitted to each subject's data, with six additional nuisance regressors. The 5 s black screen at the end of each trial was used to register baseline activity.

6.2.8 Multivariate analysis

To investigate whether the experience of abstract paintings as beautiful is associated with specific spatial patterns of neural activity, we used representational similarity analysis (RSA) [33]. As explained in chapter 2.2.11, we started by running a GLM for each subject in which each trial was treated as an independent condition, thereby generating a parameter estimate (beta) map for each trial. Next, for each subject, the beta maps corresponding to the 10 highest and 10 lowest rated paintings were selected and projected to the brain surface.

A whole-brain, surface-based searchlight analysis was performed using cortical patches with a 6 mm radius. These essentially served as ROIs from which the pattern similarity between each pair of trials for every region in the brain could be determined. So, for each searchlight ROI, the Pearson correlation distance, *d*, was calculated for each pair of trials. Next, in order to represent the (dis)similarity between pairs of trials in each searchlight ROI, neural representational dissimilarity matrices (RDMs) were generated for each subject.

To test whether the similarity was significant only for beautiful trials, the mean group neural RDM was calculated for each searchlight ROI, and these RDMs were then compared to a model RDM (Figure 6.7). The correlation between the neural and model RDMs was assessed using the Spearman rank correlation and statistical significance was determined by means of permutation testing.

The first model RDM that we tested (Figure 6.7) assumed a high similarity in the activity patterns associated with viewing 'very beautiful' paintings (i.e., $d = 0.0$), and no similarity when viewing paintings which were deemed 'not beautiful' or between the patterns of 'very beautiful' and 'not beautiful' paintings (i.e., $d = 0.5$). No pairs of trials were expected to have anti-correlated patterns (i.e., $d = 1.0$). A second RDM model was also tested, which conversely assumed high similarity in activity patterns for 'not beautiful' paintings (Figure 6.7).

6.2.9 Anatomical atlases

Two atlases of cortical regions were used to label the results. The first was specifically used for the visual areas and is based on a retinotopic mapping study [34] (this is the same

atlas that was used in previous chapters). The second was the default atlas used by *FreeSurfer*, namely the Desikan-Killiany atlas [35].

6.3 RESULTS

6.3.1 Behavioural results

The mean beauty rating for the abstract paintings was 3.97 (*sd* = 0.70). There was a low mean correlation of *r* = 0.16 (lowest Pearson *r* = -0.34, highest *r* = 0.61) when comparing each subject's ratings to every other subject's ratings, indicating that there was little agreement among subjects about each painting's beauty score (Figure 6.2). For comparison purposes, behavioural data from a previous study on facial beauty [2] was reanalysed. This revealed that the agreement among subjects is much higher for faces than it is for abstract art, with a mean correlation of *r* = 0.72 (lowest *r* = 0.42, highest *r* = 0.88), which is in accordance with previous studies [22].

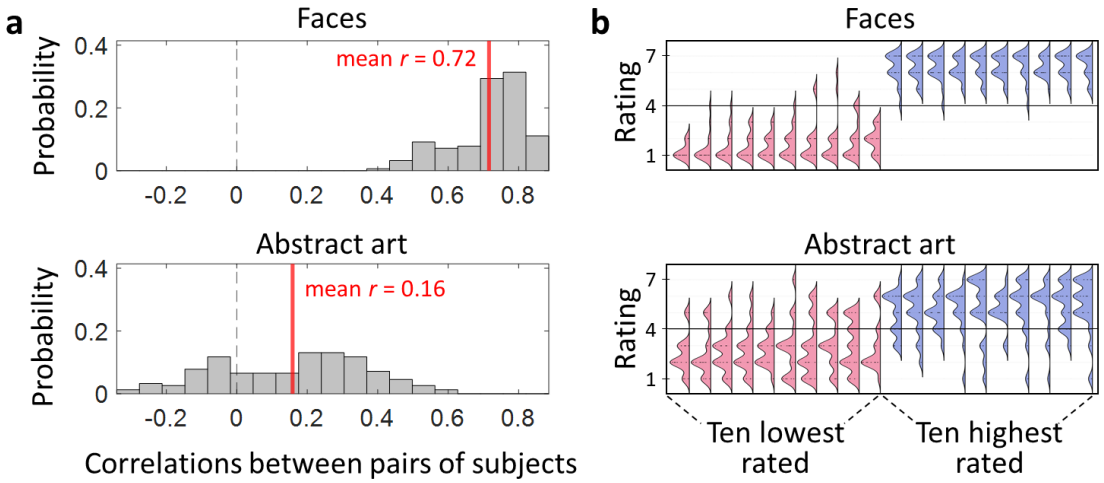

Figure 6.2. Behavioural results and comparison with data on face beauty.
(a) Histograms showing the distribution of inter-subject correlations for beauty ratings given to a set of 120 faces [2] and 120 abstract art paintings (this study). For each study, the Pearson correlation coefficient was calculated between the beauty ratings of every pair of subjects. The plot represents the probability distributions of these correlations. The mean correlation score is indicated by the red lines. **(b)** Density plots showing the probability of ratings given to the 10 faces [2] and 10 abstract paintings (this study) with the best average (blue) and worst average (pink) scores. Each density plot was constructed using the scores given by all participants for each of these stimuli.

The great variability in the aesthetic ratings of abstract art is also well captured by the distributions of the ratings given by all subjects to the 10 abstract paintings and the 10 faces with the highest and lowest mean beauty scores (Figure 6.2). With faces, the highest rated stimuli (on average) were predominantly given high ratings (higher than the neutral point of four), and those with the lowest mean beauty scores showed a similar trend, with most subjects scoring them less than four. However, with abstract art, the highest rated stimuli still received low ratings (as low as one), and the lowest scoring paintings still received scores as high as seven. This indicates that there is greater universal agreement among subjects on the beauty of faces, and much less agreement on the aesthetic status of abstract art paintings. These findings sit well with the theory that proposes a distinction between biological and artifactual stimuli [4].

6.3.2 Univariate categorical activations

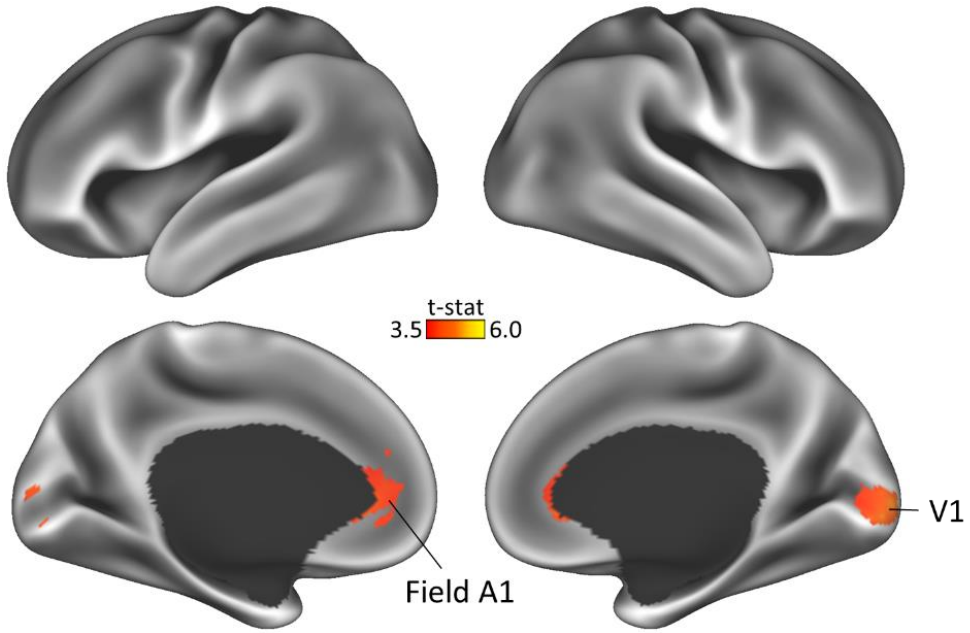

Figure 6.3. Categorical analysis of 'very beautiful' > 'not beautiful' abstract art.
Cortical locations where 'very beautiful' (scores of 6 and 7) abstract art stimuli elicited stronger activations compared with 'not beautiful' (scores of 1 and 2) stimuli. There was activity in primary visual cortex (V1) and field A1 (specifically, anterior cingulate cortex). Additional subcortical activations include the head of the caudate (not shown here).

As expected from previous literature on the experience of beauty [9–13], comparing the 'very beautiful' condition with the 'not beautiful' one showed increased activity in field A1 and primary visual cortex (V1) (Figure 6.3 and Table 6.1). When comparing the 'very beautiful' condition with the 'neutral' condition, increased activations in additional areas were revealed; besides field A1 and V1, there was increased activity in the lateral orbitofrontal cortex (lOFC), V3, lateral occipital cortex and the striatum including the nucleus accumbens (Figure 6.4 and Table 6.1). Note that for this comparison the activity in field A1 was widespread, extending bilaterally to the superior frontal gyrus, frontal pole and lOFC.

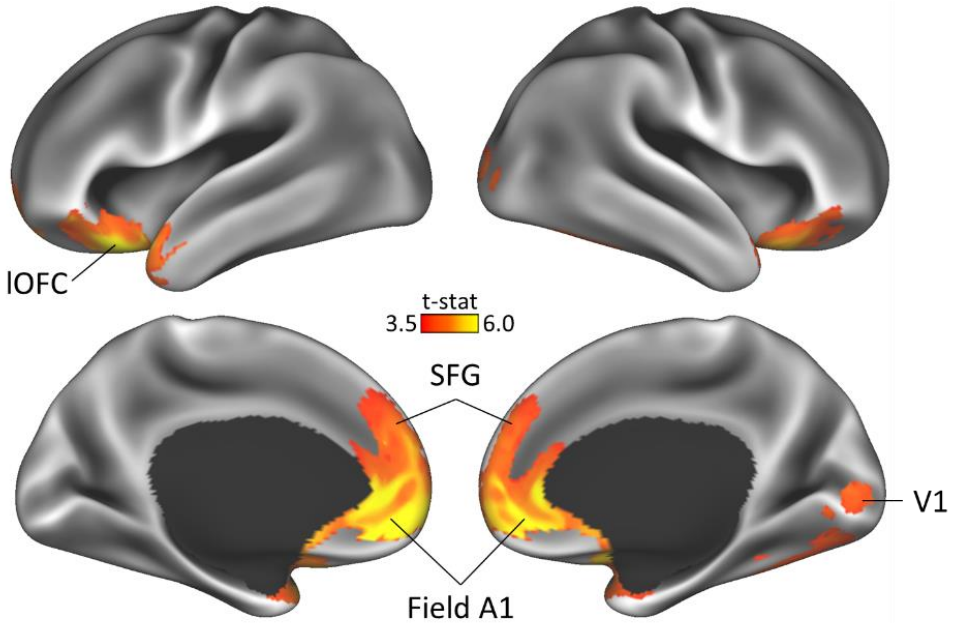

Figure 6.4. Categorical analysis of 'very beautiful' > 'neutral' abstract art.
Cortical locations where 'very beautiful' (scores of 6 and 7) abstract art stimuli elicited stronger activations compared with 'neutral' (score of 4) stimuli. The main activations were in visual cortex, field A1, lateral orbitofrontal cortex (lOFC), the superior frontal gyrus, and the striatum (not shown here).

CLUSTER AND/OR REGION	VOXELS	$P_{Clust-FWE}$	T	Coordinates (mm)		
				x	y	z
Very beautiful > Not beautiful						
R V1	109	0.0488	5.10	6	-96	0
Medial prefrontal lobe and caudate	136	0.0422				
Anterior cingulate cortex (aCC)			4.49	0	30	0
R Caudate			4.49	9	21	3
aCC			4.14	6	30	9
Very beautiful > Neutral						
Prefrontal cortex and striatum	2083	0.0004				

Lateral orbitofrontal cortex (lOFC)			6.89	-33	18	-21
Field A1 (aCC)			6.80	-3	48	-3
Field A1 (right posterior OFC)			5.70	18	12	-18
Visual cortex	299	0.0154				
R V1			5.11	18	-87	3
R V3v			4.68	21	-81	-3
R Lateral occipital cortex (LO1)			4.58	27	-84	6

Table 6.1. Results of the categorical fMRI analysis.
Categorical univariate analyses revealed significantly higher activity in the visual cortex, field A1, lateral orbitofrontal cortex (lOFC), and the striatum during the experience of 'very beautiful' compared with 'not beautiful' or 'neutral' abstract art. Note that the size of the prefrontal cluster in the 'very beautiful > neutral' comparison is very large (2083 voxels). This cluster covers a large swath of bilateral lOFC and mOFC, and the bilateral striatum including the nucleus accumbens, which may not be clear by simply examining the peak coordinates. These results are shown on the cortical surface in Figure 6.3 and Figure 6.4.

For control purposes, we assessed how activity at different levels of aesthetic appeal compares with activity at rest, that is, without any visual stimulation. To this end, we conducted a categorical fMRI comparison of each of the three categories – 'not beautiful', 'neutral', and 'very beautiful' – against baseline activations. As expected, this revealed extensive increases in activity in the visual cortex for all three categories.

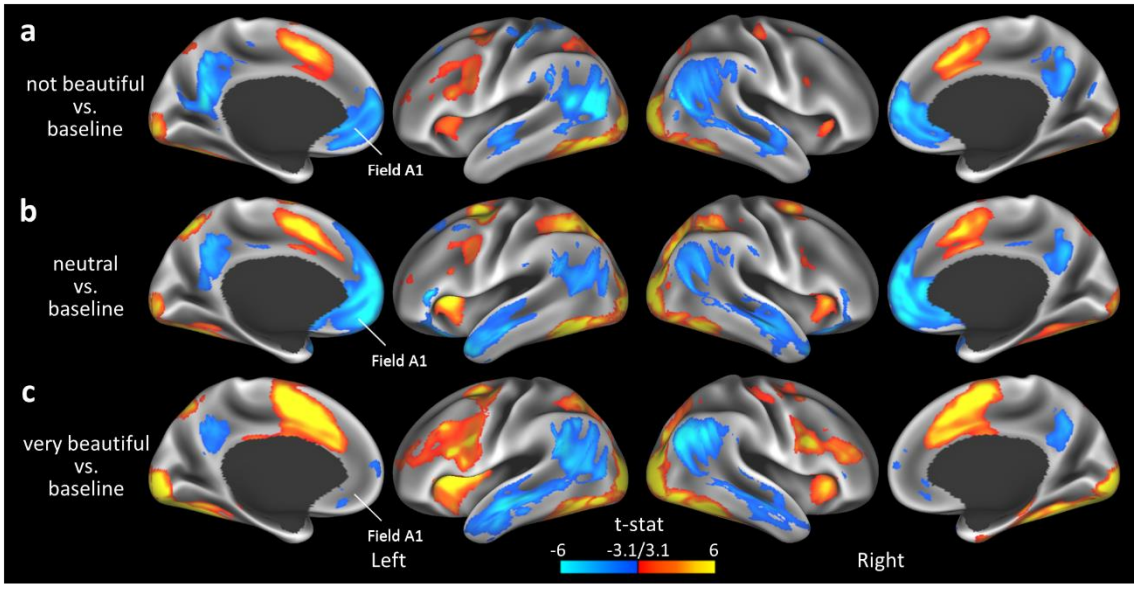

Figure 6.5. Categorical comparison between task conditions and baseline activity.
BOLD signal changes associated with viewing a) not beautiful, b) neutral, and c) very beautiful abstract art were compared with the baseline (rest) signal. All three conditions activate a wide array of cortical regions, including extended visual cortex, the supplementary motor area, frontal eye fields and insula. The was decreased activity in the default-mode network. All visualisations here are significant at $p_{unc.} < .001$.

Of special interest here is field A1. This area of the brain is part of the default mode network (DMN) and is active during rest [36,37]. This means that when a comparison is made against baseline, a decrease in activity is expected in field A1 (and in the rest of the DMN), unless the area is involved in the particular task. Thus, as expected, we found a strong deactivation of field A1 in the 'neutral' and 'not beautiful' conditions compared with baseline, while this deactivation was no longer present when the 'very beautiful' condition was compared with it (Figure 6.5). These findings have been observed before [34] and indicate that with beauty, the increased activity reflects a decrease of inhibition in field A1.

6.3.3 Univariate parametric activations

Several studies have reported that activity in field A1 increases linearly with the declared intensity of the experience of beauty, attraction, or desire, or that a more intense experience of beauty is associated with a categorically stronger activity in that region [2,13,38,39]. Yet some of the same reports, as well as others, have also pointed to a non-linear relationship between the level of the declared experience of beauty and BOLD signal changes in field A1, with neutral beauty ratings being associated with the weakest BOLD signal [38,40,41]. To further explore this observation, the BOLD signal changes were assessed according to three parametric models.

CLUSTER AND/OR REGION	VOXELS	$P_{Clust-FWE}$	T	Coordinates (mm)		
				x	y	z
Linear parametric activations						
Visual cortex	288	0.0196				
R V1			5.92	9	-96	3
L V2 and V3			4.05	-12	-90	-18
L V4			4.01	-27	-84	-15
V-shaped parametric activations						
Superior frontal gyrus	334	0.0156	7.31	3	51	36
L lateral orbitofrontal cortex	239	0.0230	5.62	-39	27	-15
R lateral orbitofrontal cortex	171	0.0336	4.87	27	18	-18
Checkmark-shaped parametric activations						
Prefrontal cortex	1644	0.0020				
L posterior OFC and ventral striatum			6.22	-18	9	-24
Field A1			6.09	-3	48	0
R posterior OFC and ventral striatum			5.89	21	15	-21

Visual cortex	96	0.0496				
R V1			4.47	15	-87	3
R V1			4.16	9	-84	-3
R V2 and V3			4.04	21	-81	-3

Table 6.2. Results of the parametric fMRI analyses.
Results of the three univariate parametric models assessing the relationship between BOLD activity and beauty ratings. The group-level analysis was carried out using permutation testing, with a cluster-forming threshold of $p < .001$ and FWE correction ($p_{clust\text{-}FWE} < .05$). The results and models are visualised in Figure 6.6.

Linear relationship with beauty

A linear parametric analysis of fMRI data with beauty as a modulator, that is, assuming a linear increase in brain activity as a function of increasing aesthetic appeal, revealed significant clusters in visual cortex (V1, V2, V3 and V4), but not field A1 (Figure 6.6 and Table 6.2).

Deviation from neutrality: V-shaped model

A V-shaped parametric model, assuming an equal increase in brain activity in either direction ('not beautiful' or 'very beautiful') compared to neutrality, revealed increased activity in a large portion of the superior frontal gyrus (SFG) and bilateral lateral orbitofrontal cortex (lOFC) with more extreme beauty judgments, both toward the high and low ends of the scale (Figure 6.6 and Table 6.2).

Deviation from neutrality: Checkmark-shaped model

Finally, a checkmark-shaped parametric model also assumed an increase in brain activity in either direction ('not beautiful' or 'very beautiful') compared to neutrality, but to a different extent: activity related to 'not beautiful' stimuli was expected to be weaker than that related to 'very beautiful' stimuli. This model revealed strong activations in field A1, bilateral lOFC, SFG and visual cortex (V1, V2 and V3) (Figure 6.6 and Table 6.2).

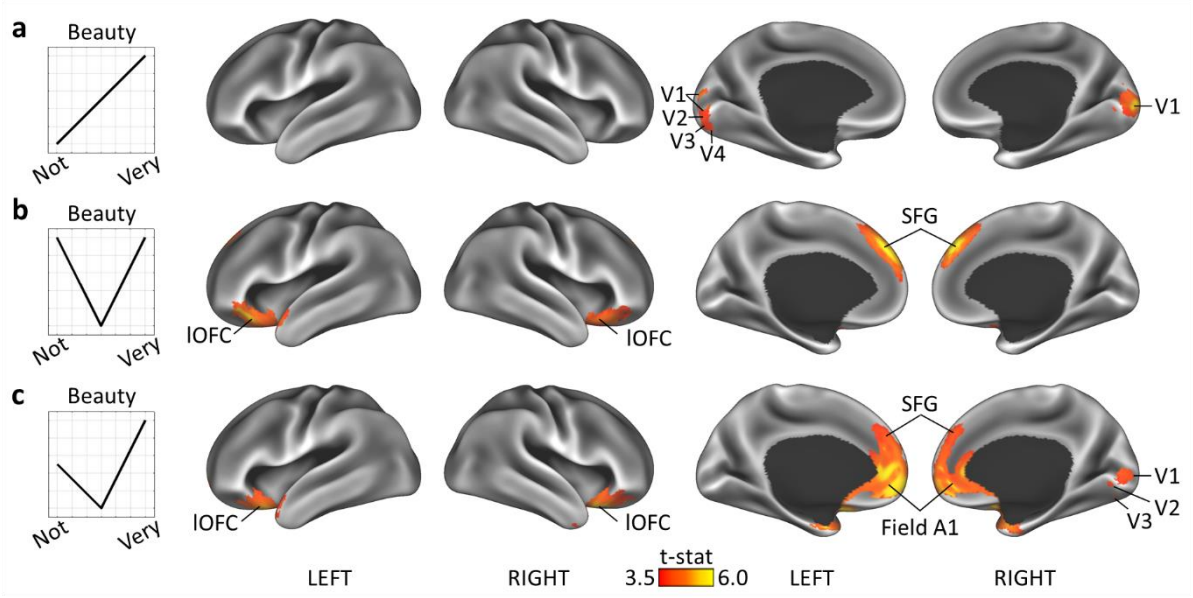

Figure 6.6. Parametric BOLD activity during aesthetic experiences.
BOLD activity during the beauty rating task was assessed according to three parametric models. (a) Model 1 assumed a linear increase in activity with increasing beauty ratings. The only cluster revealed by this model was in visual cortex (V1, V2, V3 and V4). (b) Model 2 assumed a V-shaped relationship between beauty ratings and brain activity, whereby 'very beautiful' and 'not beautiful' stimuli would lead to a similar level of activity, and 'neutral' stimuli would be associated with the lowest activity. This model revealed clusters in lateral orbitofrontal cortex (lOFC) and the superior frontal gyrus (SFG), bilaterally. (c) Model 3 assumed a 'checkmark-shaped' relationship, whereby 'very beautiful' stimuli are associated with the highest activity, followed by 'not beautiful' stimuli, and finally by 'neutral' stimuli. This model revealed activity in field A1 of the medial frontal cortex, SFG, lOFC and in the ventral striatum (not shown here). All results are based on non-parametric permutation testing (pclust-FWE < .05).

6.3.4 Representational similarity analysis

A whole-brain searchlight RSA using the Pearson correlation distance revealed clusters in visual areas with common patterns in response to beautiful stimuli. Specifically, we compared the representational dissimilarity matrices (RDMs), which contain the dissimilarity scores between pairs of trials, to a model RDM that assumed similar patterns only for 'very beautiful' stimuli. Spearman correlations between the neural and the model RDM revealed the following visual regions with significant correlations after permutation testing: left V1, right V2v/V3v, bilateral V3, left VO2 (anterior to V4α), left V7/IPS0, bilateral anterior fusiform gyrus and left SFG (Figure 6.7 and Table 6.3). Model 2, which assumed similar patterns only for the 'not beautiful' stimuli, only correlated significantly with the neural RDM of anterior right V1. The opposite correlation observed in V1 with

Model 1 and Model 2 may possibly relate to the scale, as ratings of 'very beautiful' always coincide with the pointer moving to the right, and ratings of 'not beautiful at all' with the pointer moving to the left. Nevertheless, these opposing correlations were not observed when the same scale was used but a different stimulus, namely facial stimuli [2], suggesting that the pattern similarity may indeed be induced by the abstract paintings (which consisted of oriented lines).

The results obtained from the two models indicate that the patterns in visual cortex are indeed specific to the 'very beautiful' category. Figure 6.7 shows that most visual regions correlated positively with Model 1 and negatively with Model 2. This is expected to some degree given that the two models assume almost opposite trends but the two need not be fully anti-correlated. For control purposes, Figure 6.7 and Table 6.3 also shows that the neural RDM of a region that is not expected to be involved in the task, namely primary auditory cortex, did not correlate with either model.

REGION	***Model 1*** r_S	***Model 1*** $-log_{10}(p)$	***Model 2*** r_S	***Model 2*** $-log_{10}(p)$	**MNI Coordinates (mm)**		
					x	**y**	**z**
L V1	0.4	8	-0.26	3	-7	-97	-5
R V2-V3	0.27	3	-0.18	2	19	-76	-15
L V3	0.26	3	-0.14	1	-17	-97	23
R V3	0.36	6	-0.13	1	29	-90	-6
L VO2	0.27	4	-0.23	3	-30	-61	-9
L V7	0.29	4	-0.24	3	-31	-76	21
L FG ant lat	0.27	3	-0.13	1	-41	-50	-22
R FG ant lat	0.35	6	-0.2	2	48	-43	-27
L SFG	0.31	5	-0.02	0	-21	35	50
R V1	-0.15	1	0.42	8	15	-77	4
L Auditory ctx	-0.03	0	-0.01	0	-42	-28	11
R Auditory ctx	0.06	0	-0.03	0	42	-23	12

Table 6.3. Results of the multivariate fMRI analysis with RSA.
Representational similarity analysis (RSA) revealed significant pattern similarity in various areas in the visual cortex when 'very beautiful' stimuli were grouped together. We also found one location, namely right V1, in which significant pattern similarity appeared when 'not beautiful' stimuli were grouped together. The data in this table is visualised in Figure 6.7.

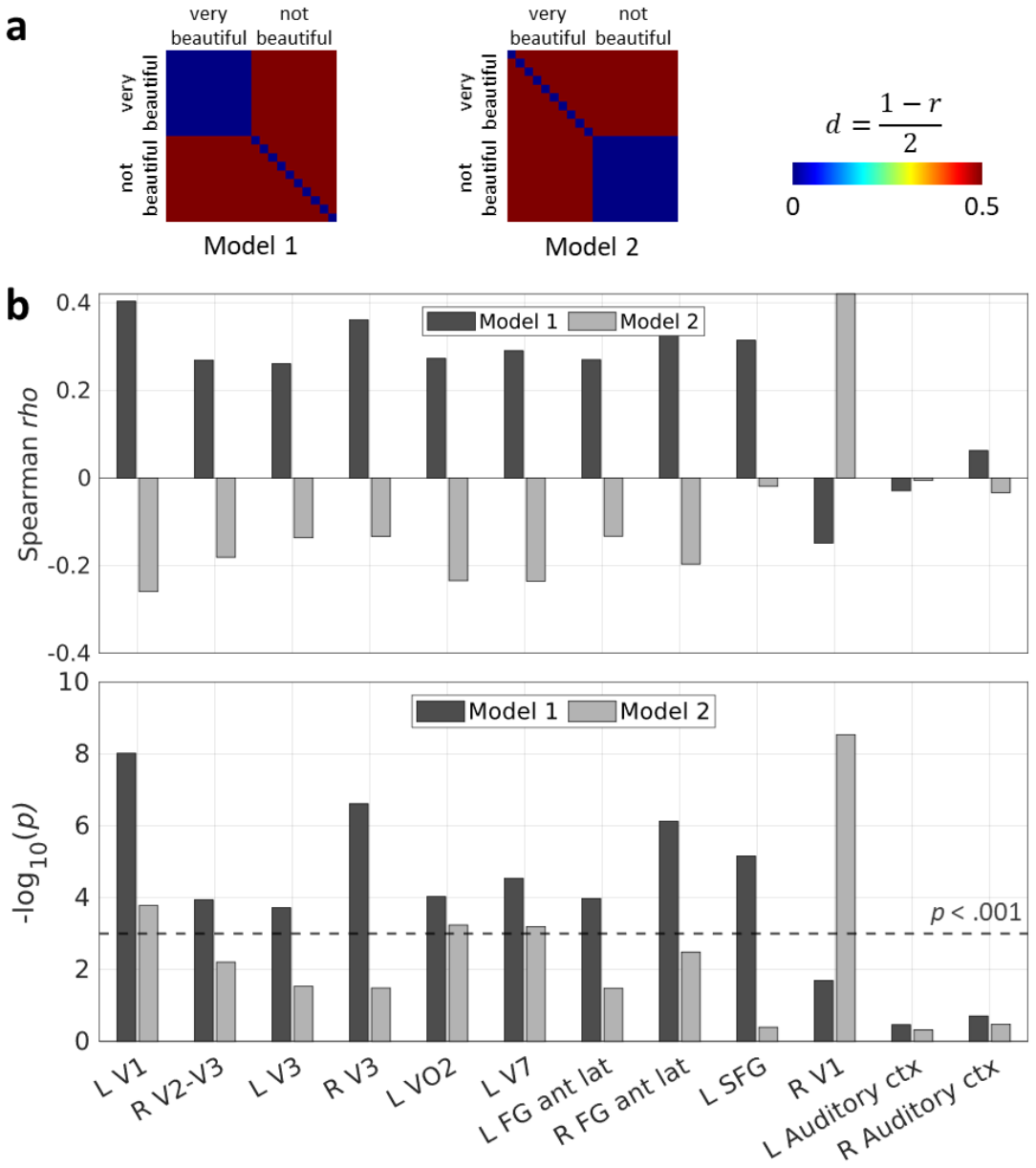

Figure 6.7. Results of the representational similarity analysis.
(a) The model representational dissimilarity matrices (RDMs) used in the representational similarity analysis (RSA). The RDMs represent the relationship between pairs of trials based on the Pearson distance metric, calculated based on the displayed equation. Smaller distances equal greater similarity between pairs of trials. Model 1 assumes that only 'very beautiful' stimuli share similar neural patterns, whereas Model 2 assumes that only 'not beautiful' stimuli share similar patterns. **(b)** The top bar plot shows the Spearman rank correlation between the neural RDMs and the two model RDMs for a set of regions obtained through a searchlight analysis with permutation testing. The bottom bar plot displays the significance of each reported correlation. Most of the regions that were positively and significantly correlated with Model 1 were in visual cortex. The dashed line represents the threshold for significance at $p < .001$. For comparison, a region which is not expected to be involved in the task was included, namely the primary auditory cortex, which indeed did not show any correlation with either model. MNI coordinates are shown in Table 6.3.

6.4 DISCUSSION

6.4.1 Biological vs. artifactual beauty

We enquired into whether the experience of beauty derived from viewing abstract works of art – consisting of arbitrary assemblies of lines and colours – leads to broadly similar engagement of neural mechanisms as that resulting from viewing beautiful human faces based on previous studies. Though both can arouse an experience of beauty, the two categories of stimuli differ significantly. While the experience of facial beauty is mediated through inherited or rapidly acquired concepts and is resistant to revision through peer opinion [42,43], the experience of works created through human agency, including abstract works of art, is much less resistant to revision in light of peer opinion and is probably not interfaced through any known inherited brain concept [3,4,22]. Yet the fact that they can both arouse the "aesthetic emotion", or the experience of beauty, implies that aesthetic experiences aroused through a combination of lines and colours in abstract paintings may engage broadly similar brain mechanisms. It thus became interesting to learn whether the experience of beauty in abstract works of art would result in decodable activity within sensory visual areas on the one hand and within field A1 of medial prefrontal cortex on the other.

By placing abstract art in the artifactual category, it is not implied that the perception of visual attributes that abstract art consists of may not be the result of inherited physiological mechanisms. It is almost certain, for example, that orientation selectivity is inherited [44]; however, the exact assembly of lines and colours in different works of art is not. This is distinct from faces where the constituent elements usually have to take their correct place in an overall composition in order to be recognised as a face. Consistent with previous results [22], the behavioural results show that there is much greater variability in rating the beauty of abstract paintings than there is for faces, making of the experience of beauty in abstract art a more subjective one than the experience of facial beauty.

Despite these differences, a similar strategy is used by the brain for the two categories; both involve the emergence of decodable patterns in sensory areas; with facial beauty the decodable activity was in the sensory areas known to be critical for the perception of faces [2], while for beautiful abstract art it was in sensory visual areas known to contain

large concentrations of orientation selective and chromatic cells. In addition, there is increased activity in field A1 as revealed by the univariate analyses. However, there remains one difference: whereas Yang et al. [2] found distinct patterns in field A1 for beautiful faces, we did not find such patterns in field A1 for beautiful abstract art. Therefore, these results suggest that a principal difference between facial and abstract beauty is that for faces (biological beauty), a pattern emerges in both the sensory areas and field A1, but for abstract art (artifactual beauty), a pattern emerges in the sensory areas only. This explanation is presented tentatively and with diffidence because it seems overwhelmingly simple, and future studies need to confirm it. The hesitation can also be traced to the fact that the study of Vessel et al. [11] reported decodable activity in field A1 in response to both beautiful buildings (artifactual) as well as to beautiful faces (biological). However, the method used here (RSA with the Pearson correlation distance) is more suitable for handling the specific question addressed in this study, that of detecting patterns of neural activity, as opposed to using multi-voxel pattern analysis (MVPA) which is sensitive to both patterns or overall amplitude of activity [33].

6.4.2 The selective function of sensory areas

These results, and those of Yang et al. [2], show that the so-called visual 'sensory' areas cannot be mere passive recipients of signals related to their specialities. Rather, it seems that these sensory areas are also able to classify stimuli according to their aesthetic appeal. This appears to be true regardless of whether the viewed stimuli belong to the biological category (faces) or the artifactual one (abstract art). This is because decodable patterns emerge in the sensory areas only with stimuli that are experienced as beautiful, regardless of category, and when such patterns emerge there is, as a correlate, activity in field A1.

It is tempting to suggest that it is the emergence of such decodable patterns in sensory areas that engages field A1. However, in the absence of temporal studies, the possibility that field A1 is activated prior to the sensory areas and that the latter are only activated through feedback cannot be excluded. A precedent for this may be found in studies which have shown, for example, that activity in the amygdala precedes activity in face-processing sensory areas when fearful stimuli are viewed [45]. Whatever the temporal relationship in activity between the sensory areas and field A1 may be, we cannot escape the conclusion that, in addition to processing the attributes of the stimulus, the sensory

areas are also involved – either before, simultaneously with, or after activation of field A1 – in ordering the stimuli according to criteria that give them an aesthetic status. They are therefore involved in a selective process.

One criticism may be that certain low-level features, such as colour or brightness, may be more abundant in beautiful paintings than in not beautiful ones, thereby driving the increased response in visual cortex, instead of beauty itself [46]. However, we believe that this point is circumvented by the variance in aesthetic ratings that we observed in our cohort; what was regarded as beautiful by some was regarded as not beautiful by others. Because of this, there was no fixed beauty condition that applied across subjects, which means that when making any comparison, a given painting is not consistently present in any category. Further, previous neuroimaging studies have specifically assessed the neural correlates of aesthetic judgement and judgement of other features of visual stimuli such as brightness and symmetry, and found that the network of orbitofrontal (medial and lateral) regions that we report is more involved in aesthetic judgements [39,47].

Finally, the engagement of the sensory areas may reflect an attentional effect. Beauty captures attention; for example, introducing a beautiful, task-irrelevant stimulus can significantly impair task performance [48,49], and studies have shown that subjects fixate for a longer time on attractive faces [50]. These attentional effects hint to a possible stronger or prolonged engagement of sensory areas when exposed to beautiful stimuli.

6.4.3 Co-activity between sensory areas and field A1 is the basis of the experience of beauty

Another conclusion that we can draw is that when the observer experiences stimuli as beautiful, there are decodable patterns of activity in sensory areas, with activity in field A1 as a correlate. We compared the neural activity associated with the perception of works of abstract art at three levels of aesthetic experience – 'very beautiful', 'neutral', and 'not beautiful'. The results showed that visual cortex is more engaged when the declared experience of beauty increases, and this engagement is further supported by the emergence of specific neural patterns in visual cortex. Moreover, there were important differences within the medial prefrontal region: beautiful stimuli fully engaged field A1, while the other categories did not, or did so to a limited degree. Indeed, direct comparisons between the 'very beautiful' category and the other categories (Figure 6.3

and Figure 6.4), as well as the parametric analysis of brain activity according to the 'checkmark-shaped' model (Figure 6.6), showed strong activations in the medial frontal cortex in a region that included field A1, among others. This indicates that field A1 in the medial prefrontal region is involved in assigning a positive aesthetic attribute to a stimulus, or in processing the reward related to that stimulus, though it is not intended to imply that that is its only function. In conclusion, it is the unique combination of increased activity in sensory cortex according to certain configurations and increased activity in field A1 that underlies the experience of beauty. The relationship between these seemingly distant areas is therefore revealed through a specific experience, in this case that of beauty.

The activity in field A1 itself also raises interesting questions. For example, there may be different sub-regions of it active with different aesthetic experiences [12]. Hence, one pointer to future work that emerges from these studies is the importance of detailing the pattern of anatomical connectivity within field A1 and between it and other areas in both the sensory and frontal cortices. In light of our present studies and those of others, we also suggest that the boundaries of A1, as defined by Ishizu and Zeki [10], be expanded, especially ventrally, to include other areas implicated in the experience of beauty reported in other studies [51]. It is likely that the variability in reported activations is largely caused by (poor) fMRI signal quality in that region of the brain, especially across studies using different scanners and acquisition parameters [52]. It is therefore desirable that field A1 should have a diameter of around 30 mm with the same central coordinates.

Activity in other prefrontal areas, such as the lateral orbitofrontal cortex (lOFC) and the superior frontal gyrus (SFG), also showed up consistently when subjects gave non-neutral ratings to the abstract art stimuli, indicating that these regions are also involved in aesthetic judgement. However, the exact role of these regions in the context of neuroaesthetics is yet to be determined. For example, are these regions involved because they play a general role in judgement, or could their role be more specific within beauty tasks? Previous research suggests that general involvement in judgement may be the driving factor [47,53,54].

6.4.4 'Not-beautiful' does not necessarily mean 'ugly'

In this study the main focus was the experience of beauty. Given that the 7-point rating scale went from 'not-beautiful' to 'very-beautiful', we cannot make any claims about negative aesthetic judgements, such as ugliness, which may be a different category of aesthetic experience altogether.

In light of these results, the experience of ugliness nevertheless raises interesting questions; for example, given that the 'checkmark-shaped' model showed strong engagement of field A1, does it mean that this region, which plays a cardinal role in the experience of beauty, is also involved in the experience of ugliness? Second, do the experience of beauty and ugliness engage a different brain network, implying two distinct aesthetic concepts, or are the same regions involved, implying a continuum of the same experience, with ugliness and beauty being the extremes of the spectrum? And finally, do any specific decodable activity patterns emerge in sensory areas with the experience of ugliness? Studying the experience of ugliness will thus not only inform us about ugliness, but about beauty as well. We therefore set out to investigate this aesthetic experience separately, which I shall discuss in the next chapter.

REFERENCES

1. Bell, C. (1914). Art (Chatto & Windus).
2. Yang, T., Formuli, A., Paolini, M., and Zeki, S. (2022). The neural determinants of beauty. European Journal of Neuroscience *55*, 91–106. 10.1111/EJN.15543.
3. Zeki, S. (2009). Splendors and Miseries of the Brain: Love, Creativity and the Quest for Human Happiness (Wiley-Blackwell).
4. Zeki, S., and Chén, O.Y. (2020). The Bayesian-Laplacian brain. European Journal of Neuroscience *51*, 1441–1462. 10.1111/ejn.14540.
5. Allison, T., Puce, A., Spencer, D.D., and McCarthy, G. (1999). Electrophysiological studies of human face perception. I: potentials generated in occipitotemporal cortex by face and non-face stimuli. Cerebral Cortex *9*, 415–430. 10.1093/cercor/9.5.415.
6. Kanwisher, N., McDermott, J., and Chun, M.M. (1997). The fusiform face area: a module in human extrastriate cortex specialized for face perception. The Journal of Neuroscience *17*, 4302–4311. 10.1523/JNEUROSCI.17-11-04302.1997.
7. Sergent, J., Ohta, S., and Macdonald, B. (1992). Functional neuroanatomy of face and object processing: a positron emission tomography study. Brain *115*, 15–36. 10.1093/brain/115.1.15.
8. Haxby, J. V., Hoffman, E.A., and Gobbini, M.I. (2000). The distributed human neural system for face perception. Trends Cogn Sci *4*, 223–233. 10.1016/S1364-6613(00)01482-0.
9. Kawabata, H., and Zeki, S. (2004). Neural correlates of beauty. J Neurophysiol *91*, 1699–1705. 10.1152/JN.00696.2003/ASSET/IMAGES/LARGE/Z9K0040437760007.JPEG.
10. Ishizu, T., and Zeki, S. (2011). Toward a brain-based theory of beauty. PLoS One *6*, e21852. 10.1371/journal.pone.0021852.
11. Vessel, E.A., Isik, A.I., Belfi, A.M., Stahl, J.L., and Gabrielle Starr, G. (2019). The default-mode network represents aesthetic appeal that generalizes across visual domains. Proc Natl Acad Sci U S A *116*, 19155–19164. 10.1073/PNAS.1902650116/-/DCSUPPLEMENTAL.
12. Pegors, T.K., Kable, J.W., Chatterjee, A., and Epstein, R.A. (2015). Common and unique representations in pFC for face and place attractiveness. J Cogn Neurosci *27*, 959–973. 10.1162/JOCN_A_00777.
13. O'Doherty, J., Winston, J., Critchley, H., Perrett, D., Burt, D.M., and Dolan, R.J. (2003). Beauty in a smile: the role of medial orbitofrontal cortex in facial attractiveness. Neuropsychologia *41*, 147–155. 10.1016/S0028-3932(02)00145-8.
14. Hubel, D.H., and Wiesel, T.N. (1968). Receptive fields and functional architecture of monkey striate cortex. J Physiol *195*, 215–243. 10.1113/jphysiol.1968.sp008455.
15. Zeki, S.M. (1978). Uniformity and diversity of structure and function in rhesus monkey prestriate visual cortex. J Physiol *277*, 273–290. 10.1113/jphysiol.1978.sp012272.
16. Zeki, S, Perry, RJ and Bartels, A. (2003). The processing of kinetic contours in the brain. Cerebral Cortex *13*, 189-202 doi:10.1093/cercor/13.2.189.
17. Brouwer, G.J., and Heeger, D.J. (2009). Decoding and reconstructing color from responses in human visual cortex. Journal of Neuroscience *29*, 13992–14003. 10.1523/JNEUROSCI.3577-09.2009.

18. Brouwer, G.J., and Heeger, D.J. (2013). Categorical clustering of the neural representation of color. The Journal of Neuroscience *33*, 15454–15465. 10.1523/JNEUROSCI.2472-13.2013.

19. Montaser-Kouhsari, L., Landy, M.S., Heeger, D.J., and Larsson, J. (2007). Orientation-selective adaptation to illusory contours in human visual cortex. Journal of Neuroscience *27*, 2186–2195. 10.1523/JNEUROSCI.4173-06.2007.

20. Zeki, S., and Stutters, J. (2013). Functional specialization and generalization for grouping of stimuli based on colour and motion. Neuroimage *73*, 156–166. 10.1016/j.neuroimage.2013.02.001.

21. Cheadle, S.W., and Zeki, S. (2014). The role of parietal cortex in the formation of color and motion based concepts. Front Hum Neurosci *8*, 1–10. 10.3389/fnhum.2014.00535.

22. Bignardi, G., Ishizu, T., and Zeki, S. (2020). The differential power of extraneous influences to modify aesthetic judgments of biological and artifactual stimuli. Psych J, pchj.415. 10.1002/pchj.415.

23. Lutkenhoff, E.S., Rosenberg, M., Chiang, J., Zhang, K., Pickard, J.D., Owen, A.M., and Monti, M.M. (2014). Optimized brain extraction for pathological brains (optiBET). PLoS One *9*, e115551. 10.1371/journal.pone.0115551.

24. Tustison, N.J., Avants, B.B., Cook, P.A., Zheng, Y., Egan, A., Yushkevich, P.A., and Gee, J.C. (2010). N4ITK: Improved N3 bias correction. IEEE Trans Med Imaging *29*, 1310–1320. 10.1109/TMI.2010.2046908.

25. Fonov, V., Evans, A.C., Botteron, K., Almli, C.R., McKinstry, R.C., and Collins, D.L. (2011). Unbiased average age-appropriate atlases for pediatric studies. Neuroimage *54*, 313–327. 10.1016/J.NEUROIMAGE.2010.07.033.

26. Jenkinson, M., Bannister, P., Brady, M., and Smith, S. (2002). Improved optimization for the robust and accurate linear registration and motion correction of brain images. Neuroimage *17*, 825–841. 10.1006/NIMG.2002.1132.

27. Avants, B.B., Tustison, N.J., Song, G., Cook, P.A., Klein, A., and Gee, J.C. (2011). A reproducible evaluation of ANTs similarity metric performance in brain image registration. Neuroimage *54*, 2033–2044. 10.1016/J.NEUROIMAGE.2010.09.025.

28. Fischl, B. (2012). FreeSurfer. Neuroimage *62*, 774–781. 10.1016/j.neuroimage.2012.01.021.

29. Greve, D.N., and Fischl, B. (2009). Accurate and robust brain image alignment using boundary-based registration. Neuroimage *48*, 63–72. 10.1016/J.NEUROIMAGE.2009.06.060.

30. Holmes, A.P., Blair, R.C., Watson, J.D.G., and Ford, I. (1996). Nonparametric analysis of statistic images from functional mapping experiments. Journal of Cerebral Blood Flow and Metabolism *16*, 7–22. 10.1097/00004647-199601000-00002/ASSET/IMAGES/LARGE/10.1097_00004647-199601000-00002-FIG2.JPEG.

31. Winkler, A.M., Ridgway, G.R., Webster, M.A., Smith, S.M., and Nichols, T.E. (2014). Permutation inference for the general linear model. Neuroimage *92*, 381–397. 10.1016/J.NEUROIMAGE.2014.01.060.

32. Eklund, A., Nichols, T.E., and Knutsson, H. (2016). Cluster failure: Why fMRI inferences for spatial extent have inflated false-positive rates. Proc Natl Acad Sci U S A *113*, 7900–7905. 10.1073/PNAS.1602413113/SUPPL_FILE/PNAS.1602413113.SAPP.PDF.

33. Kriegeskorte, N., Mur, M., and Bandettini, P. (2008). Representational similarity analysis – connecting the branches of systems neuroscience. Front Syst Neurosci *2*. 10.3389/neuro.06.004.2008.

34. Wang, L., Mruczek, R.E.B., Arcaro, M.J., and Kastner, S. (2015). Probabilistic maps of visual topography in human cortex. Cerebral Cortex *25*, 3911–3931. 10.1093/cercor/bhu277.

35. Desikan, R.S., Ségonne, F., Fischl, B., Quinn, B.T., Dickerson, B.C., Blacker, D., Buckner, R.L., Dale, A.M., Maguire, R.P., Hyman, B.T., et al. (2006). An automated labeling system for subdividing the human cerebral cortex on MRI scans into gyral based regions of interest. Neuroimage *31*, 968–980. 10.1016/J.NEUROIMAGE.2006.01.021.

36. Raichle, M.E., MacLeod, A.M., Snyder, A.Z., Powers, W.J., Gusnard, D.A., and Shulman, G.L. (2001). A default mode of brain function. Proceedings of the National Academy of Sciences *98*, 676–682. 10.1073/pnas.98.2.676.

37. Shulman, G.L., Corbetta, M., Buckner, R.L., Fiez, J.A., Miezin, F.M., Raichle, M.E., and Petersen, S.E. (1997). Common blood flow changes across visual tasks: I. increases in subcortical structures and cerebellum but not in nonvisual cortex. J Cogn Neurosci *9*, 624–647. 10.1162/jocn.1997.9.5.624.

38. Zeki, S., Romaya, J.P., Benincasa, D.M.T., and Atiyah, M.F. (2014). The experience of mathematical beauty and its neural correlates. Front Hum Neurosci *8*, 68. 10.3389/fnhum.2014.00068.

39. Jacobsen, T., Schubotz, R.I., Höfel, L., and Cramon, D.Y. V. (2006). Brain correlates of aesthetic judgment of beauty. Neuroimage *29*, 276–285. 10.1016/J.NEUROIMAGE.2005.07.010.

40. Kawabata, H., and Zeki, S. (2008). The neural correlates of desire. PLoS One *3*, e3027. 10.1371/JOURNAL.PONE.0003027.

41. Martín-Loeches, M., Hernández-Tamames, J.A., Martín, A., and Urrutia, M. (2014). Beauty and ugliness in the bodies and faces of others: An fMRI study of person esthetic judgement. Neuroscience *277*, 486–497. 10.1016/J.NEUROSCIENCE.2014.07.040.

42. Glennon, M.J., and Zeki, S. (2021). The power of external influences to modify judgments of facial and moral beauty. Psych J. 10.1002/PCHJ.492.

43. Chen, C.-H., and Zeki, S. (2011). Frontoparietal activation distinguishes face and space from artifact concepts. J Cogn Neurosci *23*, 2558–2568. 10.1162/JOCN.2011.21617.

44. Hubel, D.H., and Wiesel, T.N. (1977). Ferrier Lecture: Functional Architecture of Macaque Monkey Visual Cortex. Proceedings of the Royal Society B: Biological Sciences *198*, 1–59. 10.1098/rspb.1977.0085.

45. Méndez-Bértolo, C., Moratti, S., Toledano, R., Lopez-Sosa, F., Martínez-Alvarez, R., Mah, Y.H., Vuilleumier, P., Gil-Nagel, A., and Strange, B.A. (2016). A fast pathway for fear in human amygdala. Nat Neurosci *19*, 1041–1049. 10.1038/nn.4324.

46. Iigaya, K., Yi, S., Wahle, I.A., Tanwisuth, K., and O'Doherty, J.P. (2021). Aesthetic preference for art can be predicted from a mixture of low- and high-level visual features. Nat Hum Behav. 10.1038/s41562-021-01124-6.

47. Ishizu, T., and Zeki, S. (2013). The brain's specialized systems for aesthetic and perceptual judgment. European Journal of Neuroscience *37*, 1413–1420. 10.1111/EJN.12135.

48. Chen, W., Liu, C.H., and Nakabayashi, K. (2012). Beauty hinders attention switch in change detection: the role of facial attractiveness and distinctiveness. PLoS One *7*, e32897. 10.1371/journal.pone.0032897.

49. Sui, J., and Liu, C.H. (2009). Can beauty be ignored? Effects of facial attractiveness on covert attention. Psychon Bull Rev *16*, 276–281. 10.3758/PBR.16.2.276.

50. DeWall, C.N., and Maner, J.K. (2008). High status men (but not women) capture the eye of the beholder. Evolutionary Psychology *6*, 147470490800600. 10.1177/147470490800600209.

51. Tsukiura, T., and Cabeza, R. (2011). Shared brain activity for aesthetic and moral judgments: implications for the Beauty-is-Good stereotype. Soc Cogn Affect Neurosci *6*, 138–148. 10.1093/SCAN/NSQ025.

52. Weiskopf, N., Hutton, C., Josephs, O., and Deichmann, R. (2006). Optimal EPI parameters for reduction of susceptibility-induced BOLD sensitivity losses: A whole-brain analysis at 3 T and 1.5 T. Neuroimage *33*, 493–504. 10.1016/J.NEUROIMAGE.2006.07.029.

53. Elliott, R., Dolan, R.J., and Frith, C.D. (2000). Dissociable functions in the medial and lateral orbitofrontal cortex: evidence from human neuroimaging studies. Cerebral Cortex *10*, 308–317. 10.1093/CERCOR/10.3.308.

54. Kringelbach, M.L. (2005). The human orbitofrontal cortex: linking reward to hedonic experience. Preprint, 10.1038/nrn1747 10.1038/nrn1747.

7.

Neural Correlates of the Experience of Ugliness

Our enquiry into the experience of abstract beauty suggests that this experience is dependent upon the co-activity between medial frontal and sensory areas. This leaves us with the question of ugliness; are the same neural mechanisms involved in this experience, including neural activity patterns, or are different mechanisms at play? This question arises because ugliness, although often regarded as the opposite of beauty, could possibly be a distinct aesthetic category. We therefore conducted another study which was almost identical to the one described in the previous chapter. This time, however, instead of rating abstract paintings according to beauty, subjects were asked to rate faces according to how ugly they found them to be. There was moderate agreement in the experience of ugliness of faces among subjects. Univariate parametric analyses did not reveal any brain regions with increasing activity as the declared intensity of the experience of ugliness increased. However, increasing activity appeared in the striatum and primary visual cortex with decreasing levels of ugliness. As with studies on facial beauty, RSA revealed distinct neural activity patterns in sensory areas relevant for face processing and in field A1 of the medial frontal cortex. Thus, similar neural mechanisms appear to be involved in the experience of facial beauty and ugliness, the difference being heightened activity in field A1 of the medial frontal cortex with beauty. This suggests that ugliness and beauty are indeed interdependent opposites, existing on a continuum, of the same aesthetic concept.

7.1 INTRODUCTION

We have observed that decodable patterns emerged with the experience of abstract beauty in sensory areas implicated in the processing of lines and colours, while with beautiful faces it was in visual areas implicated in the processing of faces, suggesting that certain ineffable qualities that make us perceive a stimulus as beautiful are represented in these areas [1,2]. Moreover, it is only when such a stimulus is experienced as beautiful that, in addition to the sensory areas, there is engagement of field A1 of the medial frontal cortex; without the experience of beauty, there is no obvious connection between these distant regions of the brain. This naturally raises a question about ugliness; does this aesthetic experience, too, engage a specific neural network, and does it have a common neural representation in the form of activity patterns?

Studies have addressed the experience of ugliness alongside and in comparison with beauty, and found involvement of various brain areas in the experience of ugliness, including the amygdala, insula, cingulate gyrus and lateral frontal cortices [3–6]. However, by placing ugliness on the same scale and thus continuum as beauty, it is implied that this experience is simply the opposite of that of beauty, rather than a distinct aesthetic category. But ugliness often has characteristics attached to it that are well removed from those that are attached to beauty, among them dislike and disgust [7], and the experience may serve as a warning signal that the stimulus contains a pathogen threat [8]. It is therefore possible that ugliness is a separate category from that of beauty rather than being simply a gradation of it. The exact neural mechanisms underlying the experience of ugliness as a specific perceptual category are thus not yet fully understood.

An area of special interest is field A1 of the mOFC, which has been shown to be involved during the experience of beauty, regardless of its source [3,9]. Could it be that a stimulus of another aesthetic quality, i.e. ugliness, also elicits decodable activity in field A1? If beauty and ugliness are indeed opposites, it is reasonable to expect that both have a distinct neural representation in the areas involved in the experience. There are, in fact, some indications that this pivotal area for beauty may be engaged with ugliness as well. The experiment from the previous chapter indicated a stronger involvement of field A1 when comparing beautiful stimuli to neutral stimuli instead of 'not beautiful' stimuli. Some even argue that field A1 is activated to a similar extent by ugly and beautiful stimuli [5]. This

observation is however not conclusive since a direct comparison of activity between ugly and neutral stimuli fails to reveal increased activity in field A1. Thus, the exact role of field A1 in the experience of ugliness, if any, remains to be determined.

To address these questions, we specifically investigated the experience of facial ugliness, treating ugliness as a category in its own right, that is to say, not the extreme opposite of beauty. This was done by having subjects indicate the degree of 'ugliness' of various faces on a scale that did not include beauty.

7.2 METHODS

7.2.1 Participants

Twenty-three healthy subjects (12 female, 11 male; ages 19-33 years; mean age 24.8 ± 2.7) from six different self-identified ethnic backgrounds (Black, Chinese, Indian, Middle Eastern, South-East Asian, White) formed the final sample used in the study; all were right-handed and had normal or corrected-to-normal vision. The initial sample included 40 participants, of whom four were excluded due to excessive head movements during the scan, three for sleeping during the scan, four due to problems with the imaging data files, five for not properly engaging with the task (minimal variability in the ratings), and one due to an incidental finding of a brain anomaly. The experiment was approved by the ethical committee of Ludwig-Maximilians-Universität Munich (LMU) where the imaging experiments were conducted. All subjects gave informed consent.

7.2.2 Stimuli

The stimuli consisted of 120 images of faces with a neutral expression. These were obtained from the Chicago Face Database [10–12] and included an equal number of Asian, Indian, Latino, Black, White and mixed-race faces (20 of each category, split equally between males and females). The stimuli were scaled to 500×500 pixels and were presented in their original colour without cropping or modification. The task was programmed in the *Presentation* software package (Neurobehavioral Systems, Inc., Albany, CA).

7.2.3 Procedure

Subjects performed the same task and number of trials as described in 6.2.3, but were presented with faces instead of abstract paintings. The question was also different; instead of being asked to rate beauty, participants were asked to rate the degree ugliness of the faces on a scale from one to seven, one corresponding to 'not ugly at all' and seven corresponding to 'very ugly'.

7.2.4 Image acquisition and pre-processing

Brain images were again collected at the University Hospital of the LMU on a 3.0 T Philips Ingenia scanner (Philips Healthcare, Best, The Netherlands), where the same structural and functional sequences were acquired as described in 6.2.4. The imaging data was pre-processed and smoothed in the exact same way as the previous study on beauty, described in 6.2.5. For the multivariate analysis, no smoothing was applied to maintain spatial specificity. The beta images (parameter estimates of each trial) were again projected onto the cortical surface (obtained from *FreeSurfer*).

7.2.5 Univariate analysis

We again performed parametric analyses to identify in which brain regions activity increased or decreased linearly (parametrically) with ugliness ratings, concentrating this time on standard linear relationships (in contrast to the non-linear ones described in the previous chapter). A GLM was fit to each participant's BOLD time-series and incorporated a single task effect (stimulus presentation) along with regressors that accounted for responses and rest periods. In addition, six motion correction parameters were included as nuisance regressors. To capture any unexplained variance in the BOLD signal, the ugliness score given at each trial was introduced as an additional regressor. The first-level analysis on each participant's time series was performed using *SPM12* and the second-level modelling was again done using non-parametric permutation testing with the *SnPM* toolbox [13,14].

Categorical analyses comparing the 'very ugly' condition (ratings of 6 and 7) to both 'neutral' (rating of 4) and 'not ugly' (ratings of 1 and 2) conditions were also performed to examine the brain activity related to each condition. All trials of a given condition were selected and a GLM was fitted to each subject's data, with six additional nuisance regressors. The 5 s black screen at the end of each trial was used to model rest activity.

7.2.6 Multivariate analysis

RSA was again performed to examine what brain regions, if any, had a specific spatial arrangement of neural activity related to the experience of ugliness. First, we ran a first-level GLM which considered each trial as an independent condition. This generated a parameter estimate (beta) map for each trial, from which 20 were selected (the 10 lowest- and 10 highest-rated trials) for our comparison. The whole-brain searchlight analysis was conducted in the same way as previously described (6.2.8), from which the group neural RDMs were obtained.

Next, we compared the mean group RDM of each searchlight ROI to the model RDM. This model assumed that, on average, 'ugly' trials would share very similar neural patterns (d = 0.0) and that there would be no clear relationship between these and the 'not ugly' trials (d = 0.5), which were not assumed to share a common pattern. Spearman rank correlation was used to assess the similarity between the neural and model RDM, and permutation testing was again performed to determine statistical significance. Finally, further thresholding was done by imposing a minimum cluster size (surface area) of 36 mm^2 to reveal meaningful clusters.

7.3 RESULTS

7.3.1 Behavioural results

There was significant inter-participant agreement on the ugliness ratings provided to the set of 120 faces (mean Pearson correlation r = 0.42, p < .001, lowest r = 0.01, highest r = 0.70, Figure 7.1), suggesting a moderate-to-high consensus among individuals in perceiving faces as ugly. Interestingly, in the previous chapter we saw that there was an even higher consistency among subjects in facial beauty ratings (r = 0.72 on average), but the current result nevertheless exceeds the considerably lower inter-subject agreement observed when assessing abstract beauty (r = 0.16 on average). These findings therefore align as well with the proposed division between biological and artefactual stimuli [15].

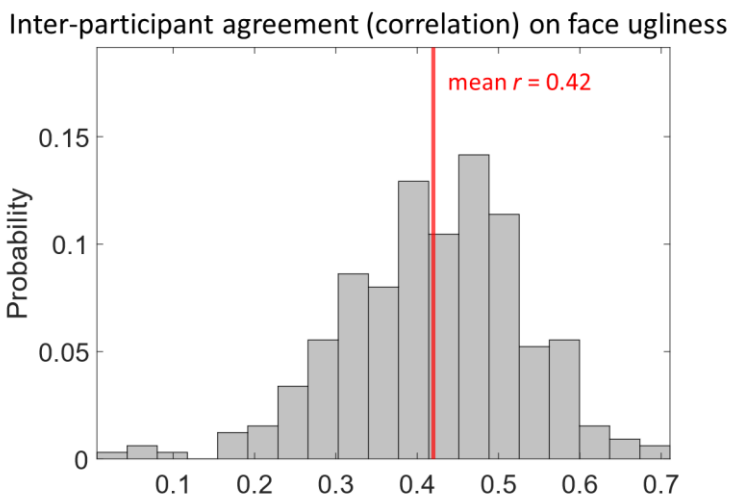

Figure 7.1. Inter-participant agreement on face ugliness.
The agreement between the ugliness scores given by each participant (N=23) for the 120 faces was assessed using Pearson correlations. This figure shows the distribution of these correlation scores and indicate that there was moderate-to-high agreement between participants about the ugliness of faces. The average correlation was r = 0.42, with the lowest score being 0.01 and the highest being 0.70.

7.3.4 Univariate parametric activations

To determine which brain regions are involved in the experience of ugliness, linear parametric activity changes with increasing and decreasing ugliness ratings were examined. No brain regions showed linearly increasing activity with the declared intensity of the experience of ugliness. However, there was a parametric relationship between the experience of decreasing levels of ugliness and increasing levels of activity in a region that is at the intersection between the ventral striatum and the posterior part of the medial orbitofrontal cortex, as well as in the primary visual cortex (Figure 7.2 and Table 7.1). These regions have been associated with beauty, likability, and reward [5,16–19].

7.3.3 Univariate categorical results

The categorical analysis did not reveal any significant activations when comparing 'very ugly' with 'not ugly' or 'neutral'. Conversely, comparing 'not ugly' with 'very ugly' revealed only a cluster in primary visual cortex, which is in line with the parametric result.

CLUSTER AND/OR REGION	VOXELS	$P_{Clust-FWE}$	T	MNI coordinates (mm)		
				x	y	z
Linear parametric increasing activations						
No significant activations.						
Linear parametric decreasing activations						
Striatum	67	.0402	6.82	0	9	-6
L Primary visual cortex (V1)	94	.0262	4.48	-9	-90	-6
L V1			4.32	-12	-96	3

Table 7.1. Results of the parametric fMRI analysis.
Results of the linear parametric model assessing the relationship between BOLD activity and ugliness ratings. The group-level analysis was carried out using permutation testing, with a cluster-forming threshold of $p < .001$ and FWE correction ($p_{clust-FWE} < .05$). The clusters are visualised in Figure 7.2.

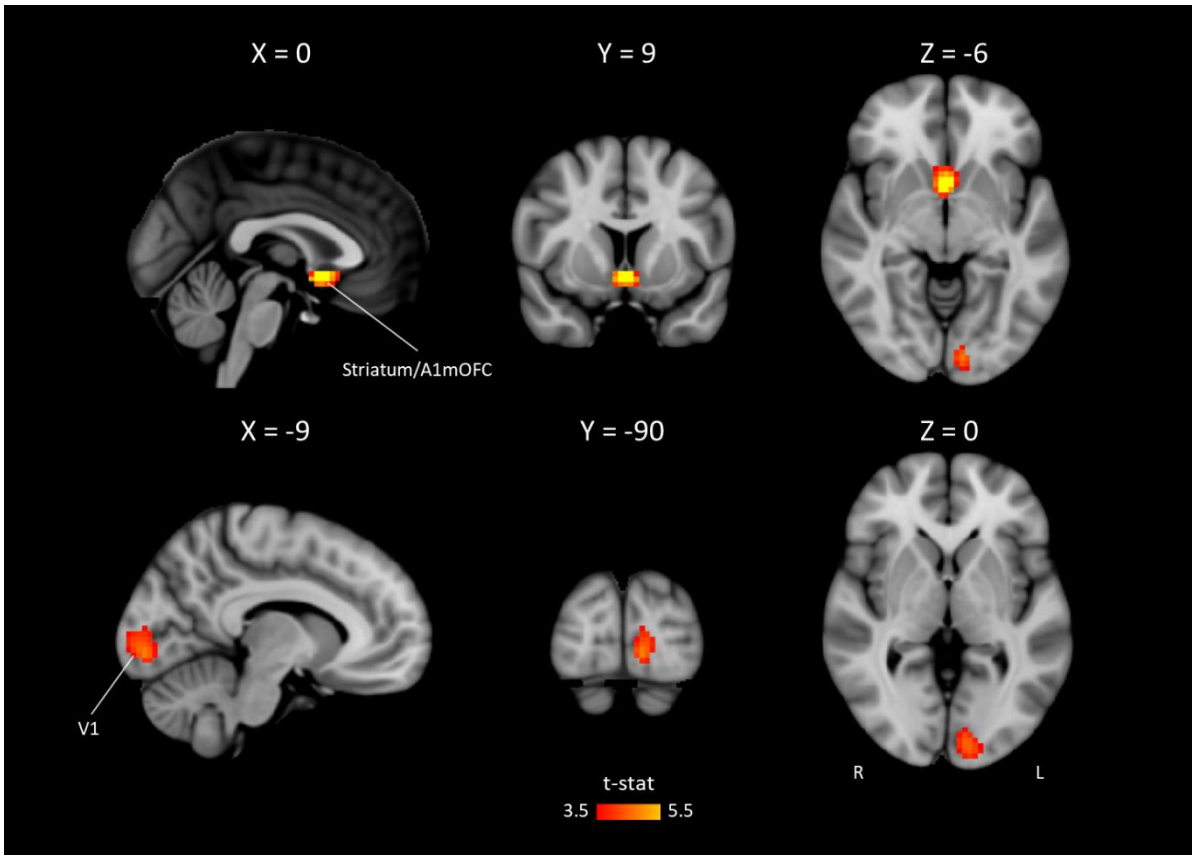

Figure 7.2. Parametric activations with decreasing levels of ugliness.
Regions with increasing levels of activity as the declared intensity of the experience of ugliness decreases. The group-level analysis was carried out using permutation testing, with a cluster-forming threshold of $p < .001$ and FWE correction ($p_{clust-FWE} < .05$). The clusters are reported in detail in Table 7.1.

7.3.4 Multivariate analysis results

A whole-brain searchlight RSA was conducted to determine whether any common neural activity patterns emerge in response to viewing faces that individuals experience as ugly. We compared the neural RDM with a model RDM that assumes that a distinct pattern only emerges for 'ugly' faces, that is, high pattern similarity between faces that are perceived as 'ugly' and no similarity between faces that are perceived as 'not-ugly'.

Several clusters showed significant pattern similarity when the faces were experienced as 'ugly' by the participants (Figure 7.3). Specifically, there were distinct neural patterns in the occipito-temporal cortex (including the occipital and fusiform face areas), frontal pole (FP), right pre- and postcentral gyri, precuneus, field A1 of the mOFC and the left middle temporal gyrus, among others. All clusters are reported in detail in Table 7.2.

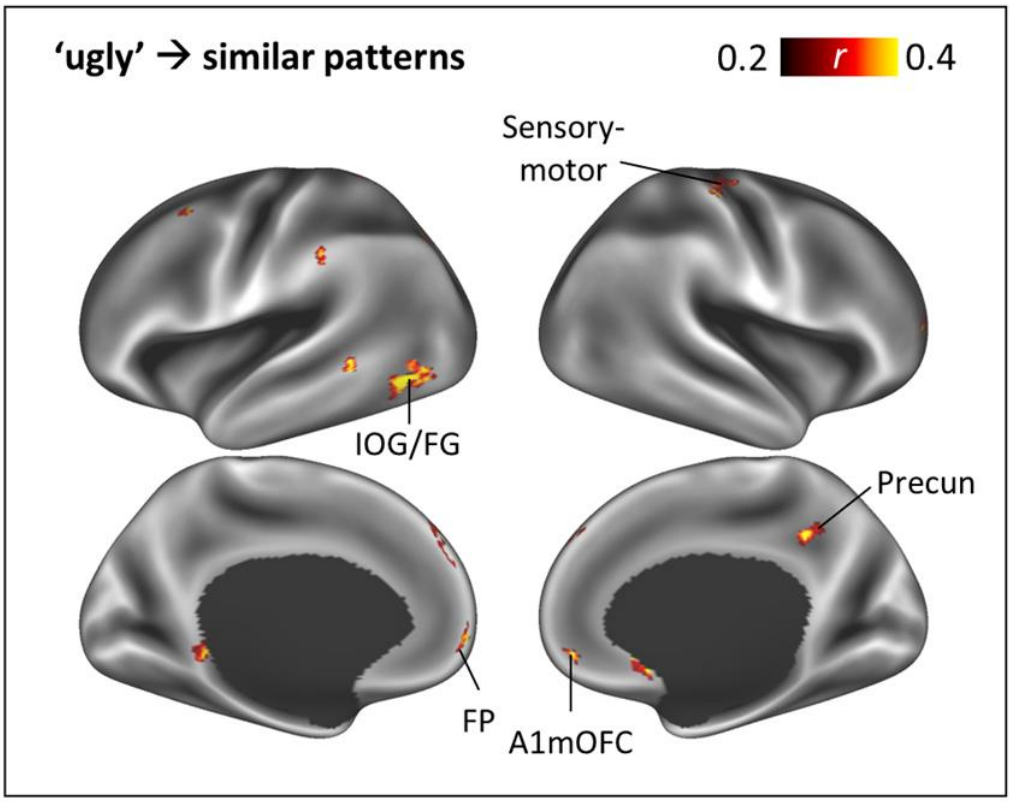

Figure 7.3. Searchlight RSA results displayed on the inflated brain surface.
A whole-brain surface-based searchlight RSA revealed several clusters where similar neural patterns emerge when a subject experiences a face as 'ugly'; there was a large cluster in the inferior occipital gyrus (IOG) and fusiform gyrus (FG) that borders the occipital face area (OFA) and fusiform face area (FFA), and other clusters in the precuneus (Precun), frontal pole (FP) and field A1 of the medial frontal cortex. These results are based on permutation testing with a vertex-wise p-value threshold of .001 and a minimum cluster size of 36 mm^2.

CLUSTER	r_{peak}	-log10 *p*	Area (mm^2)	MNI (mm)		
				x	y	z
L fusiform / inferior temporal / lateral occipital cortex	0.61	6.15	548	-44	-69	0
R post- and precentral gyri	0.45	3.94	242	37	-24	53
L middle temporal gyrus	0.53	5.53	123	-64	-45	1
R precuneus	0.45	4.26	89	13	-44	37
L supramarginal gyrus	0.43	4.42	85	-64	-29	40
L middle frontal gyrus	0.39	4.74	79	-38	11	59
Frontal pole	0.45	5.19	78	-4	66	-1
R medial orbitofrontal / rostral anterior cingulate cortex	0.46	4.19	58	4	21	-13
R medial orbitofrontal cortex	0.42	4.64	57	9	53	-9
R superior frontal cortex	0.32	3.85	56	13	52	42
L superior frontal cortex	0.38	4.50	43	-8	49	46

Table 7.2. Results of the multivariate fMRI analysis with RSA for model 1.
Several clusters were revealed by representational similarity analysis (RSA) to have significant pattern similarity when 'very ugly' stimuli were grouped together. The clusters and its size are reported along with MNI coordinates. The r_{peak} value represents the correlation between the neural RDM and model RDM. These results are based on permutation testing with a vertex-wise p-value threshold of .001 and a minimum cluster size of 36 mm^2. The clusters are labelled with the Freesurfer Desikan-Killiany atlas and are visualised in Figure 7.3.

7.4 DISCUSSION

In this study we asked subjects to make aesthetic judgments specifically about facial ugliness while simultaneously measuring their brain activity. There was no increased activity in any brain region with the declared intensity of the experience of ugliness. On the contrary, decreasing levels of ugliness showed increasing univariate activity in regions that have been associated with beauty and reward [5,16,19].

Specific neural activity patterns related to ugliness emerged in face-perceptive sensory regions and in the medial frontal cortex, including field A1 of the mOFC. This result is similar to that obtained for facial beauty; here too, there are decodable patterns in sensory regions important for face processing and in field A1, which only emerge if the face has the aesthetic quality of beauty attached to it [1]. Although the patterns are not the same ones for ugliness and beauty, it nevertheless seems that similar mechanisms are involved with the perception of both aesthetic qualities, the difference being that there is no increased activity in field A1 of the medial frontal cortex when experiencing facial

ugliness. Since during the rest state there is activity in field A1 (see chapter 6.3.2), as it is a constituent of the default mode network [20,21], this increased activity during beauty is rather a decrease of inhibition. With ugliness, there is no obvious decrease of inhibition in this region.

7.4.1 Aesthetic appeal is processed in sensory areas

First, I will reiterate a conclusion drawn in the previous chapter (6.4.2), namely that the sensory areas participate in the selection of stimuli according to aesthetic appeal. We found distinct decodable patterns in the OFA/FFA; this, together with findings from the previous chapter and other studies [1,2], suggests that the aesthetic status of a visual stimulus is registered in the visual sensory area that is specialised in the processing of it. Therefore, sensory areas are not mere passive recipients of incoming sensory input; they can also distinguish between different levels of aesthetic appeal, not only positively (beauty) but also negatively (ugliness). Just as in the case of beauty, the involvement of sensory areas with the experience of ugliness may be an attentional effect ugliness, especially since this experience may signal a potential pathogen threat [8]. Whether this sensory activity is feedforwarded to another region such as field A1, or the result of feedback is yet to be determined, but it is evident that the sensory areas are involved in aesthetic experiences.

7.4.2 A push-pull mechanism

We did not find increased activity in field A1 when the declared intensity of the experience of ugliness increased. In fact, an opposing trend was observed; as the intensity of the experience decreased, activity in the medial frontal cortex increased. Admittedly, this was not specifically in field A1 of the mOFC, but rather in more posterior parts, which have been associated with moral beauty [16]. This may be indicative of a subspecialisation within field A1, which future studies may reveal. Nevertheless, the involvement of field A1 in ugliness became evident from the multivariate analysis; the faces that were perceived as ugly elicited a specific neural activity pattern in face-perceptive areas in the fusiform gyrus and also in frontal areas, including field A1. This result, together with those obtained described by Yang et al. [1], who found a distinct pattern in these areas for beautiful faces, indicate that these areas are able to dissociate between beautiful and ugly faces, and each experience is represented by a different spatial arrangement of the

activity in them. Thus, the same network of brain areas is involved in both experiences, with face-perceptive sensory areas on the one hand and the medial frontal cortex on the other. The distinction between the experience of beauty and ugliness is therefore based not so much on the engagement of different brain regions, but rather on the engagement of different patterns of spatial distribution of activity within the same ones.

These results suggest that there is a push-pull mechanism in operation; it is modulation of activity within the same areas that are involved in beauty that lead to the experience of ugliness, and both experiences are represented by a distinct activity pattern. It thus seems probable, and is consistent with previous findings [5], that beauty and ugliness exist on a continuum, instead of being two categorically distinct concepts. We therefore come to the conclusion that beauty and ugliness are of the same category, existing on a continuum, at least in terms of underlying neurobiological mechanisms.

Involvement of other regions implicated in ugliness, such as the amygdala and insula [3,4,7], was not found. The reason for this is not known, but a difference between the study presented here and these other studies is the question that was asked; this study is the first to specifically address the experience of ugliness in isolation. Moreover, the amygdala and insula have been implicated in emotions such as disgust [22,23], which correlates with ugliness [7,8], but goes beyond. Possibly, the aesthetic judgements in this study may have been made without necessarily attaching an emotional weight to the decision. Of course, this remains speculation, but in any case, it is noteworthy that not all studies assessing ugliness find activity in these regions [5,6].

We did, however, find specific neural activity patterns in other regions that correlated with the experience of facial ugliness. First of all, patterns appeared in the precuneus and temporal cortex. These regions have also been implicated in facial processing [24,25], including facial attractiveness [26], and may therefore be part of the (extended) face-perceptive network [27]. There were also decodable patterns in the frontal cortex, including the superior and middle frontal gyri, and frontal pole, which could possibly be related to casting an aesthetic judgement, as these areas also appeared the be involved in facial [1] and abstract beauty [2]; as we saw in the previous chapter, the frontal gyri were especially implicated when subjects gave non-neutral ratings. Finally, pattern similarity in pre- and postcentral gyri may be related to motor responses involved in reporting the experience,

although previous studies have also pointed to its involvement in the experience of ugliness [6].

7.4.4. Concluding remarks

Overall, the findings in this study suggest that ugliness and beauty are opposing experiences of the same concept. Both experiences, at least when it comes to facial stimuli, involve similar neural mechanisms; it is the modulation of activity - both the level and distribution of it - in sensory areas important for face-processing and in frontal areas, including areas related to reward and emotion such as the striatum and field A1, that lie at the basis of the experience of facial ugliness and beauty.

Importantly, whereas stimulation of faces always leads to activity in face-perceptive areas [28–31], the involvement of field A1 (and other frontal areas) only becomes apparent when making an aesthetic judgement of a face, and this correlates with the emergence of specific neural activity patterns. It is therefore another instance of an experience-dependent connection in the brain; without the aesthetic experience, the relationship between these regions remains occult.

REFERENCES

1. Yang, T., Formuli, A., Paolini, M., and Zeki, S. (2022). The neural determinants of beauty. European Journal of Neuroscience *55*, 91–106. 10.1111/ejn.15543.

2. Rasche, S.E., Beyh, A., Paolini, M., and Zeki, S. (2023). The neural determinants of abstract beauty. European Journal of Neuroscience *57*, 633–645. 10.1111/ejn.15912.

3. Ishizu, T., and Zeki, S. (2011). Toward a brain-based theory of beauty. PLoS One *6*, e21852. 10.1371/journal.pone.0021852.

4. O'Doherty, J., Winston, J., Critchley, H., Perrett, D., Burt, D.M., and Dolan, R.J. (2003). Beauty in a smile: the role of medial orbitofrontal cortex in facial attractiveness. Neuropsychologia *41*, 147–155. 10.1016/S0028-3932(02)00145-8.

5. Martín-Loeches, M., Hernández-Tamames, J.A., Martín, A., and Urrutia, M. (2014). Beauty and ugliness in the bodies and faces of others: an fMRI study of person esthetic judgement. Neuroscience *277*, 486–497. 10.1016/j.neuroscience.2014.07.040.

6. Kawabata, H., and Zeki, S. (2004). Neural correlates of beauty. J Neurophysiol *91*, 1699–1705. 10.1152/jn.00696.2003.

7. Krendl, A.C., Macrae, C.N., Kelley, W.M., Fugelsang, J.A., and Heatherton, T.F. (2006). The good, the bad, and the ugly: an fMRI investigation of the functional anatomic correlates of stigma. Soc Neurosci *1*, 5–15. 10.1080/17470910600670579.

8. Klebl, C., Greenaway, K.H., Rhee, J.J., and Bastian, B. (2021). Ugliness judgments alert us to cues of pathogen presence. Soc Psychol Personal Sci *12*, 617–628. 10.1177/1948550620931655.

9. Zeki, S., Romaya, J.P., Benincasa, D.M.T., and Atiyah, M.F. (2014). The experience of mathematical beauty and its neural correlates. Front Hum Neurosci *8*. 10.3389/fnhum.2014.00068.

10. Lakshmi, A., Wittenbrink, B., Correll, J., and Ma, D.S. (2021). The India face set: international and cultural boundaries impact face impressions and perceptions of category membership. Front Psychol *12*. 10.3389/fpsyg.2021.627678.

11. Ma, D.S., Kantner, J., and Wittenbrink, B. (2021). Chicago face database: multiracial expansion. Behav Res Methods *53*, 1289–1300. 10.3758/s13428-020-01482-5.

12. Ma, D.S., Correll, J., and Wittenbrink, B. (2015). The Chicago face database: a free stimulus set of faces and norming data. Behav Res Methods *47*, 1122–1135. 10.3758/s13428-014-0532-5.

13. Winkler, A.M., Ridgway, G.R., Webster, M.A., Smith, S.M., and Nichols, T.E. (2014). Permutation inference for the general linear model. Neuroimage *92*, 381–397. 10.1016/j.neuroimage.2014.01.060.

14. Holmes, A.P., Blair, R.C., Watson, J.D.G., and Ford, I. (1996). Nonparametric analysis of statistic images from functional mapping experiments. Journal of Cerebral Blood Flow & Metabolism *16*, 7–22. 10.1097/00004647-199601000-00002.

15. Zeki, S., and Chén, O.Y. (2020). The Bayesian-Laplacian brain. European Journal of Neuroscience *51*, 1441–1462. 10.1111/ejn.14540.

16. Tsukiura, T., and Cabeza, R. (2011). Shared brain activity for aesthetic and moral judgments: implications for the beauty-is-good stereotype. Soc Cogn Affect Neurosci *6*, 138–148. 10.1093/scan/nsq025.

17. Davey, C.G., Allen, N.B., Harrison, B.J., Dwyer, D.B., and Yücel, M. (2010). Being liked activates primary reward and midline self-related brain regions. Hum Brain Mapp *31*, 660–668. 10.1002/hbm.20895.

18. Yang, T., Formuli, A., Paolini, M., and Zeki, S. (2022). The neural determinants of beauty. European Journal of Neuroscience *55*, 91–106. 10.1111/ejn.15543.

19. Fliessbach, K., Rohe, T., Linder, N.S., Trautner, P., Elger, C.E., and Weber, B. (2010). Retest reliability of reward-related BOLD signals. Neuroimage *50*, 1168–1176. 10.1016/j.neuroimage.2010.01.036.

20. Raichle, M.E., MacLeod, A.M., Snyder, A.Z., Powers, W.J., Gusnard, D.A., and Shulman, G.L. (2001). A default mode of brain function. Proceedings of the National Academy of Sciences *98*, 676–682. 10.1073/pnas.98.2.676.

21. Shulman, G.L., Corbetta, M., Buckner, R.L., Fiez, J.A., Miezin, F.M., Raichle, M.E., and Petersen, S.E. (1997). Common blood flow changes across visual tasks: I. increases in subcortical structures and cerebellum but not in nonvisual cortex. J Cogn Neurosci *9*, 624–647. 10.1162/jocn.1997.9.5.624.

22. Schienle, A., Schäfer, A., Stark, R., Walter, B., and Vaitl, D. (2005). Relationship between disgust sensitivity, trait anxiety and brain activity during disgust induction. Neuropsychobiology *51*, 86–92. 10.1159/000084165.

23. Sambataro, F., Dimalta, S., Di Giorgio, A., Taurisano, P., Blasi, G., Scarabino, T., Giannatempo, G., Nardini, M., and Bertolino, A. (2006). Preferential responses in amygdala and insula during presentation of facial contempt and disgust. European Journal of Neuroscience *24*, 2355–2362. 10.1111/j.1460-9568.2006.05120.x.

24. Huang, L., Song, Y., Li, J., Zhen, Z., Yang, Z., and Liu, J. (2014). Individual differences in cortical face selectivity predict behavioral performance in face recognition. Front Hum Neurosci *8*. 10.3389/fnhum.2014.00483.

25. Kosaka, H., Omori, M., Iidaka, T., Murata, T., Shimoyama, T., Okada, T., Sadato, N., Yonekura, Y., and Wada, Y. (2003). Neural substrates participating in acquisition of facial familiarity: an fMRI study. Neuroimage *20*, 1734–1742. 10.1016/S1053-8119(03)00447-6.

26. Vartanian, O., Goel, V., Lam, E., Fisher, M., and Granic, J. (2013). Middle temporal gyrus encodes individual differences in perceived facial attractiveness. Psychol Aesthet Creat Arts *7*, 38–47. 10.1037/a0031591.

27. Fox, C.J., Iaria, G., and Barton, J.J.S. (2009). Defining the face processing network: optimization of the functional localizer in fMRI. Hum Brain Mapp *30*, 1637–1651. 10.1002/hbm.20630.

28. Kanwisher, N., McDermott, J., and Chun, M.M. (1997). The fusiform face area: a module in human extrastriate cortex specialized for face perception. The Journal of Neuroscience *17*, 4302–4311. 10.1523/JNEUROSCI.17-11-04302.1997.

29. Allison, T., Puce, A., Spencer, D.D., and McCarthy, G. (1999). Electrophysiological studies of human face perception. I: potentials generated in occipitotemporal cortex by face and non-face stimuli. Cerebral Cortex *9*, 415–430. 10.1093/cercor/9.5.415.

30. Sergent, J., Ohta, S., and Macdonald, B. (1992). Functional neuroanatomy of face and object processing: a positron emission tomography study. Brain *115*, 15–36. 10.1093/brain/115.1.15.

31. Haxby, J. V., Hoffman, E.A., and Gobbini, M.I. (2000). The distributed human neural system for face perception. Trends Cogn Sci *4*, 223–233. 10.1016/S1364-6613(00)01482-0.

SUMMARY OF FINDINGS

The experiments discussed in this thesis have shed light on various aspects of the neurobiology of human perceptual and cognitive experience, from the processing of single visual attributes to the processing of stimuli with aesthetic qualities, revealing brain connections which only become visibly demonstrable through a specific experience. The involvement of certain brain areas in the these experiences was revealed by using both univariate and multivariate analyses.

This enquiry began by investigating the neural mechanisms involved in the awareness of a single visual attribute, namely that of motion. To appropriately induce such a state, we assessed a reduced neural system, namely that of the Riddoch syndrome. These patients, blinded due to lesions in V1, can nevertheless consciously perceive single visual attributes such as motion. The undertaking started with what seemed to be a simple question, namely of what neural mechanisms in visual areas dictate the difference of two perceptual states, one in which the patient is conscious and one in which he or she is not. We hypothesised that the spatial arrangement of activity would be different in the conscious state, which indeed turned out to be the case. It soon appeared however, that there were additional intricacies in the Riddoch syndrome, including previously unreported perceptual states such as hallucinations, which extended our studies.

The important insight from these studies, that activity patterns emerge in specialised visual areas during conscious experiences, increased our interest in these patterns, which lead us to further examine their possible emergence in other, more complex, experiences, such as aesthetic experiences, based on the assumption that these experiences involve a wider network of brain regions. These experiences also correlated with distinct neural activity patterns in areas important for the processing of the given stimulus and its aesthetic appeal. Overall, we can summarise the findings described in this thesis as follows.

V1 is not necessary for visual awareness

Our studies on patients with cortical lesions, particularly those involving V1, have revealed a nuanced understanding of how residual visual capacities and crude visual awareness may persist. Contrary to classical theories positing a complete dissociation between discrimination and awareness (as in “blindsight”), we have found that the two

are tightly linked; however, the presence of distinct perceptual states, such as agnosopsia and gnosanopsia, stresses the complexity of conscious visual experiences. Gnosanopsia is here of special interest; this scarcely reported dimension of the Riddoch syndrome, in which patients report a high degree of certainty yet are unable to discriminate, or report being aware when not visually stimulated (i.e., they hallucinate), makes this syndrome an especially powerful one to study the neural correlates of consciousness and paves the way for future research.

Despite the pre-eminent position of V1, the ineluctable conclusion seems to be that damage to this area does not lead to obliteration of visual awareness. Residual visual awareness may be sustained as long as the visual area responsible for the processing of a specific visual feature is intact and receives direct subcortical input. Moreover, this input needs to be transmitted via intact pathways; as we have seen, perturbations in the pathways can mimic the Riddoch syndrome, even when V1 is intact.

Conscious perception of single visual attributes evokes distinct neural patterns in the visual area specialised for it

Thus, V1-bypassing input into the visual cortex is sufficient to support a conscious percept. However, increased univariate activity in the relevant visual area does not seem to be a good indicator of conscious vision, as heightened activity has been found in unconscious conditions [1–3] or, as we have seen, lack in conscious ones. Our studies instead suggest that a more adequate measure of visual awareness, at least for visual motion, is a specific decodable neural activity pattern in specialised visual areas, in this case V5, as these could only be detected in conscious conditions (including hallucinatory) and not in unconscious ones. Similarly, conscious detection of coloured stimuli correlated with specific neural activity patterns in V4 complex, whereas no such pattern emerged in that area with achromatic stimuli. Thus, the conscious awareness of specific visual attributes correlates with neural activity patterns in the relevant specialised visual area. Additional brain areas were revealed as well, depending upon the experience of the subject; for instance, the experience of hallucinatory motion correlated with hippocampal activity, whereas ambiguous perception correlated with inferior frontal gyrus activity. This is therefore a demonstration of experience-dependent connections; these hidden connections between distant areas became visibly demonstrable only through these specific experiences.

Specific neural activity patterns also emerge in aesthetic experiences

Moving beyond the realm of perception of single visual attributes, we explored the neural correlates of more complex experiences, namely aesthetic experiences, particularly in response to abstract art and faces. Our findings revealed that sensory areas play a crucial role in the perception of aesthetic appeal of stimuli; both beautiful and ugly stimuli evoke specific neural activity patterns in sensory areas that are responsible for the processing of the given stimulus, whereas these activity patterns were not evident when neutral stimuli were viewed. The visual sensory areas are therefore more than passive recipients of incoming visual input; they participate, either via feedforward or feedback input, in the perception of aesthetic qualities of a stimulus. There was additional involvement of field A1 of the medial frontal cortex, but patterns could only be decoded in this region with faces (biological stimuli) and not abstract art (artifactual stimuli). We believe that this interaction between sensory and frontal cortices form the neural basis of aesthetic experiences. Again, the co-activity between these distant regions was demonstrable only through a specific experience, this time through experiences of beauty and ugliness. Simply perceiving a face does not lead to additional involvement of field A1 of the mOFC [4]; it is the aesthetic experience that reveals this connection.

The demonstration of experience-dependent connections in the human brain

Over a quarter of a century ago, Crick and Jones [5] considered it "intolerable" and "shameful" that we do not have as much information about human neuroanatomy as we do about that of monkey; they were in a search for anatomical techniques that can be used in the post-mortem human brain, based around tract-tracing; this, they hoped, might reveal a connectivity pattern in the human brain which could come close to the anatomical tracing methods used in live monkeys. Since then, many advances have been made in the study of the human brain's anatomy and function owing to advances in non-invasive brain imaging techniques, and these are of two kinds.

The first revolves around diffusion MRI and tractography which have contributed to our knowledge of the brain's anatomical connectivity. They have demonstrated, for example, the existence of direct anatomical connections between the posterior occipital cortex and the prefrontal cortex in the human brain, and have linked them to conscious visual processing and face perception [6–8]. These studies (and others) have established that the

polar occipital cortex is directly connected with the lateral and polar frontal cortex, but no direct connections have been established with the medial anatomical areas overlapping field A1. Despite these advances, the descriptions of the exact terminations of these connections are vague with respect to the many specific visual areas of the occipital lobe. It is hard to learn, from what is available, which visual areas such as V3, V3A, V4, FFA, or OFA are connected with which part of the frontal cortex.

The second approach is illustrated by the present results and those of many others, which demonstrate that connections, whether direct or indirect, between the areas enumerated above (and many more) do exist in the human brain but are currently only demonstrable during certain experiential states which, otherwise, remain occult. The studies described in this thesis serve as examples, and of course any number of previous fMRI studies could serve this purpose just as well. For instance, in a previous study [9] it was shown that ambiguous visual stimuli, in addition to engaging visual areas such as V1 and V3, also engage the mid-cingulate cortex, which had been implicated in conflict monitoring [10], though no direct connections between these visual areas and the mid-cingulate cortex have been anatomically demonstrated. Such connections also exist in other domains, such as that of motor learning [11]. Of course, all these connections are correlative and may be mediated by another, or other, unrevealed brain structures [12]. Nevertheless, the scaffolding is there, but without the experience, it remains visibly dormant.

Thus, experience itself reveals connections between different brain areas. How does this differ from (effective) functional connectivity, such as psychophysiological interaction (PPI) [13,14]? Here too, there is a temporal relationship between distant regions. However, this method makes more assumptions than experience-dependent connectivity does, as it attempts to reveal whether one area modulates the activity in another. Experience-dependent connectivity simply states that activity in areas A and B only emerge and are demonstrable during the experience, implying that they are somehow connected, without specifying exactly how they are connected; when A and B are co-active, A may modulate B, or vice versa, but this is not necessary. Moreover, it is not necessarily a direct anatomical connection; a third, or fourth, region may mediate or enable this connection. Nevertheless, it is important to explicitly emphasize that there are such highly specific state-dependent connections that are currently only demonstrable with specific experiences.

CONCLUDING REMARKS

In conclusion, the work presented in this thesis has contributed to a deeper understanding of various experiences, demonstrating that each involves a different 'experience-dependent' neural network. From these studies new questions emerge that may be addressed in future work; for instance, the discovery of hallucinations in the Riddoch syndrome may reveal interesting insights into the role of expectation in visual processing. Regarding aesthetic experiences, it would be interesting to investigate the temporal dynamics of the experience; do the sensory areas send information about aesthetic appeal to the mOFC, or does the mOFC, through feedback, engage the sensory areas? By understanding the temporal dynamics, philosophical questions regarding beauty could potentially be answered, such as whether a judgement is made first, leading to the pleasurable (emotional) experience, or whether the pleasurable experience enables an aesthetic judgement [15]. Finally, further investigations into neural activity patterns may ultimately reveal the meaning of these decodable patterns that correlate with human experience.

REFERENCES

1. Itoh, K., Fujii, Y., Kwee, I.L., and Nakada, T. (2005). MT+/V5 activation without conscious motion perception: a high-field fMRI study. Magnetic Resonance in Medical Sciences *4*, 69–74. 10.2463/mrms.4.69.
2. Moutoussis, K., and Zeki, S. (2006). Seeing invisible motion: a human fMRI study. Current Biology *16*, 574–579. 10.1016/j.cub.2006.01.062.
3. Zeki, S., and ffytche, D. (1998). The Riddoch syndrome: insights into the neurobiology of conscious vision. Brain *121*, 25–45. 10.1093/brain/121.1.25.
4. Yang, T., Formuli, A., Paolini, M., and Zeki, S. (2022). The neural determinants of beauty. European Journal of Neuroscience *55*, 91–106. 10.1111/ejn.15543.
5. Crick, F., and Jones, E. (1993). Backwardness of human neuroanatomy. Nature *361*, 109–110. 10.1038/361109a0.
6. Forkel, S.J., Thiebaut de Schotten, M., Kawadler, J.M., Dell'Acqua, F., Danek, A., and Catani, M. (2014). The anatomy of fronto-occipital connections from early blunt dissections to contemporary tractography. Cortex *56*, 73–84. 10.1016/j.cortex.2012.09.005.
7. ffytche, D.H., and Catani, M. (2005). Beyond localization: from hodology to function. Philosophical Transactions of the Royal Society B: Biological Sciences *360*, 767–779. 10.1098/rstb.2005.1621.
8. Rokem, A., Takemura, H., Bock, A.S., Scherf, K.S., Behrmann, M., Wandell, B.A., Fine, I., Bridge, H., and Pestilli, F. (2017). The visual white matter: the application of diffusion MRI and fiber tractography to vision science. J Vis *17*, 4. 10.1167/17.2.4.
9. Ishizu, T., and Zeki, S. (2014). Varieties of perceptual instability and their neural correlates. Neuroimage *91*, 203–209. 10.1016/j.neuroimage.2014.01.040.
10. Botvinick, M.M., Carter, C.S., Braver, T.S., Barch, D.M., and Cohen, J.D. (2001). Conflict monitoring and cognitive control. Psychol Rev *108*, 652. 10.1037/0033-295X.108.3.624.
11. Laureys, S., Peigneux, P., Phillips, C., Fuchs, S., Degueldre, C., Aerts, J., Del Fiore, G., Petiau, C., Luxen, A., Van der Linden, M., et al. (2001). Experience-dependent changes in cerebral functional connectivity during human rapid eye movement sleep. Neuroscience *105*, 521–525. 10.1016/S0306-4522(01)00269-X.
12. Eickhoff, S.B., and Müller, V.I. (2015). Functional Connectivity. In Brain Mapping: An Encyclopedic Reference, A. W. Toga, ed. (Elsevier), pp. 187–201. 10.1016/B978-0-12-397025-1.00212-8.
13. Friston, K.J. (1994). Functional and effective connectivity in neuroimaging: a synthesis. Hum Brain Mapp *2*, 56–78. 10.1002/hbm.460020107.
14. Friston, K.J., Buechel, C., Fink, G.R., Morris, J., Rolls, E., and Dolan, R.J. (1997). Psychophysiological and modulatory interactions in neuroimaging. Neuroimage *6*, 218–229. 10.1006/nimg.1997.0291.
15. Kant, I. (1790). Critique of Judgement H. Bernard, ed. (Barnes & Noble).